THESIS

RE-EVALUATING EFFECTS OF WATER QUALITY CHANGES ON SOIL HYDRAULIC PROPERTIES

Submitted by

David P. Huber

Department of Soil and Crop Sciences

In partial fulfillment of the requirements

For the Degree of Master of Science

Colorado State University

Fort Collins, Colorado

Summer 2011

Master's Committee:

Advisor: Greg Butters
Co-Advisor: Luis Garcia

Kenneth Barbarick

ABSTRACT

RE-EVALUATING EFFECTS OF WATER QUALITY CHANGES ON SOIL HYDRAULIC PROPERTIES

Elevated soil salinity has long been an agricultural concern, causing reductions in infiltration and crop yields, and in extreme cases loss of agricultural land. This study re-examines how salinity affects soil hydraulic properties in order to address deficiencies in prediction methods and management of salinity's impacts on soils. This research project explores the effects of both changing irrigation water electrical conductivity (EC) and sodium adsorption ratio (SAR) on soil hydraulic conductivity, K, and soil moisture retention, θ, over a range of soil water tensions. The Results show that a decrease in EC from 20 to 0.25 dS m^{-1}, with SAR held constant at low to moderate levels, causes changes in $K(\theta)$ only after dropping below 1.5 dS m^{-1} for soils at this particular site. The initial $K(\theta)$ could not be recovered by increasing the EC to its original level, indicating that irreversible clay dispersion had taken place. Increasing SAR from approximately 4 to 25 with EC held at 0.5 dS m^{-1} caused slight reductions in $K(\theta)$. In contrast to the EC treatment, $K(\theta)$ partially recovered after the SAR was reduced to its initial condition. The mechanism for the SAR effect is clay swelling and is reversible with changing soil water chemistry. The results from both EC and SAR treatments are consistent with other research reports. However, in contrast to previous studies and of particular interest is the

magnitude of change in K with changing EC or SAR and decreasing θ. Unlike current models that assume the decline in K due to solution chemistry is constant over the entire K(θ) range, equal to the change at K_{sat}, this study observes an exponential increase in the solution chemistry's effect on K with decreasing θ. These findings suggest that current models that ignore solution chemistry, or models that assume a constant K reduction for the entire K(θ) function, are over-estimating the drainage in these systems. Adoption of a more characteristic solution chemistry model, similar to the one presented here, could help better manage irrigation water quality, reduce salt accumulation, and improve crop yields.

ACKNOWLEDGEMENTS

Thanks to my wife Cory for supporting me through my late nights and stressful times. Thanks to my Mom, Diane and my Dad, Joe for always supporting me and allowing me to take risks in life. Thanks to my Grandpa for being a source of wisdom and inspiration in both my professional and private lives. Thanks to my advisor Greg Butters for allowing me to explore my interests as well as helping me achieve my goals. In addition, I'd like to thank Greg for his incredible patience with my slow completion of this project. Thanks to my other committee members Luis Garcia, Kenneth Barbarick, and former member Jim Ippolito for lending me their support and extensive expertise. Thanks to the Colorado Agricultural Experimental Station and Luis Garcia for providing my RA funding. Thanks to the Department of Biology and Tracy Halward for providing me with the opportunity to TA. Thanks to my fellow students at Colorado State University including James Wittler, Curtis Cooper, Aida Jiménez-Esquilín, Dan MacKinnon, Bob Brobst, and Daniel Gillham. Thanks to all my friends and colleagues at Arizona State University for encouraging me and providing me with the opportunity to apply my knowledge to new research fields and interests. Finally, since this degree has taken me so long, I now have to thank my daughter, Sophia who didn't yet exist while I worked at Colorado State University but now is a great source of inspiration and motivation for me to go on and do great things.

PROJECT SUMMARY AND MAJOR FINDINGS

This study re-examines how salinity affects soil hydraulic properties in order to address deficiencies in prediction methods and management of salinity's impacts on soils. This research provides data, tables, and figures characterizing the native soil hydraulic properties in a select area of the lower Colorado Arkansas River Valley, east of Lamar. Correlation between soil hydraulic properties and soil physical and chemical properties are also shown. The effects of both changing irrigation water electrical conductivity and sodium adsorption ratio on soil hydraulic conductivity and soil water content are provided in tables and figures. All the soil hydraulic parameters describing the soil hydraulic and moisture retention functions are listed in tables in the supplemental appendix. Below is a brief summary of the major findings of this research project.

- The hysteresis, or difference, between the draining and wetting K and θ functions in these soils was shown to become more pronounced with reduced EC and unchanged or slightly less hysteretic with increased SAR. The ratio of α_w/α_d was show to increase with changing decreasing soil water EC, and for most treated soils the assumption that α_w equaled $2*\alpha_d$ failed, with α_w for some treatments reaching greater than 5 times α_d.

- The soil water tension at air entry for the soils varied between both native low and high salinity regions and between electrical conductivity or sodium adsorption ratio treatments. The soil water tension at air entry was significantly lower (i.e. closer to zero) for the high salinity region vs. the low salinity region. The soil water tension at air entry decreased with reduced electrical conductivity and varied for changing sodium adsorption ratio.

- Considering data from both *in situ* and lab analyses, solution chemistry with an electrical conductivity below 1.5 dS m^{-1} and with a low to moderate sodium adsorption ratio (approx. 5), appears to be a threshold value for clay dispersion and disruption of these specific soils. The threshold value was approximately constant between all soils collected from salinity regions (low, medium, and high) and for *in situ* infiltration measurements.

- A key finding of this research project is the change in soil hydraulic conductivity as a function of both solution chemistry and water content indicates the effect of solution chemistry on hydraulic conductivity is not constant with increasing soil water tension. Nearly all models that consider solution chemistry effects on hydraulic conductivity assume a constant reduction in hydraulic conductivity over the entire range of the conductivity function.

TABLE OF CONTENTS

INTRODUCTION 1
Research Objectives 6
METHODS 8
Site Characterization 8
Site Description 8
Field Sampling 9
Soil Characterization 12
Field Infiltration 12
Soil Chemical Analysis 15
Soil Physical Analysis 17
Supplemental Physical Characteristics 19
Clay Mineralogical Analysis 20
Data Analysis 21
Statistical Analysis 21
Direct Estimation of Soil Hydraulic Properties 21
Inverse Analysis of Soil Hydraulic Properties 24
RESULTS AND DISCUSSION 26
Soil Chemical and Physical Properties 26
Field Infiltration 32
Native Hydraulic Conductivity and Moisture Retention Characterization 38
Electrical Conductivity Reduction Series 50
EC Effects on K(h) and θ(h) 53
Sodium Adsorption Ratio Series 56
SAR Effects on K(h) and θ(h) 59
Hysteresis and Soil Solution Chemistry 61
Spatial and Treatment Effects on Soil Air Entry Pressure 69
Effects of Solution Chemistry with Changing Soil Water Content 70

Relative Conductivity for the EC Reduction Series 72
Relative Conductivity for the SAR Reduction Series 77
CONCLUSIONS AND IMPLICATIONS 81
Solution Chemistry and Relative Hydraulic Conductivity 81
Model Parameterization and Soil Heterogeneity 83
Surface Crusting and Leaching Efficiency 84
Implications of Soil Water Hysteresis 88
Recommendations 91
REFERENCES 93
SUPPLEMENTAL APPENDIX 100

FIGURE INDEX

Figure 1: Map of the Colorado Arkansas River Basin……14
Figure 2: Map of the lower Colorado Arkansas River Valley and regions of interest.. 20
Figure 3: Map of field 1 soil salinity and selected sampling regions……. 21
Figure 4: Photograph of intact soil cores sampled for laboratory analysis……..... 22
Figure 5: Photographs of the relative infiltration plots in field 2……... 24
Figure 6: Saturated hydraulic conductivity sampling layout in field 2…….. 25
Figure 7: Diagram of continuous flow cell for K(h) and θ(h) determination…… 29
Figure 8: Mineralogical analysis using XRD for the medium and high salinity……
regions……. 42
Figure 9: Mineralogical analysis using XRD for the low and high salinity regions….. 43
Figure 10: Total pore volumes leached for salinity treatments…….. 44
Figure 11: Change in relative infiltration time with changing solution chemistry…… 45
Figure 12: Change in relative infiltration rates between control and gypsum amended
plots……46
Figure 13: Change in saturated hydraulic conductivity with changing solution……
Chemistry……...47
Figure 14: Trendline of saturated hydraulic conductivity change with changing……..
solution chemistry……..48
Figure 15: The K(h) and θ(h) parameters between salinity regions under native soil…
conditions……...50
Figure 16: Hydraulic conductivity and moisture retention functions between salinity.
regions……53
Figure 17: Change in soil water pressure at air entry between salinity regions……. 54
Figure 18: The difference in hysteresis of soil hydraulic functions between salinity…
regions……55
Figure 19: A comparison of predicted vs. measured soil hydraulic properties…….. 59
Figure 20: Comparison of predicted vs. measured soil hydraulic functions between…
salinity regions……...60
Figure 21: The change in saturated hydraulic conductivity and water content with….
reduced solution EC……...62
Figure 22: Change in hydraulic conductivity and moisture retention functions with…
reduced soil solution EC – low salinity region……..65
Figure 23: Changes in soil hydraulic and moisture retention functions with reduced..
EC – medium salinity region……. 66

Figure 24: Change in hydraulic conductivity and moisture retention with reduced soil solution EC – high salinity region……. 67
Figure 25: Change in saturated hydraulic conductivity and water content with…… increase in SAR……. 68
Figure 26: Change in soil hydraulic and moisture retention functions with increasing SAR – low salinity region……..70
Figure 27: Hysteresis in hydraulic conductivity and moisture retention for the EC….. reduction series – low salinity region…… 72
Figure 28: Hysteresis in hydraulic conductivity and moisture retention for the EC….. reduction series – medium salinity region……. 73
Figure 29: Hysteresis in hydraulic conductivity and moisture retention for the EC….. reduction series – high salinity region……... 73
Figure 30: The difference in van Genuchten L parameters between salinity regions… 74
Figure 31: The change in the van Genuchten L parameter with changing EC……... 75
Figure 32: Hysteresis in hydraulic conductivity and moisture retention for the SAR… series – low salinity region…… 76
Figure 33: Hysteresis in hydraulic conductivity and moisture retention for the SAR… series – high salinity region……... 76
Figure 34: The change in the van Genuchten L parameter with changing SAR for the low salinity region……..77
Figure 35: The change in the van Genuchten L parameter with changing SAR for the high salinity region…… 78
Figure 36: Correlation between van Genuchten L parameter and inverse fit sum of… squares……79
Figure 37: Change in soil water pressure at air entry with changing solution……... Chemistry……...81
Figure 38: Relative hydraulic conductivity for EC reduction series – low salinity…… region……. 84
Figure 39: Relative hydraulic conductivity for EC reduction series – medium salinity region……. 85
Figure 40: Relative hydraulic conductivity for EC reduction series – high salinity….. region……. 85
Figure 41: Relative hydraulic conductivity for the SAR series – low salinity region… 89
Figure 42: Relative hydraulic conductivity for the SAR series – high salinity region... 89
Figure 43: Regression of the relative hydraulic conductivity with reduced water…….. content – low salinity region at 1.5 dS m^{-1}…… 93
Figure 44: Simulated changes in soil hydraulic conductivity with changing solution.. chemistry……99
Figure 45: Hysteresis effects on cumulative soil drainage and evaporation…….. 101

TABLE INDEX

Table 1: Soil nutrient properties for field 1 salinity regions……...38
Table 2: Soil salinity and physical properties for field 1 salinity regions…….. 40
Table 3: Soil properties for field 2 salinity regions…… 41
Table 4: Hysteresis in the α parameter between draining and wetting curves…….. 53
Table 5: Comparison between field 1 and 2 soil hydraulic properties…….. 56
Table 6: Intra-salinity region heterogeneity of hydraulic conductivity and water…… content…….. 57
Table 7: Measured vs. predicted Ks values for the EC reduction series…… 87
Table 8: Measured vs. predicted Ks for SAR series……...90
Table 9: Chemistry of irrigation water applied for cumulative infiltration simulation. 98

EQUATION INDEX

[Eq.1].....25
[Eq.2].....26
[Eq.3].....27
[Eq.4].....27
[Eq.5].....16
[Eq.6].....17
[Eq.7].....33
[Eq.8].....33
[Eq.9].....33
[Eq.10].....34
[Eq.11].....34
[Eq.12].....82
[Eq.13].....82

INTRODUCTION

Salinity has long been a problem in agriculture (Hillel, 2000). In nearly every irrigated agricultural system, addition of water to augment seasonal rainfall eventually results in raised water tables, water-logging, and salt accumulation (Singh *et al*., 2010; Hillel, 2000; Ayers and Westcott, 1985) – over a quarter of irrigated land in the U.S. is seriously affected by salinization (Ghassemi *et al.*, 1995; Lefkoff and Gorelick, 1990). Salinization can cause a number of problems, often resulting in reduced crop yields, adjacent environmental and habitat degradation, and in extreme cases the temporary or permanent loss of agricultural land (Singh *et al*., 2010; Purkey and Wallender, 2001a; Ghassemi *et al*., 1997). In general, areas under intense irrigation develop salinity problems within two decades to 100 years (Gates *et al*., 2002). Problems associated with high salt concentrations include decreased germination rates, increased osmotic stress, plant toxicity, and mineral depletion (Hillel, 2000; Mer *et al*., 2000; Khavai-Nejad and Chaparzadeh, 1998). High salt concentrations can also cause a decrease in soil organic matter, shifts in soil fauna, and reduction of the soil's fertility and structural stability (Rietz and Haynes, 2003; Sarig *et al*., 1993).

Salt accumulation in agricultural soils is often caused by a combination of *in situ* conditions and unfavorable management practices that may or may not be directly related to irrigation strategies. A combination of field and upstream geology, irrigation water quality and storage, and the soil's drainage capacity all greatly affect the salinization of a

region (Gates *et al*., 2006; Gates and Grismer, 1989). In addition, water rights of upstream and downstream users and changes in water policy with increasing urban water demand can reduce the amount of water and the number of strategies available to remediate salt affected regions (Gates *et al*., 2006; Thorvaldson and Pritchett, 2006). In regions with salt accumulation, management practices to stop or reverse damage and reduced yields can become very complex.

The lower Arkansas River Valley in southeastern Colorado (Figure 1) is one such area identified as having moderate to severe salinity problems (Burkhalter and Gates 2005). The groundwater electrical conductivity (EC) sampled from wells throughout the valley between 1999 and 2005, averaged between 3.0 to 5.78 dS m^{-1} (Gates *et al*., 2006). Water EC sampled from the river channel now average over 4.29 dS m^{-1} as it approaches the Kansas state border (Whittemore *et al*., 2000), and the EC in the alluvial aquifer ranges from 2.57 to 5.86 dS m^{-1} moving down the valley (Goff *et al*., 1998). For perspective, average rainwater EC equals 0.015 dS m^{-1}, and excellent quality irrigation water ranges between 0.285 to 0.715 dS m^{-1} (Duncan *et al*., 2000). Electrical conductivity values of 2.86 dS m^{-1} constitute the upper limit of acceptable irrigation water but only if leaching and other remediation strategies are available to prevent salt loading.

The first signs of salinization in the lower Arkansas River Valley appeared in the early twentieth century (Whittemore et al., 2000; Miles, 1977). Installation of subsurface drains in the 1930's helped lower the water table and reduce salinization temporarily (Gates *et al*., 2002). However, in the 1970's water tables began to rise again as did the rate of salinization (Gates et *al*., 2002; Burkhalter and Gates 2005).

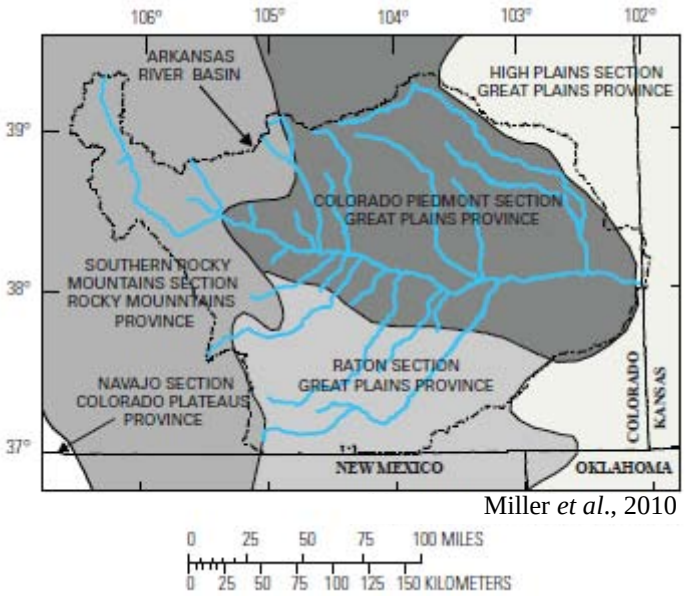

Figure 1: Map of the Colorado Arkansas River Basin.

Problems were exacerbated by the building of two reservoirs on the lower Arkansas River (Gates *et al*., 2006), John Martin Reservoir in 1948 downriver of La Junta, and Pueblo Reservoir in 1975 just west of the city of Pueblo. The reservoirs did two things: first, because of flood control the river channel began to widen and sediment accumulation on the riverbed caused the water table to rise (Gates *et al*., 2002). Second, because of the storage capacity of the reservoirs, water was available year round. This year round storage of water in canals, retention ponds, and water application increased water tables and increased salt application to soils (Gates *et al*., 2002; Burkhalter and Gates 2005). All these factors combined, the lower Arkansas River is now one of the most saline rivers in the U.S. (Whittemore *et al*., 2000) and much of the valley's agricultural land is classified with the Environmental Protection Agency's highest salinity hazard rating (Burkhalter and Gates 2005). This, combined with the fact that 33 percent of the local economy in the Lower Arkansas River Valley--the largest agricultural basin in Colorado--is derived from farming, 23 percent of which is directly from irrigated land

(Thorvaldson and Pritchett, 2006), makes it apparent how critical salinity management is for the region.

Recognizing that more research is required on water and salinity issues in order to effectively manage agriculture in the lower Arkansas River Valley, a multidisciplinary research group was formed to study the effects of salinity. This project, "Multidisciplinary Research on Salinity Issues in the Arkansas River Valley," funded in part through the Colorado Agricultural Experimental Station (Project COL00694) and in part by the U.S. Department of the Interior Geological Survey and Colorado Water Resources Research Institute (Project 2002CO6B), includes numerous researchers and integrates socio-economic, agronomic, natural and physical sciences, and engineering disciplines. The *characterization of soils for field scale modeling of salinity* is included in the core science goals of the project and is the focus of this Master's project.

Characterization of soils in the lower Arkansas River Valley for the purpose of modeling salinity's effects on soil properties and processes involves analysis of soil physical, chemical, and hydrological properties. Worldwide, there has been extensive research on the impact salts have on soils and crops. Typically, stable concentrations of salts (e.g. halite, calcite, and gypsum) have little direct effect on the physical state of the soil matrix themselves. Alone, salts become a problem in most systems when they reach concentrations in solution that cause osmotic stress to plants, prevent adsorption of important ions, or disrupt protein synthesis in cells (Mer, 2000; Khavai-Nejad, 1998). These adverse effects are often managed by leaching of the soils to remove excess salts (Hillel, 2000). In the case of sodium (Na^+) and chloride (Cl^-), which can be toxic to plants at high concentrations, salts composed of less harmful ions like calcium (Ca^{2+}) and

sulfate ($SO4^{2-}$) (e.g. gypsum) are applied to the soil surface and leached into the soil as an effective management strategy (Hillel, 2000; Keren and O'Connor, 1982; Keren and Shainberg, 1981). An exception to the direct effects salts have on the physical state of the soil matrix is in the presence of smectitic, i.e. shrink-swell, soils. Although many soils contain cations between clay platelets, smectitic soils can accept cations with large hydration spheres, causing the soils to swell when wet, thus reducing porosity and water infiltration (McNeal 1968; McNeal *et al*., 1966). The magnitude to which soil infiltration rates are affected by this process depends largely on the mixture of 1:1 and 2:1 clays in a particular region and the type and concentration of salts (Mamedov *et al*., 2001; Quirk, 1994; Oster, 1994; Shainberg and Letey, 1984; Dane and Klute, 1977).

The primary factor associating salinity with soil physical and hydrologic processes arises when salts are leached from the soil. It is during this process that clay dispersion is common when fields, traditionally irrigated with poor quality water (i.e. high salt concentrations), are irrigated with less saline water. This causes interlayer cations binding clay platelets together to diffuse into solution, dispersing the platelets, and thus clogging soil pores and disrupting the structural stability of the soil (Dane and Klute, 1977; Shainberg and Letey, 1984). These problems often cause a reduction in the hydraulic conductivity and drainage of the soils (Levy *et al*., 2005). This disruption can lead to further problems related to salt buildup such as water seepage and salt crusting. In the lower Arkansas River Valley, what soil hydrological data there is comes from work done by Burkhalter and Gates (2005), Gillham (2004), and National Resources Conservation Service soil survey data for surface soils (http://websoilsurvey.nrcs.usda.gov). However, the majority of research in the valley has

focused on surveying and mapping soil salinity along with depth to water table (Houk *et al*., 2006; Gates *et al*., 2002). Research in the lower Arkansas River Valley has up to now, been the basis for field and basin scale salinity and groundwater modeling associated with Colorado Water Resources Research Institute projects and is aimed at more effective irrigation management. What is now required, is a detailed characterization of soil physical and hydrologic properties.

Research Objectives

The goal of this research project is to examine the effects of salt concentration and composition on the hydraulic conductivity and water content of a small cluster of agricultural soils in the lower Arkansas River Valley to better parameterize hydrologic models and aid management decisions for the region.

The objectives of this project are 1) To characterize the hydrologic parameters of a representative soil type along an in-field salinity gradient using direct, lab based measurements of K(h) and moisture retention, $\theta(h)$, and employing inverse hydrologic modeling techniques; 2) To determine the effects of variable salt concentrations and compositions on K(h) and $\theta(h)$ of soils in lab based experiments. A decline in K(h) and increase in $\theta(h)$ is expected with decreasing EC and increasing SAR (Dane and Klute, 1977). In addition, it is expected that the changes observed due to reduction of EC are not reversible in the short term. In contrast to changes in EC, changes in K(h) and $\theta(h)$ associated with an increase in SAR are expected to be reversible; 3) To examine *in situ* K(h) changes with variable salt concentrations. Specifically, to determine whether surface soils contain sufficient salt concentrations to prevent sealing with large rain

events or irrigation water with low TDS. Surveys of the soils in the Arkansas River Basin suggest high concentrations of gypsum, which may buffer any changes in solution chemistry under normal agronomic operations. However, it is expected that typical agronomic soils will develop some degree of surface sealing due to application of irrigation water with low ion concentrations; 4) To express change in hydraulic conductivity as a function of both changing EC or SAR and θ. These functions will be compared to current models considering solution chemistry effects on $K(\theta)$. Several studies consider solution chemistry effects on $\theta(h)$ (Russo and Bresler, 1976; Wesseling and Oster, 1973), but focus more on changes in K with changing chemistry as opposed to changes in K as a function of both θ and changing chemistry. Other models exist but only consider solution chemistry effects on saturated hydraulic conductivity, K_{sat}, (e.g. Šimůnek *et al*., 2009). A case will be made for the need to consider solution chemistry at $K(\theta) < K_{sat}$.

METHODS

Site Characterization

Site Description

The region encompassing the Colorado Arkansas River Basin is classified as semi arid, receiving 350 to 400 mm of annual precipitation. Mean annual temperature is 11 to 13 degrees Celsius with 150 to 170 frost free days. The Colorado Arkansas River Basin is home to approximately 900,000 people (CSWSI, 2005) and ranges from central Colorado near Leadville to the southeast boarder with Kansas. The Colorado Arkansas River Basin accounts for 15 percent of the total water diversion in Colorado and provides water to over 405,000 acres of irrigated land, making it Colorado's second largest agricultural center (CSWSI, 2005). Primary crops for the lower basin include alfalfa (*Medicago sativa* L.), corn (*Zea mays* L.), wheat (*Triticum aestivum* L.), onion (*Allium cepa* L.), and cantaloupe (*Cucumis melo* L. subsp. *melo* var. *cantalupensis* Naudin) (Eldeiry and Garcia, 2008). The lower Arkansas River Basin is divided into two regions: the upper section from Pueblo, Colorado to John Martin Reservoir and the lower section spanning from John Martin Reservoir to the Kansas state line (Figure 2). Both regions are greatly impacted by high salinity and high water tables.

Two adjacent fields in the lower section of the Arkansas River Basin (Prowers County), located approximately 10 miles east of the town of Lamar, were selected for this

study (731839 m E 4218762 m N; elevation 1065 m). Both fields were cultivated with alfalfa (*Medicago sativa* L.) and furrow irrigated. Both fields were under no-till management during and 2 years prior to sample collection and measurement. Fields were selected based on their high salinity, high water tables, and similar crop and management regimes. Soils at the two fields are classified as fine-loamy, mixed, superactive, calcareous, mesic Aquic Ustifluvents and are defined as saline loams to clay loams underlined by calcareous sandy alluvium. Soils in this series often contain 2 percent gypsum, with an average EC of 10 dS m^{-1} and a SAR between 3 to 5.

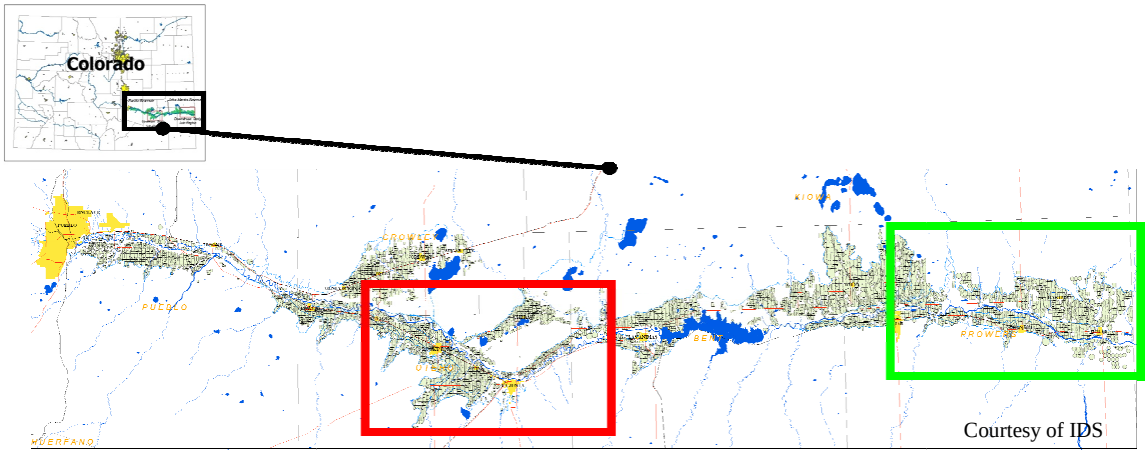

Figure 2: Map of the lower Colorado Arkansas River Valley and regions of interest.

Field Sampling

Field 1 was used to collect samples for laboratory analysis. Samples were collected at 3 locations along a salinity gradient spanning the width of the field (Figure 3); the average EC at each sampling region was 3.73, 10.0, and 19.87 dS m^{-1} respectively. Each sampling area consists of a 2 m^2 plot visually uniform in soil surface topography and plant cover. For field 1, six intact soil cores measuring 4 cm tall by 7 cm in diameter were collected from each plot for laboratory analysis.

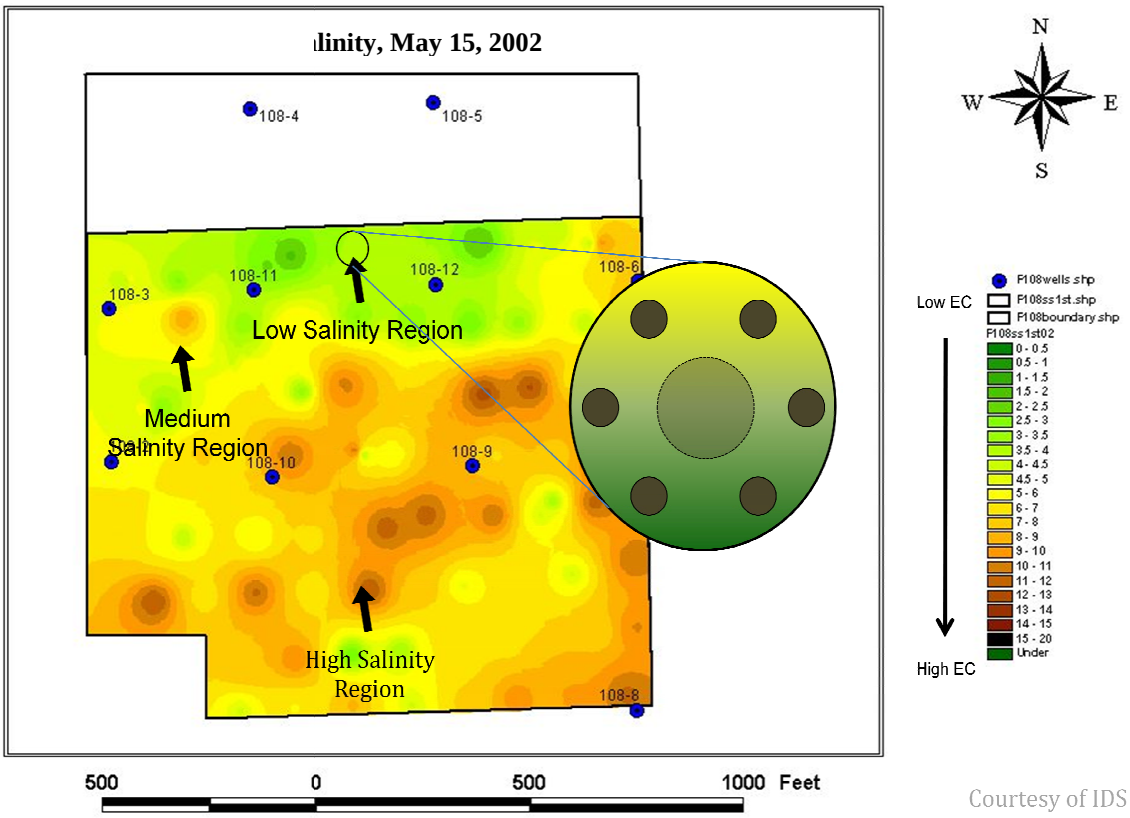

Courtesy of IDS

Figure 3: Map of field 1 soil salinity and selected sampling regions. Salinity map produced using an EM 38 salinity probe calibrated to soil paste extract EC.

The upper 2 cm of soil and any plant material were gently removed in a sod-like fashion prior to sampling to provide more consolidated and homogenous soil cores (Figure 4). The use of intact soil cores vs. repacked soil samples is crucial to accurately characterize field conditions and allows for more precise measurement of the K(h) and θ(h) functions. Repacked soil columns, which have traditionally been used to measure K(h) and θ(h) functions in the lab undergo significant consolidation during analysis resulting in changes in K(h) and θ(h) that do not reflect the physical and chemical changes undergone in the field. Four smaller cores (4 cm tall by 3.5 cm in diameter)

were taken within each plot to determine EC, bulk density, porosity, and soil moisture. Finally, bulk soil samples were collected from 2 to 6 cm in each plot for chemical, textural, and mineralogical analysis.

Figure 4: Photograph of intact soil cores sampled for laboratory analysis. The upper 2 cm of soil along with any plants have been carefully removed to produce soil cores that are more intact and homogenous.

Field 2 was selected after analysis of laboratory samples and was used to measure *in situ* soil hydraulic properties and the potential of irrigation water or rain events to cause surface sealing. A second field had to be used as opposed to the original field because the local grower had plowed field 1; the adjacent field however remained fallow. In field 2, low and high salinity regions were identified and approximately matched to EC and surface characteristics of surrogate plots in field 1. Wilcoxon rank-sum statistical comparison of soil hydraulic parameters between field 1 and 2 showed they were similar, with no differences between the parameters except for a weak difference in K_{sat}, $W_{(n1 = 6, n2 = 2)} = 12$, $p = 0.07143$. Two 1 m^2 plots were established for analysis of water quality effects and gypsum amendments on infiltration rates at each high and low EC regions. In

addition, a series of 4 transects, 8 m long were established in the high EC region adjacent to the two 1 m^2 plots for detailed analysis of *in situ* soil hydraulic conductivity. Soil sampling for field 2 consisted of three intact soil cores measuring 4 cm tall by 7 cm in diameter collected adjacent to the high EC plots only. Four smaller cores (4 cm tall by 3.5 cm in diameter) were taken immediately adjacent to both the high and low EC plots to determine EC, bulk density, porosity, and soil moisture.

Soil Characterization

Field Infiltration

Preliminary lab work indicated that soils in the Arkansas River Valley are well buffered against changes in EC due to high concentrations of naturally occurring salts. High salt concentrations throughout the soil profile makes reduction in the infiltration capacity of the soil due to improved water quality unlikely on a bulk soil basis. However, concerns were raised about surface sealing due to leaching of salts out of the top 1 to 2 cm of soil. Therefore, *in situ* infiltration tests were conducted to determine the potential for surface sealing due to leaching.

Two sets of infiltration tests were conducted. The first test compared the relative infiltration rate of soils between high and low salinity regions. The relative infiltration tests conducted in field 2 were run on duplicate plots in both the high and low EC regions.

Gypsum pellets were applied to the surface of one plot per region at a concentration of 3.8 Mg ha^{-1} to determine whether surface sealing, if a problem, could be prevented. All plots had 15 rings (H=4cm, Diameter=5.65cm) inserted to a depth of 1 cm in a semi-random distribution within the 1 m^2 area (Figure 5).

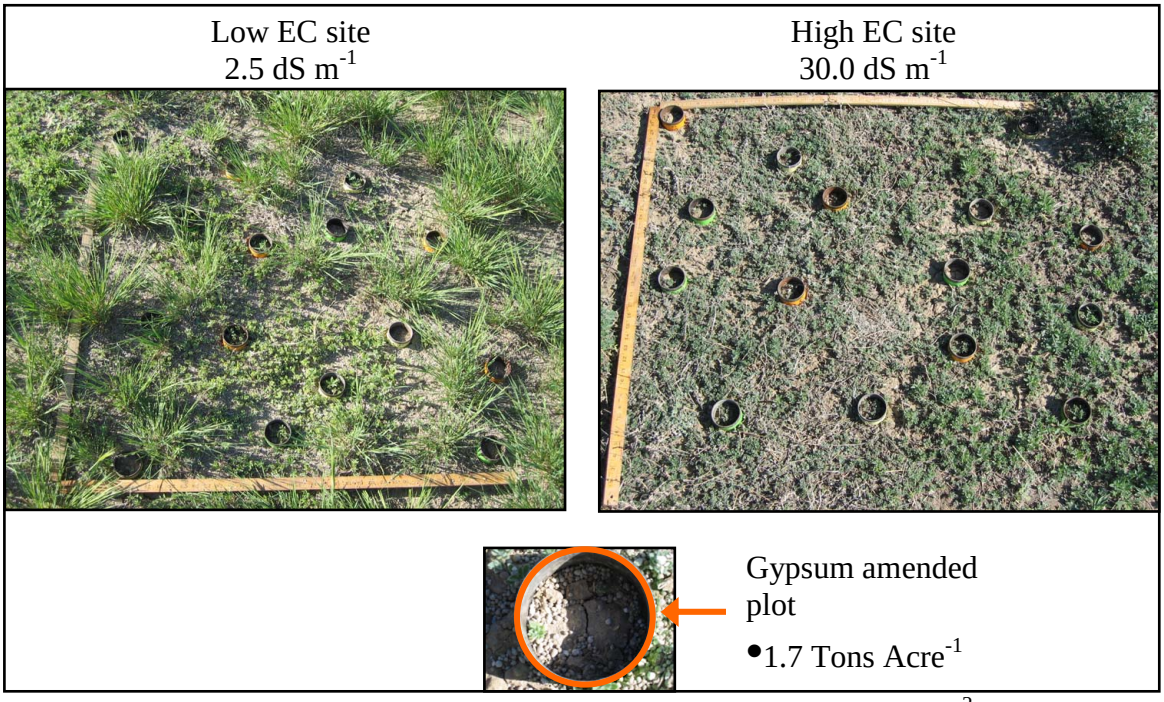

Figure 5: Photographs of the relative infiltration plots in field 2. Two 1 m^2 plots established for analysis of water quality effects and gypsum amendments on infiltration rates at each high and low salinity regions (salinity reported as the pore-water EC at the water content of the soil during the infiltration experiment).

The 15 rings were placed into 3 sets of 5, each set used to apply a different irrigation water quality (EC of 0.25, 2.0, or 4.0 dS m^{-1}; SAR = 5.0). Each irrigation water quality solution was gently poured into 5 of the 15 cores sequentially and the time to infiltrate recorded. Care was taken to place soil cores far enough away from each other to prevent saturation of the flow path of surrounding cores as this would influence infiltration time.

The second test measured the saturated hydraulic conductivity, K_{sat}, at the low salinity region of field 2 using a modified single ring, dual head infiltrometer method (Reynolds and Elrick, 1990; Youngs, 1995) and compared rates across a gradient of

irrigation water qualities. The K_{sat} was measured at 4 different water qualities (EC of 0.25, 0.5, 1.0, and 2.0 dS m^{-1}; SAR = 5.0). Thirty-two measurements were taken (n = 8), with each measurement taken 1 meter apart to avoid interference from adjacent measurements and to encompass edaphic factors of soil heterogeneity (Figure 6).

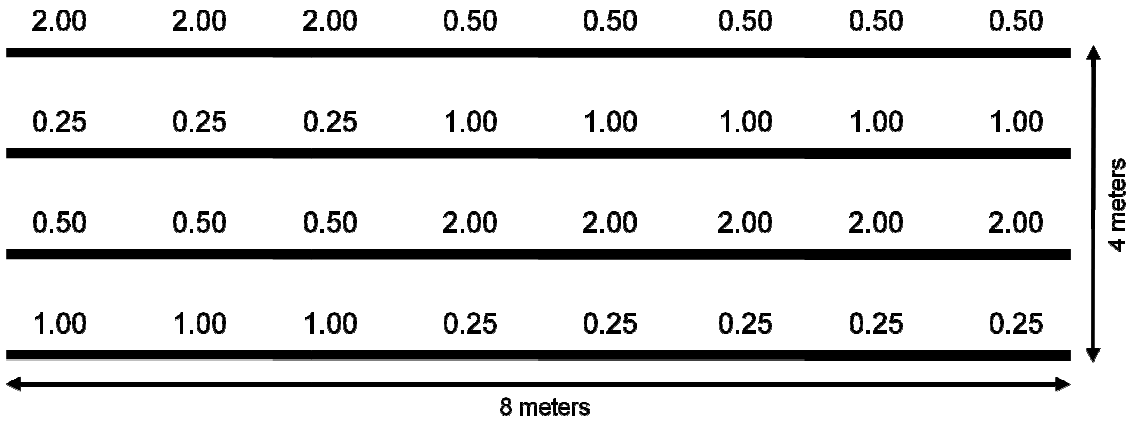

Figure 6: Saturated hydraulic conductivity sampling layout in field 2. Numbers represent the EC of the infiltration treatment solution in dS m^{-1}.

Each set of K_{sat} measurements at each water quality level were randomly distributed along each 8-meter transect. The K_{sat} was calculated from equation 1 (Reynolds and Elrick, 1990),

$$K_{sat} = \frac{G}{r} \times \frac{\Delta Q}{\Delta H} \qquad \text{[Eq. 1]}$$

where K_{sat} is saturated hydraulic conductivity (L T^{-1}), r is the radius of the ring (L), and ΔQ is the difference between the quasi-steady state flow rates for Q_1 and Q_2 (L^3 T^{-1}), which correspond to the flow rates for the two sequential ponding depths (H_1 and H_2). The ΔH is the height difference between the two ponding depths mentioned above, and G is an empirically derived shaping factor determined by Reynolds and Elrick (1990) and calculated from equation 2,

$$G = 0.316 \times \left(\frac{d}{r} \right) + 0.184 \qquad \text{[Eq. 2]}$$

where G is the shaping factor, d is the depth of ring insertion (L), r is the ring radius (L), and 0.316 and 0.184 are experimentally determined correction factors for lateral water flow in the soil matrix.

Soil Chemical Analysis

The initial chemical analysis of the soil samples from each of the 3 salinity regions in field 1 and the low salinity region in field 2 were done by the Soil, Water, and Plant Testing Lab at Colorado State University. The bulk soil taken from each region was sieved to 2 mm, homogenized, and split into three subsamples for the analysis of pH, EC, SAR, cation exchange capacity (CEC), and total/inorganic carbon content. Soil pH was determined as suggested by Thomas (1996), by adding 10 mL of deionized (DI) water to 10 g air dry soil. The soil slurry was shaken vigorously for 1 minute and then allowed to sit for 10 minutes before electrometric analysis.

Electrical conductivity was determined using the soil water extraction method (Rhoades, 1996). The EC was determined by adding 100 mL DI water to 100 g field moist soil (average 20 percent gravimetric water content) and shaking for 1 hour. Soil slurries were then filtered using Whatman 4 filters and their conductance measured using a Yellow Springs Incorporated (Yellow Springs, Ohio, USA) YSI-35 conductivity meter. Extract temperature was recorded and electrical conductivity measurements were standardized to 25 degrees Celsius using equation 3 (Rhoades, 1996),

$$EC_{25} = EC_T \times \left[1 + \alpha \left(25 - T \right) \right] \qquad \text{[Eq. 3]}$$

where EC_{25} is the temperature corrected electrical conductivity standardized to 25 degrees Celsius, and EC_T is the electrical conductivity of the soil extract and temperature T. The temperature coefficient of α is dependent on the specific ion chemistry of a solution and the specific geometry of the EC probe being used. Equation 4 shows how α was calculated,

$$\alpha = \frac{EC_T - EC_{25}}{EC_{25}\Delta T} \qquad \text{[Eq. 4]}$$

where the terms are as defined above. The soil solution and EC probe specific temperature coefficient of 0.038838 was determined using linear regression and the method outlined by Yellow Springs Incorporated (Yellow Springs, Ohio, USA) YSI-35 conductivity meter manual (1989).

In order to determine the EC of soil under field condition which is more relevant to crop productivity, EC values were multiplied by a dilution factor accounting for the soil extraction volume and field moist soil. The dilution factor calculation is:

$$EC_s = EC_e \times \left[\left(\frac{V \times \rho_w}{M_m \times \theta_m} \right) + 1 \right] \qquad \text{[Eq. 5]}$$

where EC_s is the electrical conductivity of the soil under native soil conditions (dS m^{-1}), EC_e is the extract electrical conductivity equal to the reading by the probe of the soil water extracts (dS m^{-1}), V is the volume of water added to the soil (L^3), M_m is the mass of field moist soil extracted, θ_m is the gravimetric water content of the soil (g^3 g^{-3}), and ρ_w is the density of water (g cm^{-3}).

Sodium adsorption ratio (SAR) and major cations were determined using the the AB-DTPA extraction method (Soltanpour and Schwab, 1977). Extraction solutions were refrigerated at 4 degrees Celsius until analysis at the Soil, Water, and Plant Testing

Laboratory. Major cations were determined using a Thermo Solutions IRIS Advantage High Resolution axial Inductively Coupled Plasma instrument (Thermo Scientific, Madison, WI, USA). The SAR was calculated using equation 6 (Sumner and Miller, 1996):

$$SAR = \frac{\left[Na^{+}\right]}{\left(\frac{\left[Ca^{2+}\right]+\left[Mg^{2+}\right]}{2}\right)^{\frac{1}{2}}} \qquad \text{[Eq. 6]}$$

where brackets denote the concentration of a particular cation in $mmol_c\ L^{-1}$.

The CEC of the soils was determined using the Ammonium Acetate (pH 7) method for basic soils outlined by Sumner and Miller (1996). Samples were analyzed on a Bran-Luebbe (now Seal Analytical) TRAACS 800 autoanalyzer (Mequon, WI).

Total soil carbon and nitrogen content was analyzed using a Leco CHN 600 (Nelson and Sommers, 1996). Ten subsamples from each plot were taken from the bulk soil for analysis. Soil inorganic carbon was determined on the same ten subsamples and analyzed using the modified pressure calcimeter method (Sherrod *et al.*, 2002). Organic carbon of the soils was determined by calculating the difference between total and inorganic carbon content.

Soil Physical Analysis

A continuous flow cell and procedure designed by Butters and Duchateau (2002) that operates across the tensiometry range (approximately field saturation to 0.007 MPa) was used on intact soil cores sampled from each salinity region to characterize the K(h) and θ(h) functions under field conditions (Figure 7). This approach combines direct and

indirect analysis of outflow data to estimate the K(h) and θ(h) functions (see modeling methods section below).

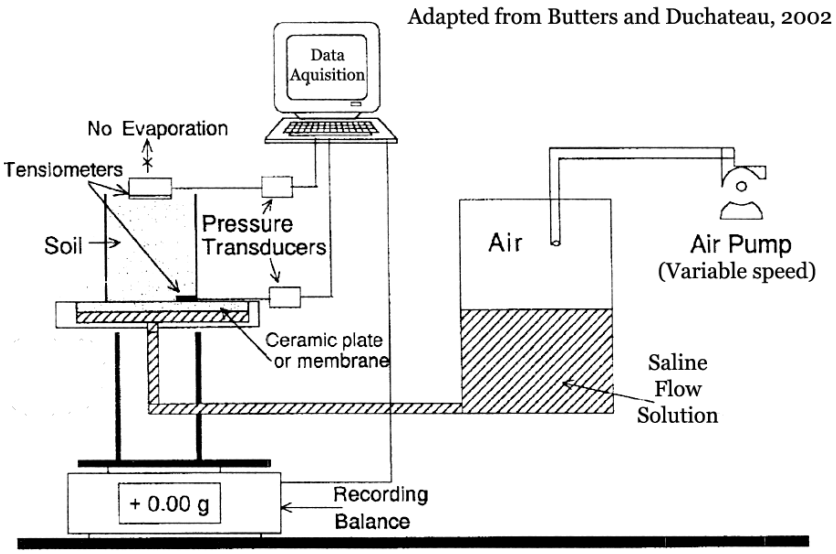

Figure 7: Diagram of continuous flow cell for K(h) and θ(h) determination.

The average EC_s value for each salinity region in both fields was used as the flow solution EC to determine K(h) and θ(h) under native conditions. It was assumed that the EC_s for each region sufficiently matched that of the intact soil cores and therefore would prevent any clay dispersion or shrink-swell behavior. Following the initial characterization of the intact soil cores, the pore water EC and/or SAR of 2 cores from each salinity region was changed in a stepwise fashion to determine how changes in EC and/or SAR affected the soil hydraulic properties. The EC of the first core from each salinity region was reduced while holding SAR constant at 5 (the average SAR of soils in field 1) to examine how changes in EC impact soil hydraulic properties. The second core from each salinity region was used to examine the affects of changing SAR on soil hydraulic properties with EC reduced and held constant at a threshold value of

0.65 dS m^{-1}, estimated from the work done by Ayers and Westcot (1985). For each core at each EC or SAR level, the soil core was run ≥3 times on the continuous flow system. At the conclusion of the EC or SAR sequence, the soil core was removed from the flow cell and its 1.5 MPa water content value measured by pressure plate extraction (Dane and Hopmans, 2002). For each soil core and for each EC or SAR treatment, average van Genuchten parameters were generated using Hydrus 1D in a similar inverse technique.

The flow solution for each run was composed of 0.05 g L-1 thymol as a microbial inhibitor (Klute, 1986) for prolonged measurements. The low concentration thymol solution had negligible impacts on soil water viscosity and surface tension and resulting measurements of K(h) and θ(h) are representative of in situ soil water behavior. In addition to thymol solution, cores that were not being actively run on the continuous flow system were sealed in plastic wrap and stored at 4 degrees Celsius.

Supplemental Physical Characteristics

In addition to the soil cores retrieved for analysis of hydraulic properties, samples were also taken for destructive analysis. Soil bulk density and gravimetric water content, which were determined using the average moist and dry soil weights of four smaller cores (4 cm tall by 3.5 cm in diameter) collected from each plot. Soil texture was determined using the standard hydrometer method (Gee and Or, 2002). Because inorganic carbon analysis indicated carbonate concentrations greater than 1 percent, carbonates were removed from the soils prior to texture analysis using the sodium acetate (pH 5) method (Gee and Or, 2002) followed by a DI water rinse to remove residual sodium acetate and gypsum. Soil organic matter (OM) was also removed prior to texture analysis as

suggested by Gee and Or (2002) using hydrogen peroxide method for soils with OM contents greater than 5 percent.

Clay Mineralogical Analysis

Clay mineralogy is important in understanding how soils will react to changes in soil solution composition. Depending on the type of clays in a particular region (e.g. 1:1, 2:1, or 2:1:1), an increase or decrease in soluble salts can cause severe changes in soil hydraulic properties. Due to the impact certain clays have on soil pore water, the clay mineralogy of the four plots in field 1 was analyzed to explain the type and extent of change in soil hydraulic properties with changes in pore water solution chemistry. Sample preparation and analysis followed the method outlined by C.H. Green (2001) as well as D.M. Moore and R.C. Reynolds, Jr. (1997). Field soil clays were determined using powder x-ray diffraction (XRD). With this method, samples are finely spread over small glass slides, which are then placed between an x-ray beam and x-ray detector. With the addition of another analytical method related to XRD, the Rietveld refinement method, structural information can be determined from the x-ray signals for finely crystalline and poorly structured minerals such as clays. X-ray diffraction patterns were compared to standards to determine the qualitative clay mineral content of the soils. The clay mineralogy data collected is meant to be a guide to better understand the physical and chemical processes that observed and is not meant to quantify individual clay fractions or to characterize the clays in the Arkansas River Valley as a whole.

Data Analysis

Statistical Analysis

All statistical analyses were conducted using R 2.12.1 (2010) and SigmaPlot 10 statistical software packages. Pair-wise statistical comparisons between salinity region properties or treatment effects on the mean of K(h) and θ(h) function parameters for each soil salinity region were analyzed using 1-way analysis of variance and covariance (ANOVA) where appropriate. All data with non-normal distributions (e.g. soil hydraulic conductivity) were transformed prior to parametric analyses and tested for equal variance to satisfy linear model assumptions. Normality was tested using the Shapiro Wilk test. Where ANOVA assumptions were not met, non-parametric analyses using the Kruskal-Wallis rank sum test or Wilcoxon rank sum test were employed. Correlation analysis including Pearson's test as well as linear regression analysis were also performed where applicable.

Direct Estimation of Soil Hydraulic Properties

As mentioned above, direct and indirect methods for estimation of the K(h) and θ(h) functions were employed. In the continuous flow method of Butters and DuChateau (2002), a soil core of height L and cross section A is drained or wetted while monitoring its weight and the water pressure at the upper and lower boundaries. By direct determination, θ(h) was calculated from the weight of the soil core and the average water pressure. The K(h) function was calculated using the discharge from the flow cell and

the hydraulic gradient between the top and bottom boundaries of the soil core measured using tensiometry (Eq. 7 and 8),

$$q(0,t) = \frac{\Delta wt}{\rho_w A \Delta t} \quad \text{and} \quad q(L,t) = 0 \qquad \text{[Eq. 7]}$$

$$\frac{\Delta H}{\Delta Z} = \frac{h(L,t) + L - h(0,t)}{L} \qquad \text{[Eq. 8]}$$

where q(0,t) is equal to the soil water flux across the lower boundary at time t, q(L,t) is the soil water flux across the upper boundary and is equal to zero (i.e. no evaporation), Δwt is the discharge of soil water, ρ_w is the density of water, and Δt is the change in time over the drainage event (usually a small time change on the order of 1 minute per measurement interval). The ΔH term is the average change in the total hydraulic head between the soil boundaries, ΔZ is the height of the soil core over which the hydraulic gradient is induced, and h(0,t) and h(L,t) are the pressure heads at time t determined by tenisometry at the lower and upper boundary layers.

The results from equations 7 and 8 were then used in equation 9, a derivation of Darcy's Law, to estimate K(h),

$$K = -\frac{q(L/2,t)}{(\Delta H/\Delta Z)} \qquad \text{[Eq. 9]}$$

where the q(L/2,t) notation is the estimated flux at L=1/2, calculated as the average flux between L and 0.

The accuracy of the direct determination of K(h) and θ(h) over the tensiometry pressure range is dependent on the satisfaction of the assumption that ΔH/ΔZ is linear for the calculation of q(L/2,t) and that |h(L,t) – h(0,t)| is not large. These conditions are most closely achieved using short samples, typically less than about 5 cm and small rates of change in the lower boundary pressure, typically less than about 0.75 cm min^{-1}. Cores

taller than this cannot maintain a linear $\Delta H/\Delta Z$ and will overestimate K (Butters and Duchateau, 2002). Recall that the intact soil cores collected for this project equaled 5 cm in height and were later reduced to approximately 4.5 cm while conditioning the soil surface for analysis. Also important is the texture or pore size distribution (PSD) of the soil core. Soils with gradual release of soil water (i.e. finer texture soils) will maintain more linear pressure head gradients.

In the operation of the flow cell method, it is common to measure the θ_s of the soil core independent of the flow cell assemblage. The θ_s values for soils in the EC and SAR treatment series were not determined this way in an effort to minimize physical disturbance of the cores. Instead, 2 extra intact soil cores from the medium EC site were treated and their θ_s determined at each step of the EC or SAR series. The change in θ_s observed on the extra soil cores was fit to a linear trendline and applied to the θ_s values for the EC and SAR series at each salinity region.

Because measurement of θ at 1.5 MPa causes changes in K not related to soil solution chemistry, the $\theta_{1.5MPa}$ values for all EC and SAR treatments were measured only once at the conclusion of the EC or SAR series treatments. It was assumed that this $\theta_{1.5MPa}$ value was the end value resulting from the series treatments. The average native $\theta_{1.5MPa}$ value for the soil cores not used for the EC or SAR series was used for the native $\theta_{1.5MPa}$ value for each treatment series specific to salinity region. Again, a linear change in $\theta_{1.5MPa}$ for the EC or SAR series was assumed and used for inverse analysis.

Inverse Analysis of Soil Hydraulic Properties

The estimated K_s, θ_s, and $\theta_{1.5MPa}$ were combined with q(0,t), h(0,t), and h(L,t) data to back-out K(h) and θ(h) functions for each core using inverse analysis. Inverse analysis was performed using the Hydrus-1D (one-dimensional) model for movement of water in variably-saturated media (Šimůnek *et al*., 2009). Hydrus-1D solves Richards' water flow equation using an iterative weighted least squares numerical approach. The van Genuchten (1980) forms of the K(h) and θ(h) were assumed,

$$S_e = \frac{\theta - \theta_r}{\theta_s - \theta_r} = \frac{1}{\left(1 + |\alpha h|^n\right)^{(1-1/n)}} \qquad \text{[Eq. 10]}$$

$$K(h) = K_s S_e^{\lambda} \left[1 - \left(1 - S_e^{1/m}\right)^m\right]^2 \qquad \text{[Eq. 11]}$$

where S_e is the effective saturation, θ_s is the saturated water content of the soil, θ_r is the residual water content of the soil approximated as $\theta_{1.5MPa}$, h is the pressure head at a given θ, and α, ℓ, and m (m = 1-1/n) are fitting parameters. All other parameters are as define above.

The power of inverse analysis is its ability to accurately determine parameters of a characteristic function that would otherwise be difficult or impossible to measure directly. By determining the flow parameters of the van Genuchten function using inverse analysis, the characteristic K(h) and θ(h) functions were determined, extrapolating from near saturation to $\theta_{1.5MPa}$ for soils specific to fields 1 and 2 in the lower Arkansas River Basin. In addition, the characteristic changes in water flow parameters for the *in situ* soil salinity gradient were determined as were the mechanistic changes in flow parameters associated with EC and SAR treatments.

Both the direct and inverse analysis of the flow cell experiment are affected by noise in the experimental data. The noise associated with measuring Δwt is dependent on the quality and significant digits associated with the scale used to measure Δwt. The noise associated with measuring $\Delta H/\Delta Z$ is dependent on the quality of the pressure transducers used and the care given to aligning the transducers with the upper and lower boundary layers of the soil core. The accuracy in determining the $\Delta wt = \Delta\theta$ was equal to that in Butters and Duchateau (2002) and equaled 0.0002 $mm^3\ mm^{-3}$. The transducers used were Validyne model DP15-42 (Validyne Engineering, Northridge, CA) with an accuracy of 0.00035MPa.

RESULTS AND DISCUSSION

Soil Chemical and Physical Properties

Soil chemical properties between salinity regions for field 1 (Table 1) are significantly different for all indices except total carbon, $F_{(2, 6)} = 2.166$, $p = 0.17$, but all are within an expected range for these soils (Burkhalter and Gates, 2005). Soil concentrations of gypsum ($CaSO_4$) are different (means = 0.21, 2.20, and 14.91, %CV = 2.37, 3.77, 6.37 for low, medium, and high salinity regions respectively) between salinity regions, $F_{(2, 6)} = 1260.0$, $p < 0.001$, and are correlated with the difference in EC between regions (Pearson's $t_{(10)} = 10.6985$, $p < 0.001$). Linear regression of percent gypsum and salinity region EC also show a high degree of correlation (r = +0.959, $p < 0.001$, n = 3). Indeed, dissolution of gypsum in the saturated paste extracted contributes to the EC_e, so the correlation between gypsum and soil EC is made even stronger. The EC_e presented here likely does not represent field conditions of the salinity levels "experienced" by plants due to the dissolution of gypsum. Soil calcite ($CaCO_3$) concentrations tend to be higher with lower EC but no significant correlation is observed (Pearson's $t_{(10)} = -0.9793$, $p = 0.3505$). Linear regression of calcite and salinity region EC show a significant negative correlation (r = -0.6636, $p = 0.0513$, n = 3) which may reflect the high concentration of $SO4^{2-}$ ions in solution and competition for Ca^{2+}. Concentrations of phosphorous are positively correlated with percent gypsum using both Pearson's test,

Table 1: Soil nutrient properties for field 1 salinity regions.

Field 1 salinity region	CaSO4		TC		TIC		SOM		TN		NO3-N		PO4-P	
	---------- (%) ----------										---------- (ug N g soil^{-1}) ----------			
	AM	%CV	AM	%CV	AM	%CV	AM	%CV	AM	%CV	AM	%CV	AM	%CV
Low	0.02a	(2.37)	1.78a	(5.41)	0.84a	(1.22)	3.97a	(8.10)	0.10a	(8.02)	6.11a	(5.51)	0.78a	(43.30)
Medium	0.22b	(3.77)	1.85a	(1.40)	0.54b	(1.07)	6.93b	(8.69)	0.15b	(2.26)	11.59b	(11.15)	2.03b	(15.56)
High	1.49c	(6.37)	1.84a	(1.08)	0.60c	(1.92)	5.57c	(1.04)	0.14b	(7.56)	3.33c	(2.09)	4.29c	(5.84)

AM = Arithmetic mean
%CV = Percent coefficient of variance

(Pearson's $t_{(10)} = 5.0773$, $p < 0.001$) and linear regression ($r = +0.9612$, $p < 0.001$, $n = 3$), which may illustrate the abundance of Ca^{2+} in these soils since phosphorous at pH levels in field 1 is effectively removed from solution to form $Ca_2(PO_4)_2$, a highly insoluble mineral, largely unavailable to plants (Lajtha and Schlesinger, 1988).

Soil physical properties (Table 2) are overall consistent with expectations for a typical agricultural soil in this region (Gates *et al*., 2006; Wittler *et al*., 2006). Soil texture varies between the salinity regions, with percent sand, silt, and clay in the medium and high salinity regions approximately equivalent (medium = 27, 41, 32; high = 26, 46, 38) but the low salinity region contains considerably more sand than the other regions (low = 41, 32, 27). The cation exchange capacity (CEC) of the soils reflects the differences in texture (specifically silt) between low, medium, and high salinity regions (Pearson's $t_{(7)} = 3.9232$, $p = 0.005726$) and is significantly different between the low vs. medium and high salinity regions, $F_{(2, 6)} = 9.1252$, $p = 0.01515$. Mean CEC values in meq $100g^{-1}$ soil for the low, medium, and high salinity regions are 17.0, 21.60, 21.70 (%CV = 4.19, 3.70, 11.17). Soil textures were sampled and measured only once at each region and therefore no statistical analysis was performed. Bulk density (BD) for these soils actually increases with increasing percent silt ($r = +0.6562$, $p = 0.0549$, $n = 3$) along with increasing salinity. Typically, the coarser the soil texture, the higher the BD. The opposite trend observed here may be caused by edaphic factors at each salinity region controlling soil structure and drainage.

Table 2: Soil salinity and physical properties for field 1 salinity regions

Field 1 salinity region	Soil type	Sand	Silt	Clay	Bulk density		pH		EC		SAR		ESP		CEC	
		--- (% by weight) ---			(g cm-3)				(dS m^{-1})				(%)		(meq $100g^{-1}$)	
		AM	AM	AM	AM	%CV	AM	%CV	AM	%CV	AM	%CV	AM	%CV	AM	%CV
Low	Loam	41.20	32.17	26.63	1.32a	(3.64)	7.97a	(0.72)	3.73a	(13.22)	7.78a	(2.35)	57.21a	(0.26)	17.00a	(4.91)
Medium	Clay loam	26.99	41.36	31.65	1.39b	(8.50)	7.90a	(0.00)	10.00b	(2.14)	8.88b	(1.67)	42.38b	(2.97)	21.60b	(3.70)
High	Silt loam	26.43	45.65	27.92	1.45b	(0.00)	7.80b	(0.00)	19.87c	(2.26)	5.45c	(2.17)	21.05c	(1.98)	21.70b	(11.17)

AM = Arithmetic mean
%CV = Percent coefficient of variance

A full suite of chemical and physical analyses were not conducted for field 2. Table 3 shows the gravimetric water content at sampling time and EC of the soils for the low and high salinity regions for relative infiltration measurements and the low salinity region for K_{sat} measurements. However, intact soil cores were collected and analyzed using the continuous flow system to estimate the soil hydraulic properties; results are reported with field 1 soil hydraulic properties below.

Table 3: Soil electrical conductivity (EC) and soil gravimetric water content (GWC) for both low and high salinity regions measured for Relative infiltration and saturated hydraulic conductivity (K_{sat}) measurements.

Analysis	Sample ID	GWC $g\ g^{-1}$	EC $dS\ m^{-1}$
Rel Infilt.	High 1	0.05	14.53
	High 2	0.05	16.30
	High 3	0.11	25.68
	Low 1	0.08	2.51
	Low 2	0.06	4.52
	Low 3	0.06	8.28
K_{sat}	Low 1	0.11	2.69
	Low 2	0.12	2.74
	Low 3	0.10	2.68

Clay mineralogy for the medium and high salinity regions was very similar based of XRD patterns (Figure 8) using suspended sediment without the sand fraction. The dominant mineral types were quartz, K-feldspar, and illite. The dominance of the phylosilicate illite explains the low potential for swelling in these soils.

Soils were treated to remove SOM, carbonates, and gypsum prior to XRD analysis so the diffraction patterns do not include the large percentage of gypsum present in these soils.

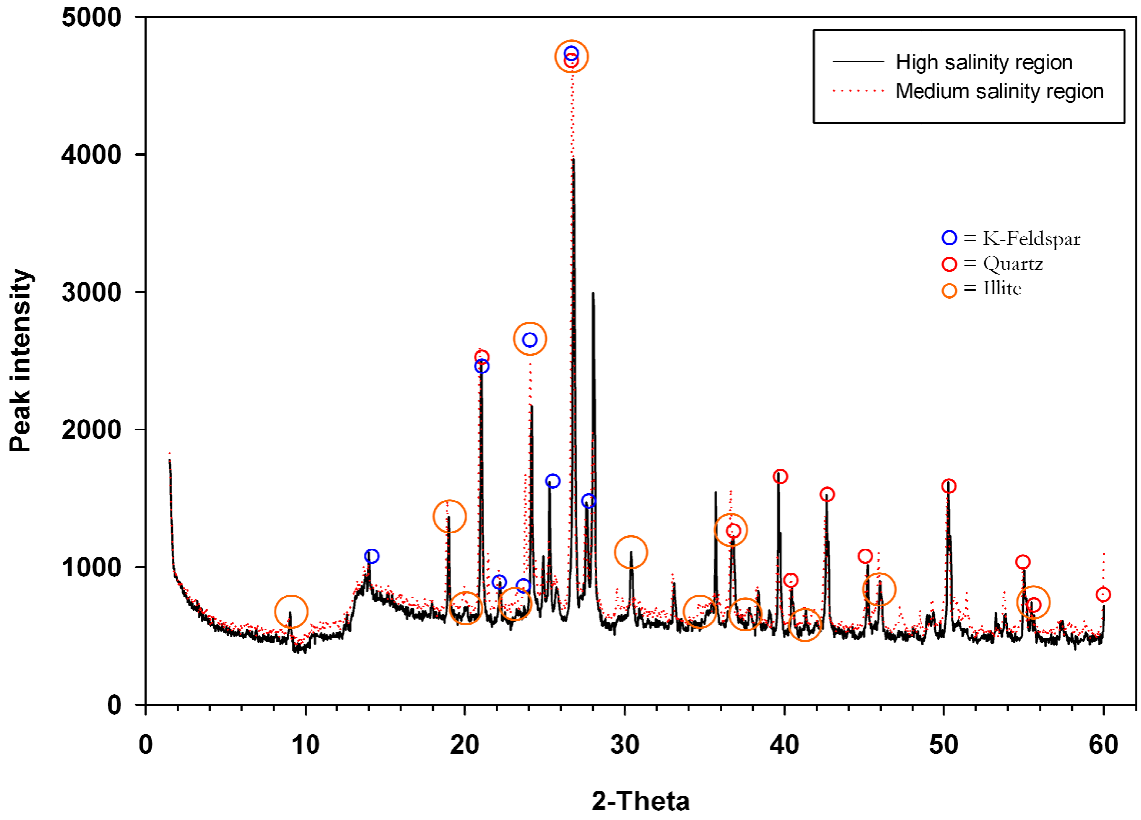

Figure 8: Mineralogical analysis using XRD for the medium and high salinity regions.

Analysis of XRD patterns using <120 micron sieved fraction showed a small amount of the phylosilicate corrensite at the high salinity region (Figure 9). Corrensite is a 2:1 layer clay mineral that is susceptible to swelling. Without quantitative methods it is difficult to determine if one salinity region had more of one mineral than the other but does appear that the percentage of 2:1 layer clays increased at the high salinity region vs. the low, although the overall percentage appeared low. It's likely this is simply representative of the smaller overall clay fraction at the low salinity region.

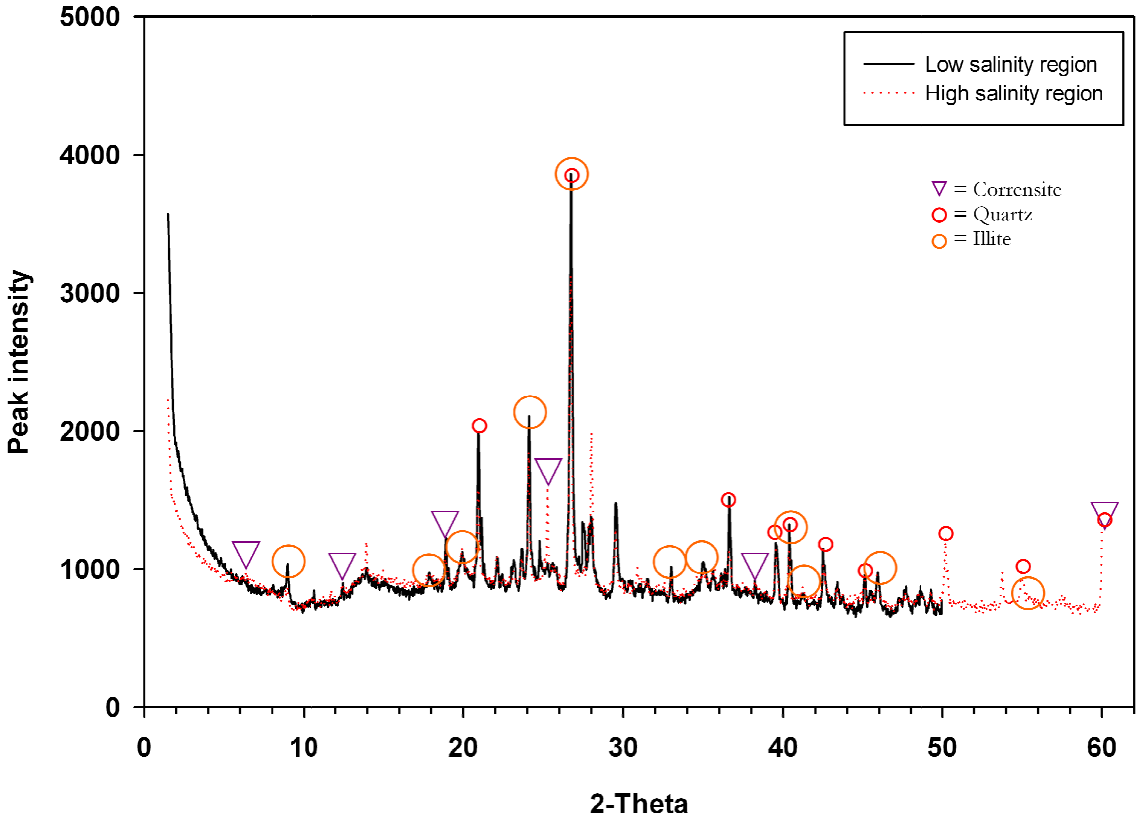

Figure 9: Mineralogical analysis using XRD for the low and high salinity regions.

Field Infiltration

The results of leaching experiments on intact soil columns, in addition to the chemical analysis reported above, indicate high adsorbed and precipitated salt concentrations in field 1 and 2 soils and therefore a high buffering capacity against moderate changes in pore-water chemistry. Results of the leaching experiments found 60 to over 200 pore volumes of water are required (depending on the salinity region) to change the pore water EC from its native condition to 0.25 dS m^{-1} (Figure 10).

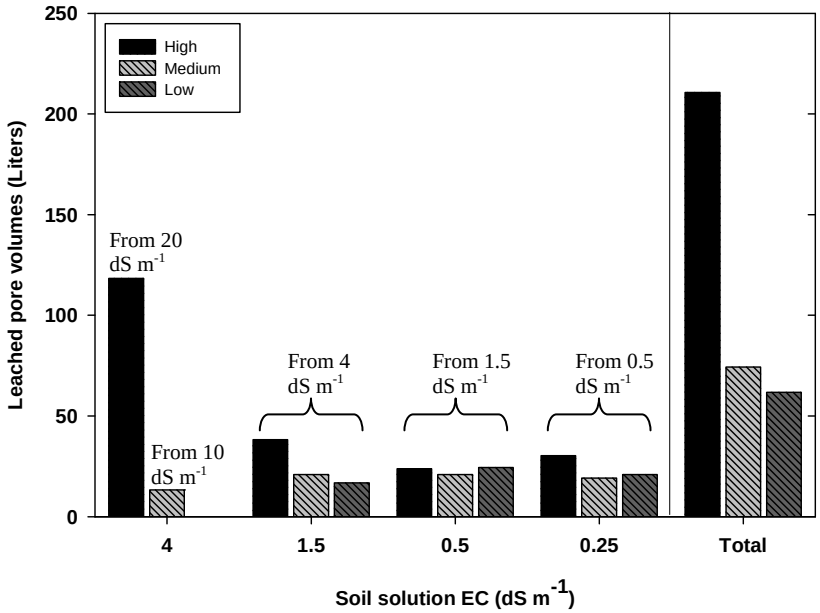

Figure 10: Total pore volumes leached for laboratory salinity treatments. High salinity region EC change was 19 to 0.25 dS m^{-1}, medium salinity region EC changed was 10 to 0.25 dS m^{-1}, and low salinity region EC change was approximately 4 to 0.25 dS m^{-1}.

Despite this resistance to EC reduction, the *in situ* infiltration tests indicate the soil surface is moderately susceptible to sealing with large rain events or improved irrigation water quality. Grouping of infiltration rates for all relative infiltration plots in field 2 between the low and high salinity regions shows a significant treatment effect when combining results from both salinity regions (Figure 11), $F_{(2, 57)} = 0.003279$, $p < 0.01$, between the 0.25dS m^{-1} irrigation water treatment (mean = 5.99 minutes, %CV = 7.18) and the 2.0 and 4.0 dS m^{-1} treatments (mean = 5.57, 5.65 minutes, %CV = 6.65, 6.90 respectively). Tests between salinity regions shows no inherent difference in infiltrations rates between salinity regions that may bias infiltration rates, $F_{(1, 58)} = 0.0219$, $p = 0.883$.

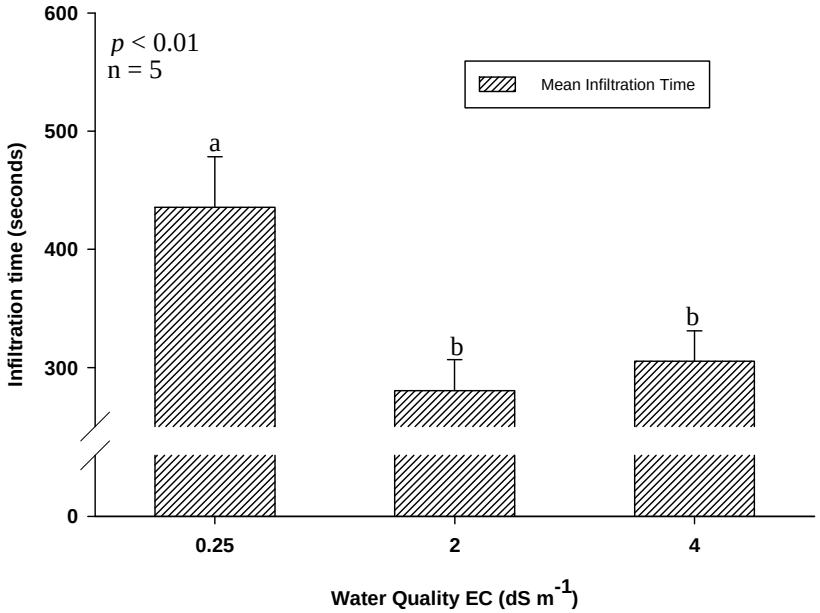

Figure 11: Change in relative infiltration time with changing solution chemistry. The mean time to infiltrate for data combined from both low and high salinity regions at three solution chemistry concentrations for field 2. Initial ponding depth was equal to 4 cm.

However, there is no significant difference in infiltration rate observed within individual salinity regions between solution treatments, $F_{(3, 56)} = 0.4127$, $p = 0.7445$. In addition, there is no significant improvement in infiltration rate with application of gypsum for individual, $F_{(3, 56)} = 1.5094$, $p = 0.2220$, or combined, $F_{(1, 58)} = 1.0391$, $p = 0.3123$ salinity regions (Figure 12). Although there was no statistically significant improvement in relative infiltration due to gypsum application, it's worth noting that gypsum amendment is a common and proven remediating practice (Wang *et al*., 1999; Keren and O'Connor, 1982) in sodium salt dominated systems. However, in a gypsum dominated system such as these, the utility of gypsum amendments seems limited. The pellet form of the

gypsum applied has a low surface area which may reduce the dissolution rate and effectiveness of the Ca^{2+} ions to prevent clay dispersion in this experiment (Keren and Shainberg, 1981).

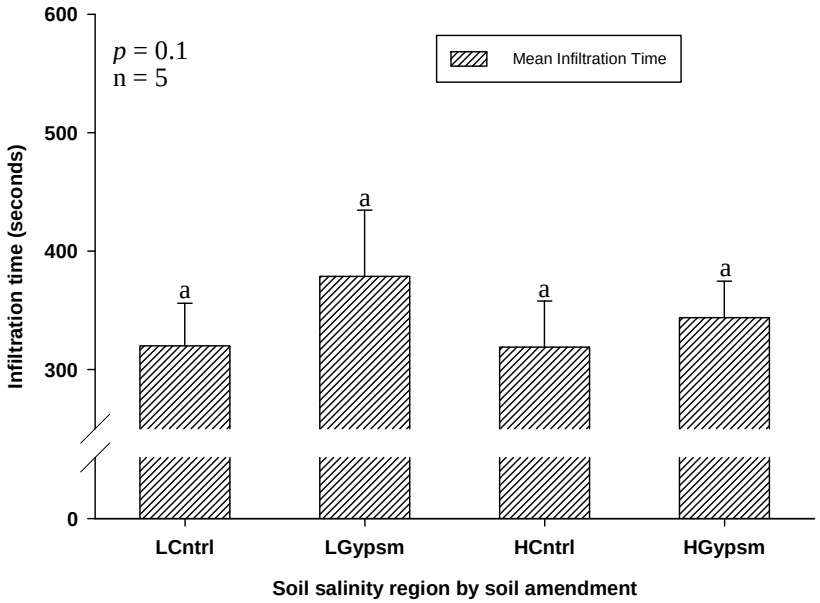

Figure 12: Change in relative infiltration rates between control and gypsum amended plots for the high and low salinity regions. Initial ponding depth was equal to 4 cm.

In addition, the dissolution of gypsum is greatly reduced in this system due to the common ion effect (as opposed to sodium dominated systems where gypsum is very soluble), and did not have time to change the solution chemistry of the infiltrating water sufficiently to prevent clay dispersion and formation of a soil crust.

Results of the relative infiltration experiment suggest a possible risk of surface sealing. However, a more detailed analysis of the soil surface's leaching potential is needed to determine whether high quality irrigation water will cause clay dispersion (soil crusting) and a reduction in infiltration rates in these fields. Therefore, saturated

hydraulic conductivity rates, K_{sat}, were measured at the high salinity region using a suite of solutions. One-way ANOVA shows significant differences between treatment means, $F_{(3,28)} = 5.1942$, $p = 0.005393$, (Figure 13).

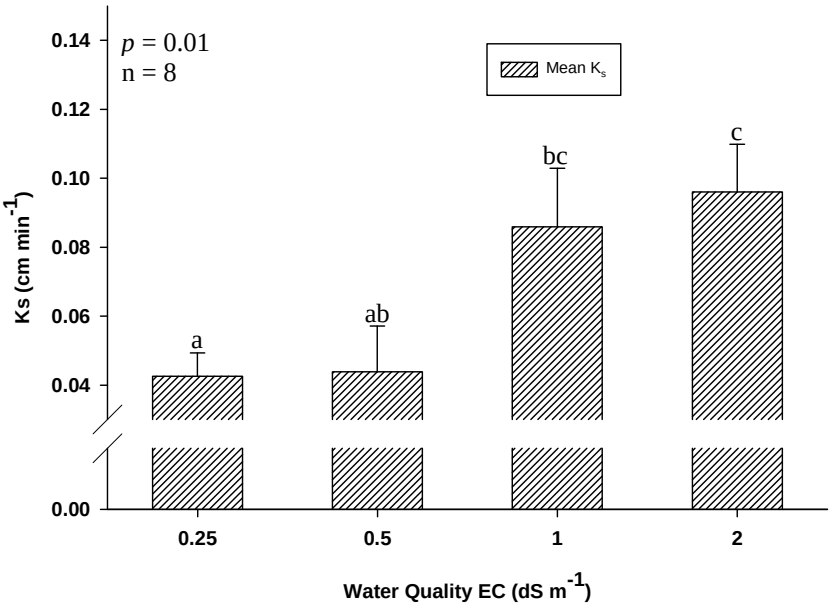

Figure 13: Change in saturated hydraulic conductivity with changing solution chemistry. The measurements were taken at the low salinity region in field 2.

Saturated hydraulic conductivity rates for the 0.25 and 0.5 dS m^{-1} solution treatments (mean = 0.043 and 0.044 cm min^{-1}, %CV = 47.3 and 85.5) are half that of 1.0 and 2.0 dS m^{-1} solution rates (mean = 0.086 and 0.096 cm min^{-1}, %CV = 56.1 and 40.7). Regression of K_{sat} with decreasing treatment solution EC (Figure 14) shows a sigmoidal relationship (f=0.0425+0.0536/(1+exp(-(x-0.8559)/0.0989))) supporting the idea of a threshold EC value for clay dispersion (Ayers and Westcot, 1985). Specific to the *in situ* soil conditions in field 2, clay dispersion appears to take place at solution EC levels of approximately 1.5 dS m^{-1}or less, and resulting in a reduction in hydraulic conductivity.

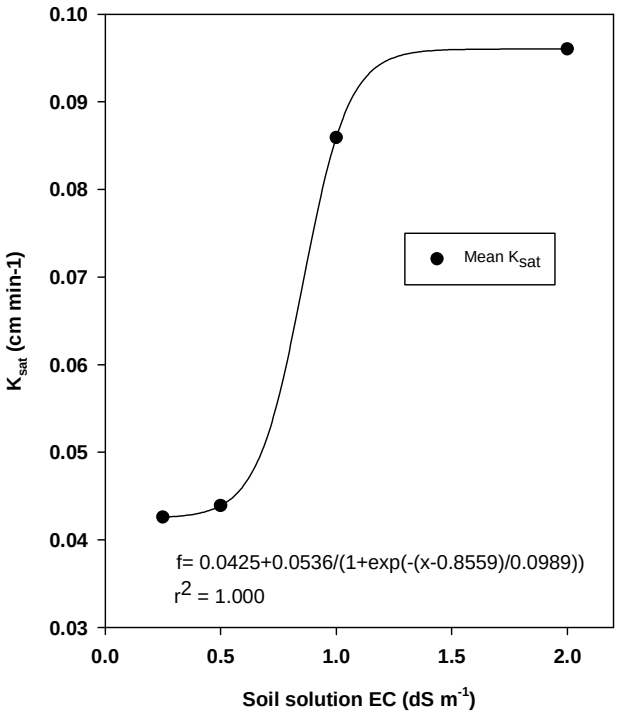

Figure 14: Trendline of saturated hydraulic conductivity change with changing solution chemistry for the low salinity region for field 2.

The relative infiltration measurements are also consistent with a threshold less than 2 dS m^{-1} for irrigation water. It is unclear from these results whether the observed reduction in K_{sat} constitutes a negative effect of solution chemistry in practice. In general however, a reduction in hydraulic conductivity equates to reduced leaching efficiency which, in a system plagued by salt accumulation, can be seen as undesirable.

Oster and Schroer (1979) speculated that the relationship between solution chemistry and hydraulic conductivity, formalized by Ayers and Westcot (1985), may be inaccurate in mixed rain/irrigation systems, and that these systems were especially sensitive to soil crusting. Oster and Schroer also note that the relationship between solution chemistry and hydraulic conductivity, formalized by Ayers and Westcot, was

derived from saturated conductivity measurements. As noted above, Oster and others have shown that the effects of solution chemistry on K change not only as a function of solution composition but also soil water tension.

The Oster and Schroer (1979) paper is of particular relevance to this project because it examines the success of leaching soils using various solution chemistries over an extended period of time (19 months). Limiting its applicability to this project is that many of the fields in the Arkansas River Valley have high water tables, which prevents leaching and the long term removal of salts below the rooting zone.

Native Hydraulic Conductivity and Moisture Retention Characterization

Analyses of native soil hydraulic properties indicate that K_{sd} for the medium and high salinity regions (mean = 0.020 and 0.017, %CV = 53.77 and 52.82) are not statistically different (Figure 15). The same is true for θ_{sd} (mean = 0.467 and 0.461, %CV = 3.39 and 1.62) and θ_r (mean = 0.268, 0.266, %CV = 3.09, 4.23). The K_{sd} for the low salinity region (mean = 0.043, %CV = 15.44) is significantly higher than both the medium and high salinity regions, $F_{(2,15)} = 14.719$, $p < 0.001$, and K_{sd} across all regions positively correlates with percent sand (r = +0.9076, $p = 0.0007$, n = 3). The low salinity region θ_{sd} and θ_r (mean = 0.441 and 0.209, %CV = 1.32 and 2.52) are significantly lower than either the medium or high salinity regions, $F_{(2,15)} = 10.114$, $p = 0.00166$ for θ_{sd} and $F_{(2,15)} = 91.08$, $p < 0.0001$ for θ_r. Correlation between θ_{sd} and percent sand across all salinity regions is strongly negative (r = -0.9197, $p = 0.0004$, n = 3). Correlation between θ_r and percent sand across all salinity regions is also strongly negative (r = -0.9721, $p < 0.0001$, n = 3). Percent sand explained differences in K_{sd}, θ_{sd}, and θ_r at all salinity regions

better than silt or clay fractions. There are no significant differences in either the α or n parameters between salinity regions for the observed drainage functions.

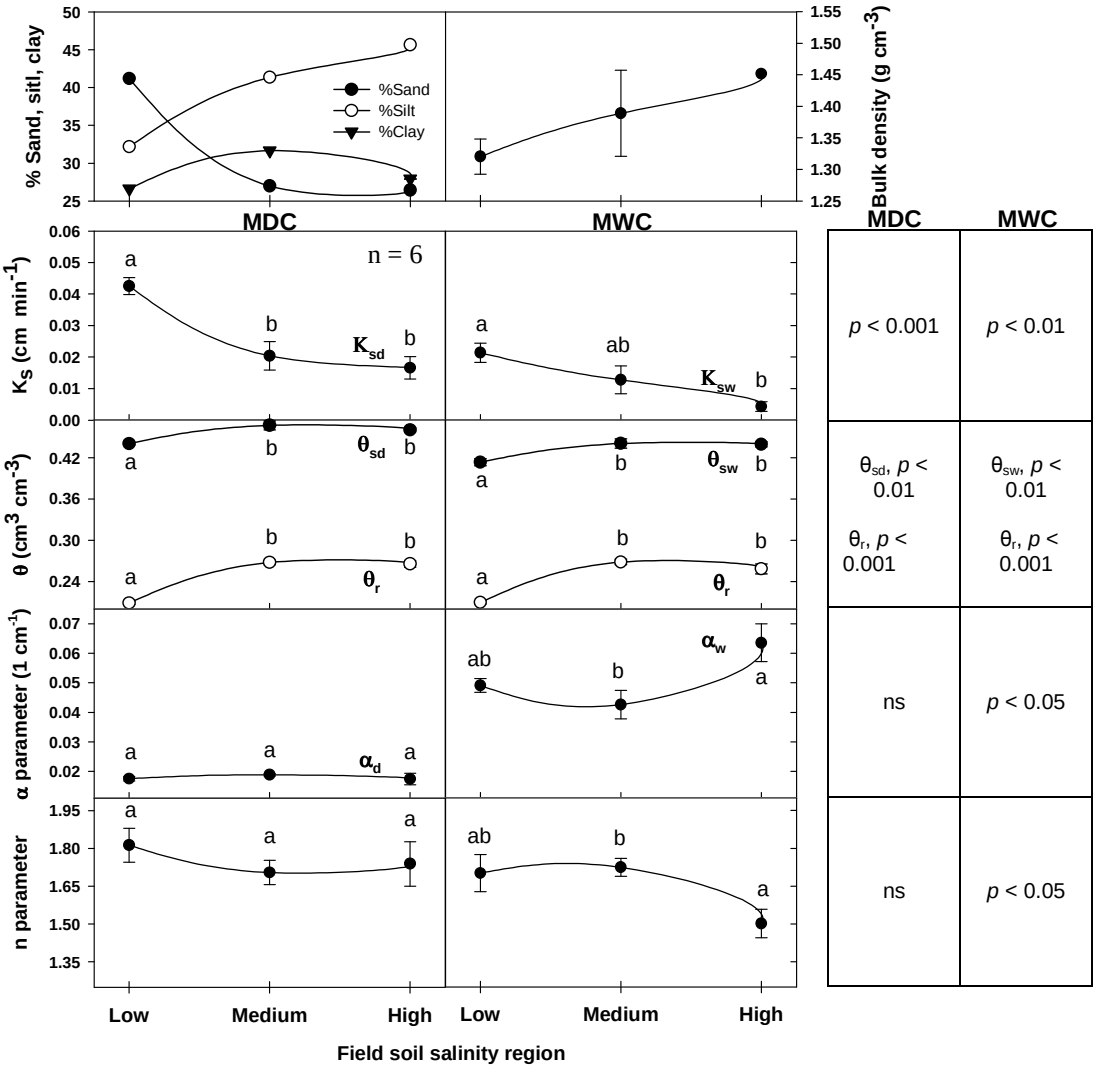

Figure 15: The K(h) and θ(h) parameters between salinity regions under native soil conditions. Function parameters are presented for both the main drainage curve, MDC, and main wetting curve, MWC. Soil texture and bulk density are also presented to assist in interpreting trends in K(h) and θ(h) parameters. Results of 1-way ANOVA statistical analysis between salinity regions are presented in the right hand column.

Estimates of the van Genuchten parameters were made for both drainage only data and for drainage/wetting loops. The van Genuchten parameter estimates for these

two different scenarios yield similar but not identical results. Because more drainage-only measurements were made than loop runs, drainage only data are reported and used for statistical analysis except where specifically noted. Differences between drainage-only and loop drainage data are not significantly different except for α at the low salinity region, $F_{(1,10)} = 15.514$, $p = 0.00278$, were α is slightly lower for drainage-only data than for loop runs (mean = 0.017 vs. 0.24; %CV = 11.02 vs. 13.59). For the high salinity region drainage only and loop runs, the van Genuchten *n* parameter is significantly different between estimates, $F_{(1,10)} = 5.1163$, $p = 0.04721$, with *n* being higher for drainage only estimates (mean = 1.74 vs. 1.50; %CV = 12.41 vs. 9.25). There is no significant difference between estimates for the medium salinity region compared to either the low or high salinity regions. Parameters from the drainage portion of the loop runs are reported along with drainage-only data and data from the main wetting curve in Tables 1, 2, and 3 of the supplemental appendix.

The wetting functions for the native salinity regions show similar trends to the drainage functions. K_{sw} for the medium and high salinity regions (mean = 0.013 and 0.004, %CV = 84.52 and 83.75) are not statistically different (Figure 15). The same is true for θ_{sw} (mean = 0.441 and 0.439, %CV = 3.84 and 2.16). The K_{sw} for the low salinity region (mean = 0.021, %CV = 34.72) is significantly higher than the high but not the medium salinity regions, $F_{(2,15)} = 7.118$, $p = 0.0067$, and K_{sw} across all regions positively correlates with percent sand (r = +0.6886, $p = 0.0403$, n = 3), although percent silt is actually better correlated (negatively) and more significant than percent sand for K_{sw} (r = -0.7629, $p = 0.0168$, n = 3). However, cores 1 and 2 from the medium salinity region are both anomalously high compared to the other 4 cores in that region. Excluding

these cores, percent sand is the best predictor of K_{sw} (r = +0.9533, $p < 0.0001$, n = 3). The low salinity region θ_{sw} (mean = 0.413, %CV = 3.02) is significantly lower than either the medium or high salinity regions, $F_{(2,15)} = 8.0611$, $p = 0.00419$. Correlation between θ_{sw} and percent sand across all salinity regions is moderately negative (r = -0.8703, $p = 0.0023$, n = 3). In contrast to the drainage functions, there are significant differences in both the α parameter, $F_{(2,15)} = 4.9783$, $p = 0.02197$ and n parameter, $F_{(2,15)} = 4.5964$, $p = 0.02773$ between salinity regions for the observed wetting functions. However, this difference is between the medium and the high salinity regions only; the low and high regions are not significantly different for either parameter. Percent sand explains differences in K_{sw} and θ_{sw} at all salinity regions better than silt or clay fractions just as it does for the drainage parameters. Neither the α parameter nor the n parameters show any significant correlation with soil texture properties. However, the difference between α_d and α_w did change with changing EC and SAR. The α parameter is typically assumed to vary predictably between the drainage and wetting curve functions, specifically α_w is assumed to equal $2*\alpha_d$. This assumption was not fixed when performing the inverse analysis of flow cell measurements in order to explore how change in EC and SAR effected the α_w/α_d ratio. For the native salinity regions, the α_w/α_d ratio was very close to 2.0 (Table 4). The α_w/α_d ratio was consistently higher for the high salinity region. For the EC reduction series, the α_w/α_d ratio increased with decreasing EC and similar to hydraulic properties, did not recover with increased EC. For the SAR series, the α_w/α_d ratio increased with increasing SAR. Similar to the EC, the α_w/α_d ratio did not decrease when solution chemistry was returned to initial conditions. It appears that the assumption that $\alpha_w = 2*\alpha_d$ is reasonable under native conditions for low to moderate salinity regions.

Table 4: Assessment of soil water hysteresis with the α_w to α_d ratio. Typically, it is assumed that $\alpha_w = 2^* \alpha_d$. All inverse fits of measured soil hydraulic properties for all salinity regions floated α_w, in order to observe any treatment or regional effects on α_w.

Salinity Region	Native		EC Series		SAR Series	
	---------- Ave (α_w/α_d) ----------					
	AM	%CV	AM	%CV	AM	%CV
Low	2.11	16.14	2.16	24.26	2.38	11.16
Medium	2.06	17.51	3.83	60.56	--	--
High	3.15	22.89	4.60	38.17	5.88	63.84

At higher salinity regions and with increased soil disturbance due to soil solution chemistry, $\alpha_w/\alpha_d > 2$ prevails.

Visual comparison of the K(h) and θ(h) functions between salinity regions (Figure 16) reiterates the correlation between K(θ) and soil texture. The K(h) function for the low salinity region shows a larger K_s and steeper characteristic decline in conductivity with decreasing θ due to its courser texture relative to the finer textured soils of the

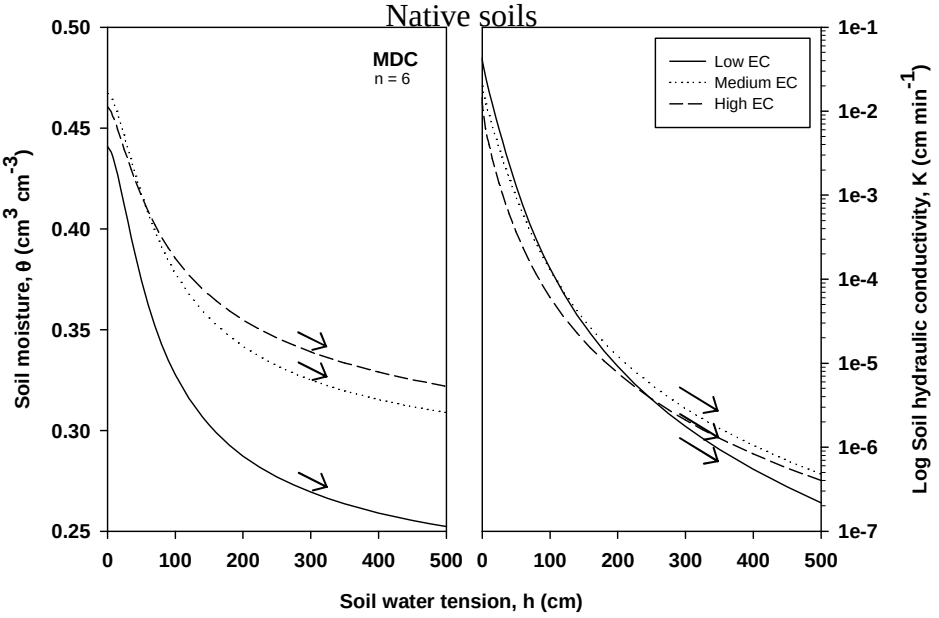

Figure 16: Hydraulic conductivity, K(h), and moisture retention, θ(h), functions between salinity regions.

medium and high salinity regions. This explains why the K(h) functions cross at lower soil water tensions. The change in texture and subsequent differences in PSD between salinity regions also impacts the air entry tension, h_i, between regions causing a decrease in h_i as soils become finer textured (i.e. moving from the low to high salinity regions). Soil silt percentage (Figure 17) explains a significant amount of the difference in h_i between regions ($r = -0.829$, $p < 0.0001$, $n = 3$), as does percent sand ($r = +0.7419$, $p = 0.0004$, $n = 3$) (figure not shown). Mean h_i values (in cm water pressure) between the low, medium, and high salinity regions are -25.54 (-6.8% CV), -20.14 (-16.27% CV), and -17.62 (-39.77% CV), and are significantly different between all three regions, $F_{(2,17)} = 4.4897$, $p = 0.02719$.

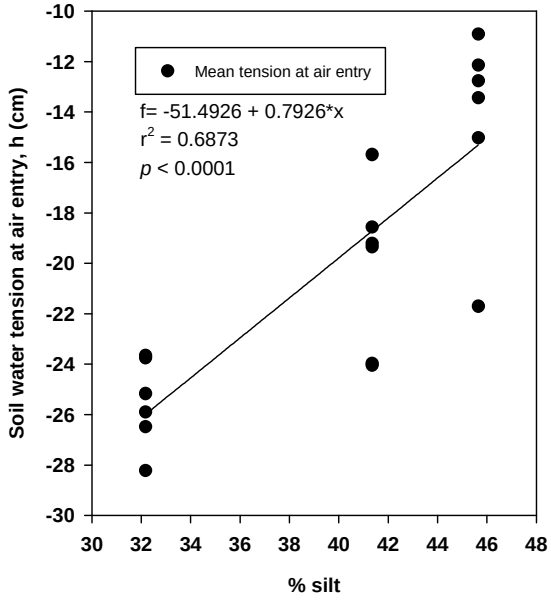

Figure 17: Change in soil water pressure at air entry, h_i, between salinity regions. Percent silt was best correlated with h_i.

Measured K_{sw} values for the native soils are observed to be lower than K_{sd} values. Figure 18 illustrates the soil water hysteresis in the K(h) and θ(h) functions for the low and high salinity regions (the medium region is not shown but is similar to the high salinity region, see supplemental table appendix). The effective magnitudes of hysteresis at the low and high salinity regions are visually equivalent except near saturation. Again, the courser texture of the low salinity regions cause the function to decline more steeply with increasing soil water tension than the finer textured, high salinity region.

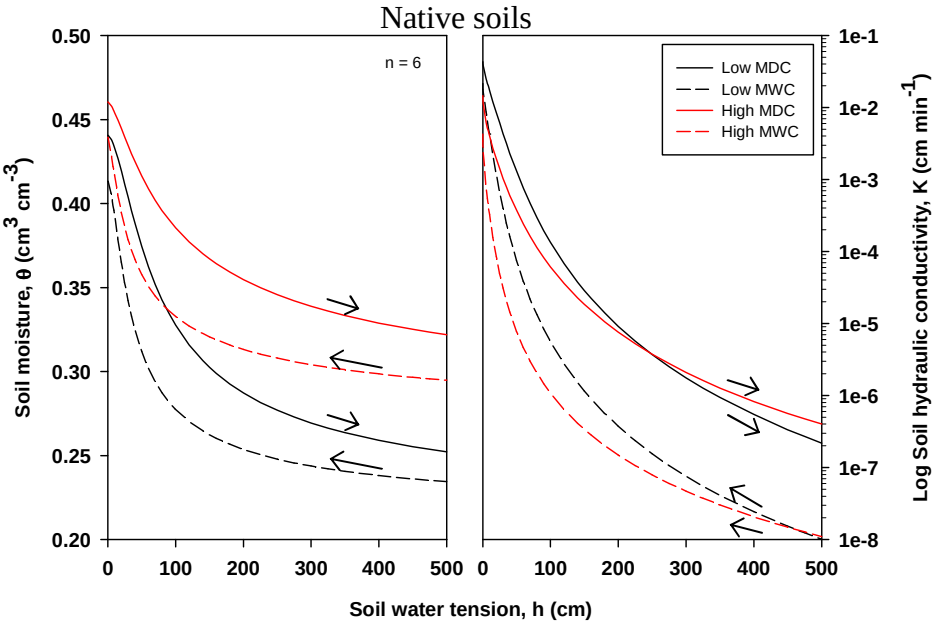

Figure 18: Hysteresis (main drainage curve, MDC, and main wetting curve, MWC) in the average measured van Genuchten soil hydraulic conductivity, K(h), and moisture retention, θ(h), functions at native conditions for the low and high salinity regions for field 1.

Field 2 soil hydraulic parameters were measured at only the low salinity region (Table 5) and are similar to the low salinity region in field 1. As stated above, Wilcoxon rank-sum comparison of soil hydraulic parameters between field 1 and 2 shows no differences between the parameters except for K_{sat} ($W_{(n1 = 6, n2 = 2)} = 12$, $p = 0.07143$).

Of particular interest when interpreting the results of native soil hydraulic characteristics in these fields, are the large differences in K(h) and θ(h) between salinity regions (as close as 150 m apart) that visually appear equivalent except for the absence of *M. sativa* L. at the high salinity region. The importance of incorporating the heterogeneity within fields when calculating changes in soil water storage, nutrient management, and salinity management could be great. Considering the highly variable soil salinity evident in the field survey (Figure 3), if salinity level is indicative of soil physical and hydraulic properties (which is reasonable to assume), then the soil hydraulic properties of field 1 are highly variable spatially.

Table 5: Comparison of soil hydraulic parameters between field 1 and field 2 low salinity regions.

Field No.	Salinity region	Rep	EC	BD	θ_s	θ_{15bar}	K_s	Ave h_i
			(dS m^{-1})	(g cm^{-3})	(cm^3 cm^{-3})		(cm min^{-1})	(1 cm^{-1})
1	Low	1	3.73	1.39	0.4413	0.2133	0.0427	-23.67
1	Low	2	3.73	1.37	0.4424	0.2064	0.0478	-25.90
1	Low	3	3.73	1.44	0.4298	0.2173	0.0504	-23.76
1	Low	4	3.73	1.44	0.4399	0.2299	0.0387	-26.49
1	Low	5	3.73	1.46	0.4401	0.2096	0.0435	-28.23
1	Low	6	3.73	1.41	0.4474	0.2031	0.032	-25.18
2	Low	2	2.74	1.43	0.4393	0.2198	0.0094	-29.73
2	Low	3	2.74	1.38	0.4521	0.2429	0.0112	-25.22

Using parameters of K(θ) from only one of the salinity regions analyzed to manage water and crops in field 1 would likely produce poor results. Even within salinity regions, there are modest differences between native soil hydraulic parameters (Table 6).

Another management issue associated with the heterogeneity of soil hydraulic properties in these fields is the amount of effort required to accurately determine these properties.

Table 6: Intra-region heterogeneity for the native soil drainage saturated hydraulic conductivity, Ksd, saturated moisture retention, θs, and residual moisture retention, θr, parameters for each of the salinity regions.

Salinity Region	θr		θsd		Ksd	
	---------- (cm^3 cm^{-3}) ----------				(cm min^{-1})	
	AM	%CV	AM	%CV	AM	%CV
Low	0.209	2.52	0.441	1.32	0.043	15.44
Medium	0.268	3.09	0.467	3.39	0.020	53.77
High	0.266	4.23	0.460	1.62	0.017	52.82

The measurement of soil hydraulic properties at the level of detail and scale required to capture the soil heterogeneity in each field in the Arkansas River Valley with the methods used above are cost and time prohibitive. However, as stated earlier, K and θ were significantly correlated with both sand and silt fraction in the soil. This relationship between soil texture and soil K and θ has been extensively examined and pedotransfer functions (PTF) developed (Schaap *et al*., 1998; Schaap and Leij, 1998a) that predict van Genuchten parameters based of soil texture, and if available other basic soil properties; the PTF employed by Hydrus-1D, Rosetta Lite (version 1.1), is one such model.

Comparison between measured van Genuchten parameters derived from the flow cell vs. the parameters derived from the Rosetta PTF (Schaap *et al*.,1998; Schaap and Leij, 1998a) help assess the utility of using a PTF, along with soil properties that are fast and simple to measure, to capture the heterogeneity between soil regions.

Figure 19 shows the flow cell derived van Genuchten parameters vs. two Rosetta PTF estimations. The closest agreement came, not surprisingly, when using the most input parameters for the PTF (sand, silt, and clay fraction, BD, and 0.033 MPa and 1.5 MPa water content values). The Rosetta estimates are consistently lower than measured values however. For some parameters such as Ks, trends observed between salinity regions using the flow cell are mirrored by the Rosetta estimates. The Rosetta estimates for θs between salinity regions are the poorest match between any of the parameters and shows nearly the opposite trend in θs compared to measured values. For the remaining parameters, correlation is modest but general trends are similar. In addition to the best fit Rosetta parameters, the variability in Rosetta estimates is plotted to illustrate the uncertainty in the PTF depending on the level of measured data provided.

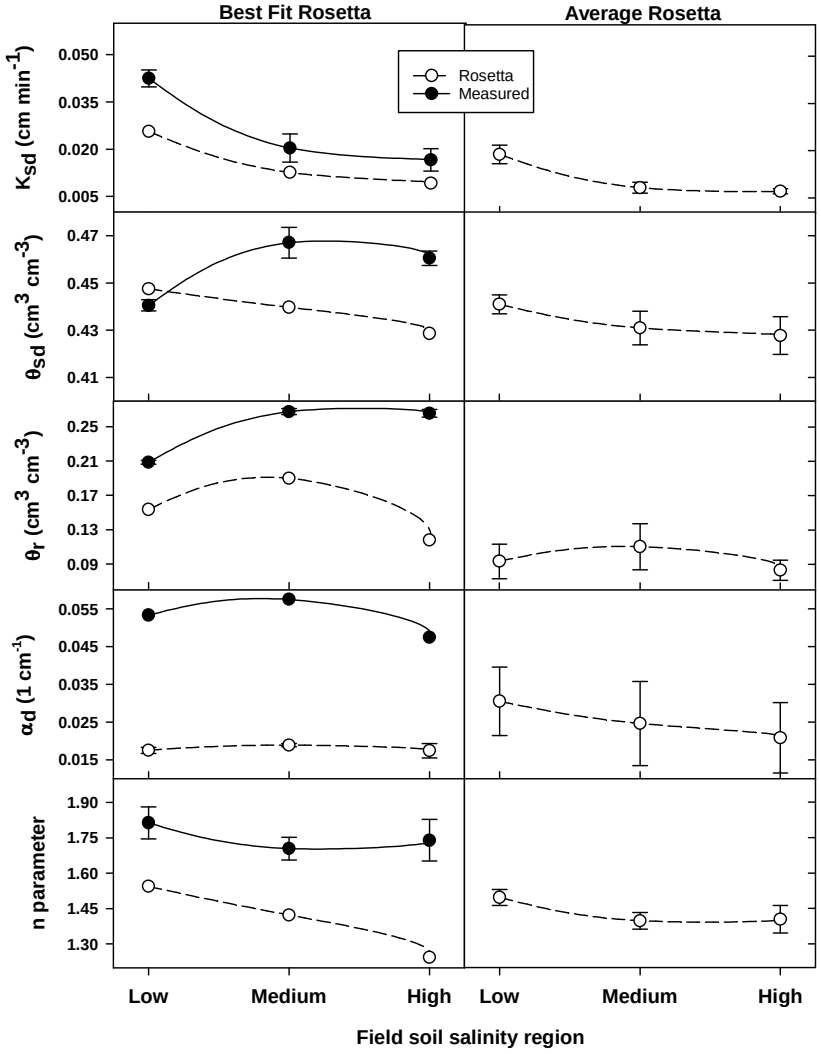

Figure 19: The predicted vs. measured soil hydraulic conductivity, K(h), and moisture retention, θ(h), parameters at native conditions for salinity regions in field 1, main drainage curve, MDC, only. Average predicted figures represent range of variability in pedotransfer predictions. Best fit figures compare measured data to predictions using inputs of percent sand, silt, and clay, bulk density, and θ at 0.033 and 1.5 MPa.

Comparing the K(h) and θ(h) by the flow cell measurement and the Rosetta indirect estimation (Figure 20) show that the relative difference between θ(h) functions for the salinity regions as estimated by the two techniques are nearly identical except near saturation.

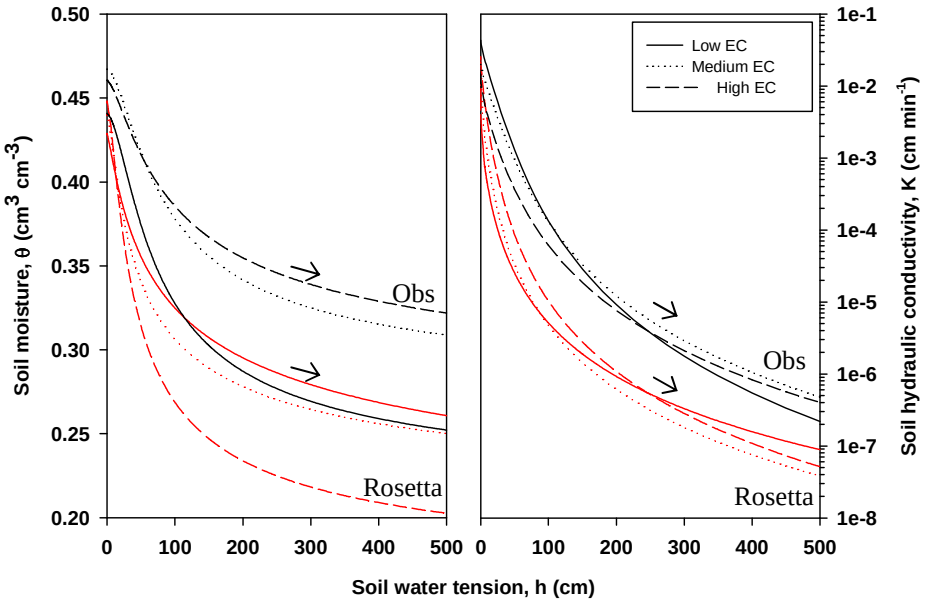

Figure 20: The predicted (Rosetta) pedotransfer (Schaap *et al*., 1998; Schaap and Leij, 1998) vs. average measured (Obs) van Genuchten soil hydraulic conductivity, K(h), and moisture retention, θ(h), functions at native conditions for the low, medium, and high salinity regions for field 1.

Again, the absolute values for the Rosetta estimates are below the measured values but for relative comparisons between sites this makes no difference. The fact that θs is poorly estimated by Rosetta as opposed to θ(h) which is very similar to measured values, suggests that the mechanism controlling unsaturated flow (i.e. alpha and n parameters) are well characterized. This is promising if detailed measurements of soil hydraulic properties are restricted. For K(h) the differences observed between salinity regions were

not duplicated by the Rosetta estimates, although the differences in both the observed and estimated functions between salinity regions were subtle and it is therefore possible that minor differences could create contrasting patterns. If the average measured K(h) functions are considered, the combined K(h) function for all salinity regions vs. the averaged Rosetta K(h) estimates are very similar, with the Rosetta estimates once again lower than measured values. Recall that at K_{sat}, Rosetta precisely estimated the differences in hydraulic conductivity between salinity regions.

Electrical Conductivity Reduction Series

Figure 21 shows the trend in saturated water content and saturated hydraulic conductivity for both the drainage and wetting functions, with decreasing EC for each salinity region. Comparing the relative change in the drainage saturated, θ_{sd}, or 15 MPa, $\theta_{1.5MPa}$, water content values from a reference EC and combining all salinity regions (n = 3 per EC treatment), there are no significant differences in treatment responses from any one salinity region, $F_{(2,9)} = 1.189$, $p = 0.3736$ for θ_{sd}, $F_{(2,9)} = 0.9954$, $p = 0.4429$ for $\theta_{1.5MPa}$. Therefore, θ_{sd} and $\theta_{1.5MPa}$ from all salinity regions were normalize and combined to allow for comparison between EC treatments. Normalization of θ_{sd} between salinity regions was accomplished by setting θ_{sd} for all EC treatments equal to the minimum θ_{sd} for the native treatment. The percent change in θ_{sd} between EC treatments was calculated for each salinity region and applied to the corrected θ_{sd} value; the same was done for $\theta_{1.5MPa}$. One-way ANOVA between EC reduction treatments (4.0 dS m^{-1} to 0.25 dS m^{-1}) shows a clear increasing trend for both θ_{sd} and θ_{15bar} but are not significantly different.

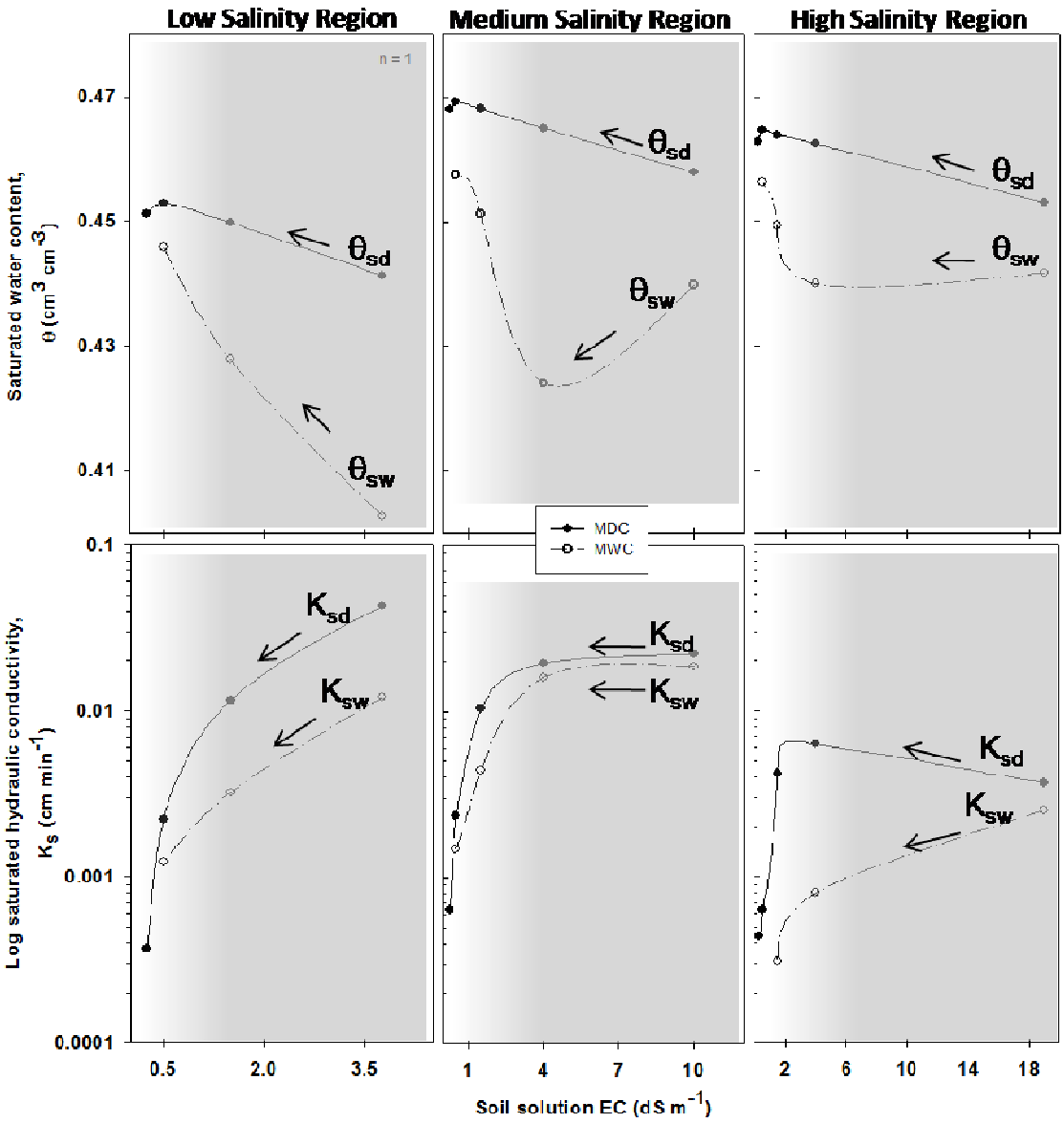

Figure 21: The measured soil saturated hydraulic conductivity, K_s, and saturated water content, θ_s, across the electrical conductivity, EC, reduction series for the low, medium, and high salinity regions for field 1. Results are presented for both the main drainage curve (denoted by subscript "d"), and main wetting curve (denoted by subscript "w").

After removing the 0.25 dS m^{-1} treatment and repeating the ANOVA, the p-values were reduced but the difference between EC treatments remained insignificant, $F_{(2,6)} = 2.0926$, $p = 0.2044$ for θ_{sd}, and $F_{(2,6)} = 1.5528$, $p = 0.2861$ for θ_{15bar}.

The proportional change in drainage saturated hydraulic conductivity, K_{sd}, between salinity regions with EC reduction is not significantly different, $F_{(2,9)} = 0.0601$, $p = 0.942$. Therefore, K_{sd} values were normalized in a similar fashion and combined for comparison between EC treatments (n = 3), which shows a significant reduction in K_{sd} with decreasing EC, $F_{(3,8)} = 77.257$, $p < 0.0001$, and is similar to observed reductions from field K_{sd} measurements.

Compared to θ_{sd}, the wetting function saturated water content, θ_{sw}, shows a similar response to the EC reduction series. The proportional change in θ_{sw} values from a reference EC and show no significant differences in treatment response from any one salinity region, $F_{(2,9)} = 1.8729$, $p = 0.2089$ for θ_{sw}. Therefore, regions were normalized and combined for θ_{sw}. One-way ANOVA between EC reduction treatments (4.0 dS m^{-1} to 0.25 dS m^{-1}) shows a significant but weak increase in θ_{sw}, $F_{(3,8)} = 3.2309$, $p = 0.08205$. After removing the 0.25 dS m^{-1} treatment and repeating the ANOVA, the p-value was reduced, $F_{(2,6)} = 7.0908$, $p = 0.02628$.

The proportional change in wetting saturated hydraulic conductivity, K_{sw}, between salinity regions is also not significantly different, $F_{(2,9)} = 0.1448$, $p = 0.8672$. Therefore, K_{sw} values were normalized and combined for comparison between EC treatments (n = 3), which shows a significant reduction in K_{sw} with decreasing EC, $F_{(3,8)} = 42.367$, $p < 0.0001$.

Attempts to recover native soil solution hydraulic properties by increasing EC back to native conditions (5 dS m^{-1}) resulted in neither the drainage nor wetting curve parameters recovering to native values. The change in $\theta_{1.5MPa}$ and θ_{sw} from 0.25 back up to 5 dS m^{-1} is not significant, $F_{(1,4)} = 0.1083$, $p = 0.7586$ for $\theta_{1.5MPa}$ and $F_{(1,4)} = 0.2616$, $p = 0.6360$ for θ_{sw} , and the change in θ_{sd}, although technically significant, is small and not close to native values, $F_{(1,4)} = 5.5777$, $p = 0.07752$ for θ_{sd}. The change in K_{sd} and K_{sw} from 0.25 back up to 5 dS m^{-1} is also not significant, $F_{(1,4)} = 0.7207$, $p = 0.4437$ for K_{sd} and $F_{(1,4)} = 0.2232$, $p = 0.6613$ for K_{sw}. Attempts to recover native soil solution hydraulic properties by increasing EC back to native conditions (5 dS m^{-1}) resulted in no significant change in h_i, $F_{(1,4)} = 1.0758$, $p = 0.3582$. Changes in all van Genuchten soil hydraulic parameters with changing EC are listed in Tables 4, 5, and 6 of the supplemental appendix.

EC Effects on K(h) and θ(h)

For both K(h) and θ(h), changes were observed between salinity regions and between EC treatments. The pattern in changing θ(h) with changing EC is consistent between salinity regions with a higher θ at any h in lower EC conditions (Figure 22, 23, 24). However, the magnitude of change differs between salinity regions, with the largest affect on θ(h) in the low salinity region. The low salinity region soil has a less uniform pore-size distribution, perhaps from structural development, than either the medium or high salinity regions (as evidenced by the slope of the θ(h)), and when soil solution EC is reduced, is severely disrupted due to clay dispersion. The medium and high salinity regions however, appear to be physically more homogenous (less Δθ with Δh) than the

low salinity region and result in only a modest increase in θ. Bulk density values from the low vs. medium and high salinity regions also support this idea. Greater soil development at the low salinity region helps explain why the BD is lower at the low salinity region where the soil texture is courser and should result in less pore space and higher BD. Although the majority of

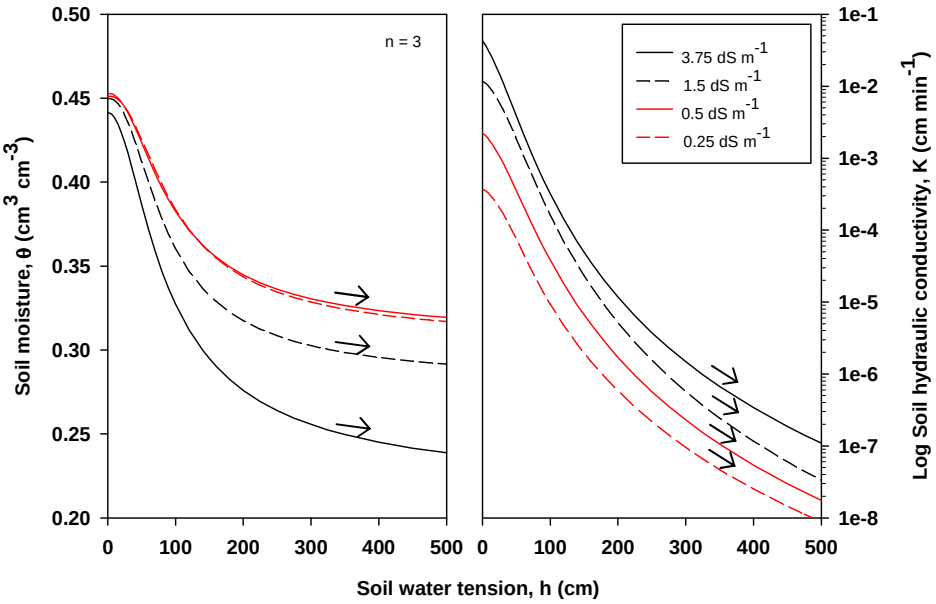

Figure 22: Change in hydraulic conductivity, K(h), and moisture retention, θ(h), functions with reduced soil solution EC – low salinity region.

support is for greater soil structure at the low salinity region, the trend in air entry values shown in Figure 15 indicates that the low salinity region actually has an air entry at higher tensions than the medium and high salinity regions, which would suggest smaller pore diameters which seems to contrast with greater structure, courser texture, and greater K_s.

The patterns in K(h) are similar between salinity regions at saturation but begin to diverge at higher water tensions. The EC treatment affects on K(h) shows similar patterns in reduced K(h) with reduced EC. For the medium salinity region, clay dispersion reduces K at saturation but K(h) at higher tensions increase due to an effective shift in PSD and more of the flow controlled by capillaries. For both the low and high salinity regions, K(h) maintain a relatively constant reduction in conductivity with

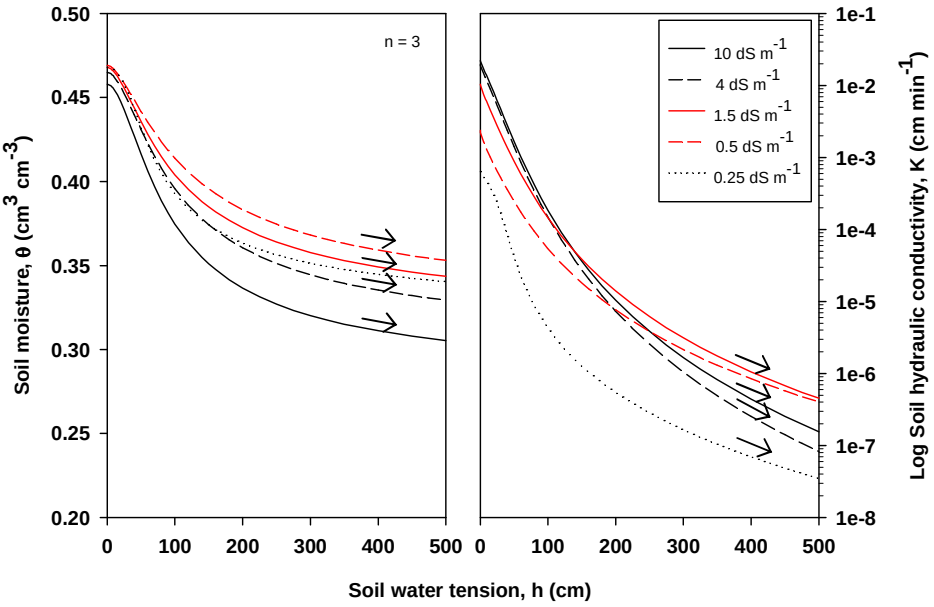

Figure 23: Changes in soil hydraulic conductivity, K(h), and moisture retention, θ(h), functions with reduced EC – medium salinity region.

increased soil water tension over the range of measured tensions. Also note that similar to the field infiltration experiments, K for the lab measurements changes little near saturation with changing solution chemistry above 1.5 dS m^{-1}. This is particularly clear for the medium and high salinity regions. For the low salinity region, the low endemic

gypsum concentrations and initial solution chemistry treatment of 1.5 dS m^{-1} appear to have begun to disperse clays.

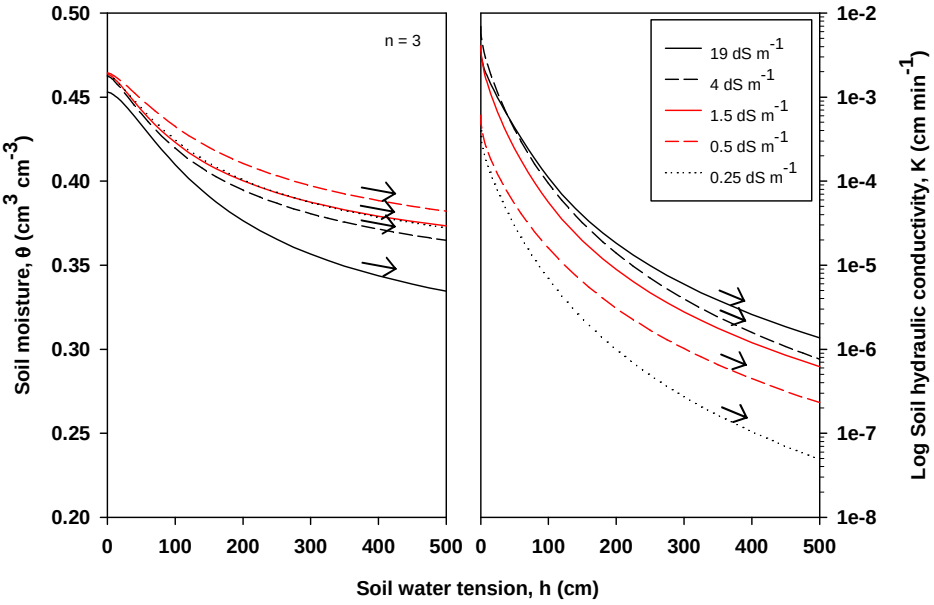

Figure 24: Change in soil hydraulic conductivity, K(h), and moisture retention, θ(h), functions with reduced soil solution EC – high salinity region.

Sodium Adsorption Ratio Series

Figure 25 shows the trend in θ_s and K_s for both the drainage and wetting functions, with increasing SAR for the low and high salinity regions (the medium salinity region did not undergo a SAR treatment series). When comparing the relative change in the θ_{sd}, or K_{sd} values from a reference SAR, and combining all salinity regions (n = 2 per SAR treatment >20, n = 1 per SAR treatment <20), there are no significant differences in treatment responses from the two salinity regions, $F_{(1,6)} = 2.5266$, $p = 0.1630$ for θ_{sd}, $F_{(1,6)} = 0.3199$, $p = 0.5922$ for K_{sd}. Therefore, θ_{sd} and K_{sd} from both salinity regions were normalized in the same fashion as the EC series and combined to allow for comparison

between SAR treatments. Non-parametric analyses accounting for unequal sample size using Kruskal-Wallis rank sum test between SAR treatments (5 to 25) shows a clear

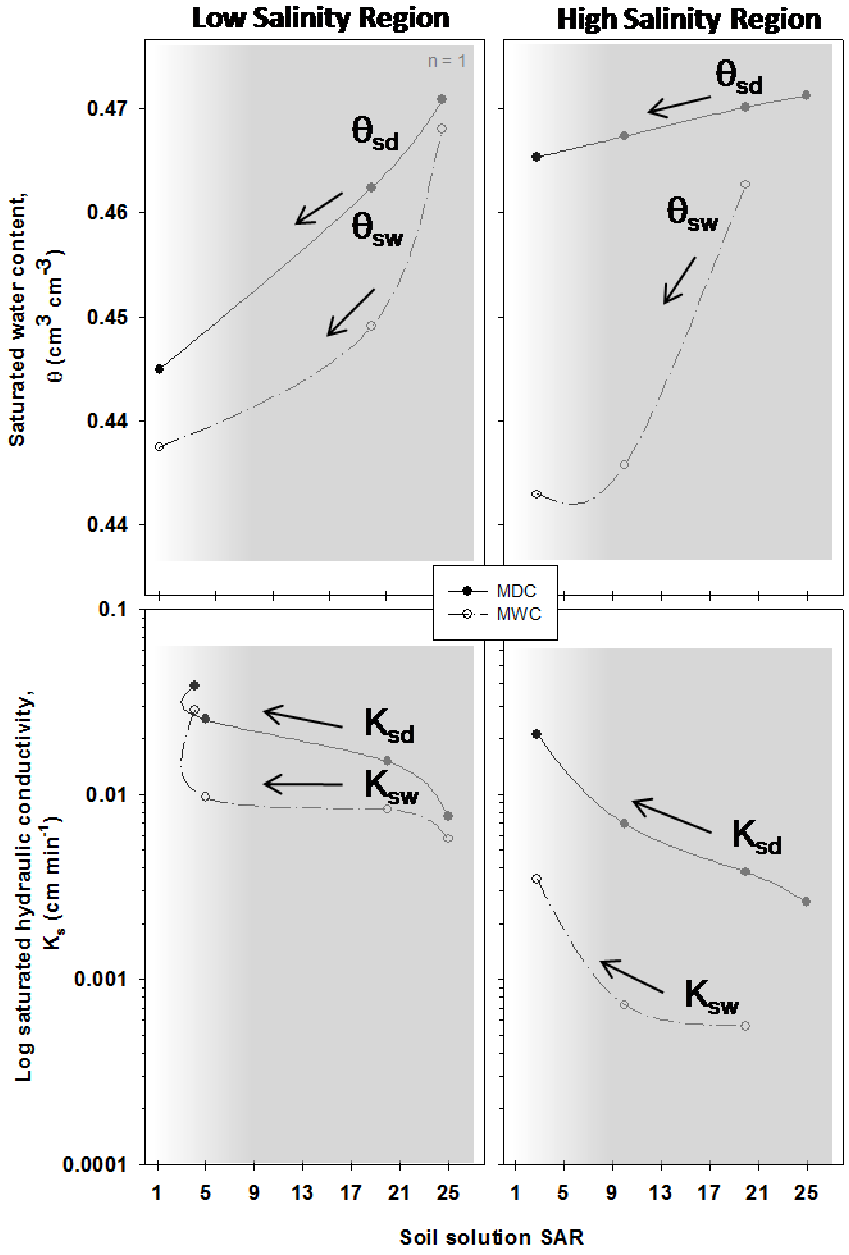

Figure 25: The measured soil saturated hydraulic conductivity, K_s, and saturated moisture retention, θ_s, across the increasing sodium adsorption ration, SAR, series for the low and high salinity regions for field 1. Results are presented for both the main drainage curve (denoted by subscript "d"), and main wetting curve (denoted by subscript "w").

increasing trend in θ_{sd} and a reduction in K_{sd} but neither is statistically significant, $H_{(5)}$ = 5.9036, p = 0.3157. Linear regression of K_{sd} shows a significant negative correlation between SAR treatments, (r = -0.8927, p = 0.0028, n = 8; f=0.0369-0.0013*x) with increasing SAR causing a reduction in K_{sd}. Comparison of the relative change in the 1.5 MPa water content, $\theta_{1.5MPa}$, values to a reference SAR $\theta_{1.5Mpa}$, and combining all salinity regions, the low and high salinity regions are significantly different, $F_{(1,6)}$ = 7.8574, p = .03014, and therefore were not combined for analysis. However, linear regression of the SAR series vs. $\theta_{1.5MPa}$ for the low salinity region shows a significant correlation, (r = +0.9998, p = 0.0002, n = 4; f=0.2081+0.0008*x) between increasing SAR and increasing $\theta_{1.5MPa}$. Linear regression of the SAR series vs. $\theta_{1.5MPa}$ for the high salinity region shows no significant correlation, (r = -0.4812, p = 0.5188, n = 4) and no clear trend due to the SAR treatments.

The wetting function saturated water content, θ_{sw}, shows a similar response to increasing SAR. The relative change in θ_{sw} values from a reference SAR and combining all salinity regions (n = 3 per SAR treatment), show no significant differences in treatment responses from either the low or high salinity regions, $F_{(1,6)}$ = 2.3843, p = 0.1735 for θ_{sw}. After normalizing and combining θ_{sw} values, a Kruskal-Wallis rank sum test performed between SAR treatments (2.8 to 25) for θ_{sw} showed no significant change in θ_{sw} with SAR, $H_{(5)}$ = 0.8005, p = 0.6369.

The relative changes in wetting saturated hydraulic conductivity, K_{sw}, between salinity regions is also not significantly different, $F_{(1,6)}$ = 8e-04, p = 0.979. Therefore, K_{sw} values were normalized and combined for comparison between SAR treatments (n = 2 per SAR treatment >20, n = 1 per SAR treatment <20). Results of the Kruskal-Wallis

rank sum test show no significant reduction in K_{sw} with increasing SAR, $H_{(5)} = 4.8916$, $p = 0.4293$.

SAR Effects on K(h) and θ(h)

For both K(h) and θ(h), changes were observed between salinity regions and between SAR treatments. The pattern in θ(h) with changing SAR, in contrast to the EC series, is inconsistent between the low and high salinity regions. Because of the uncertainty in the high salinity SAR treatment results, only the low salinity region soil is discussed below.

For the low salinity region, an increasing SAR causes an increase in θ_s (Figure 26).

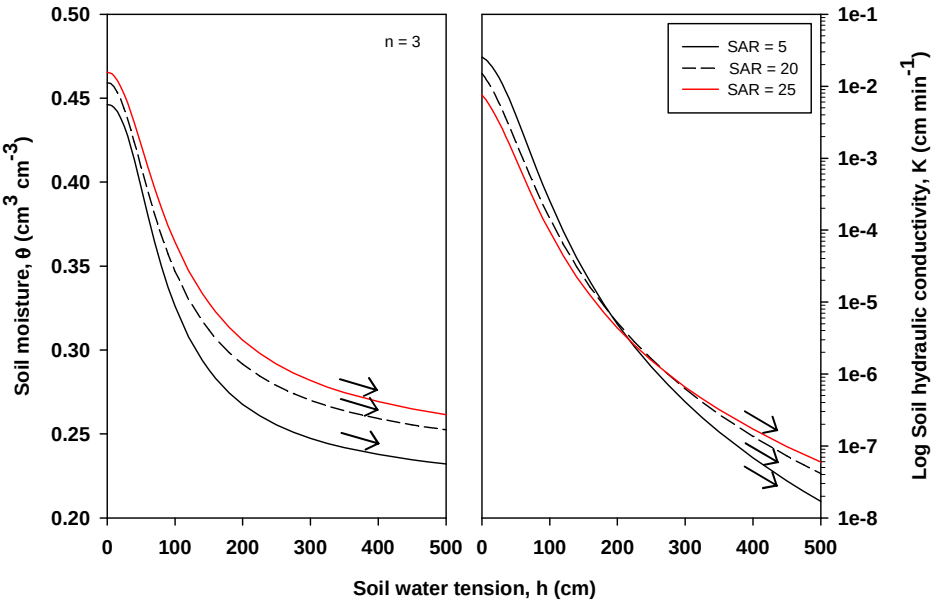

Figure 26: Change in soil hydraulic conductivity, K(h), and moisture retention, θ(h), functions with increasing SAR – low salinity region.

The effect of increased SAR on θ(h) appears to become slightly smaller or stay the same at higher water tensions. Russo and Bresler (1976) observed a decrease in the effects of SAR with increasing soil water tensions, rationalizing the change due to 1) at lower soil water tensions, movement of clay particles is reduced and no further pores become clogged, 2) as water is removed from the soil at greater soil water tensions, the swelling of the soil is reduced and hence the increase in θ caused by the swelling is reduced. For the soils in this study, the observed pattern in K(h) for the increasing SAR series does not seem to supports this theory, at least at all SAR values. The effect of increasing SAR on this soil was to reduce K near saturation but increase K at water contents less than about 0.30. Mechanistically, the observed change in K(h) with increasing SAR suggests a shift in the PSD to overall smaller pores caused by swelling. Thus, K is reduced near saturation due to fewer large pores to conduct water but remains intermediate at lower water contents due to smaller pores retaining their water longer.

Attempts to recover native soil solution hydraulic properties by reducing the SAR back to native conditions (SAR = 5) resulted in partial recovery to native conditions. However, due to an incomplete dataset, statistical analyses lack sufficient power to determine any statistical differences between salinity regions or SAR treatments with reduced SAR. Regression analysis of the low salinity region only, shows a clear reduction in θ_{sd} with lower SAR but the correlation is not significant, ($r = +0.8713$, $p = 0.3266$, $n = 1$; $f=0.4599+0.0002*x$). Neither θ_{sd} nor $\theta_{1.5MPa}$ shows any clear correlation with reduced SAR. The change in wetting curve parameters shows a slightly improved relationship with reduced SAR but once again, the correlation is not statistically significant. Change in θ_{sw} with lower SAR shows the strongest correlation ($r = +0.9733$,

p = 0.1476, n = 1; f=0.4427+0.0008*x), followed by K_{sw} (r = +0.7987, p = 0.4110, n = 1; f=0.0055+1.4785E-5*x). Changes in all van Genuchten soil hydraulic parameters with changing SAR are listed in Table 7, 8, and 9 of the supplemental appendix.

Hysteresis and Soil Solution Chemistry

Analysis of hysteretic properties showed that for K(h), a decrease in EC caused a large increase in hysteresis for the soil at all three salinity regions. Hysteresis in the θ(h) function changed very little with decreasing EC. For the low salinity region (Figure 27), hysteresis in θ(h) was actually reduced at higher soil water tensions in contrast to the trend in K(h). The θ(h) function at the medium and high salinity regions remained equivalent with reduced EC (Figure 28 and 29).

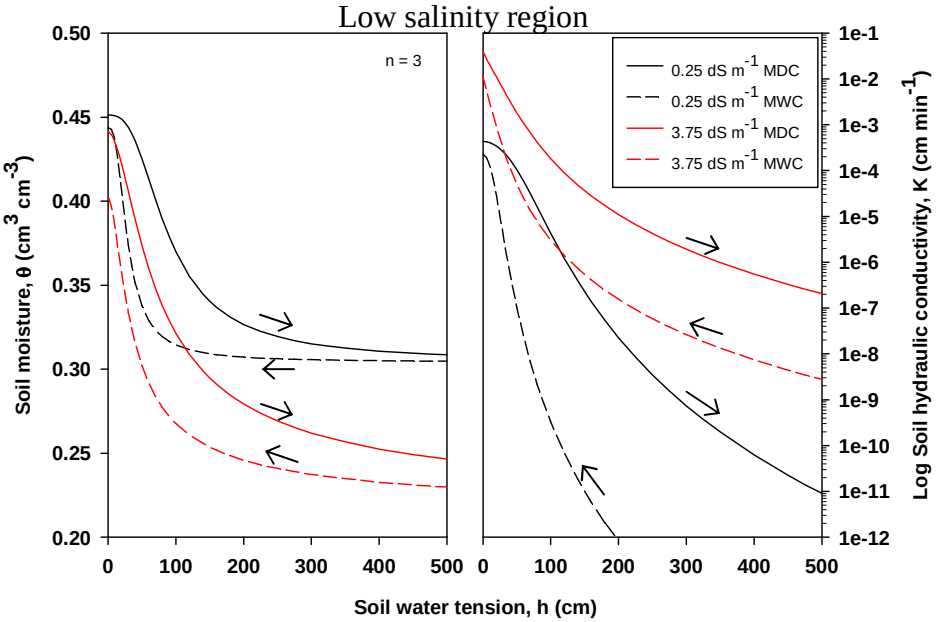

Figure 27: The change in hysteresis (main drainage curve, MDC, and main wetting curve, MWC) due to reduced soil solution EC in the average measured van Genuchten soil hydraulic conductivity, K(h), and moisture retention, θ(h), functions for the low salinity region in field 1. EC reduction for the low salinity region was reduced from the native value (3.75 dS m^{-1}) to 0.25 dS m^{-1}.

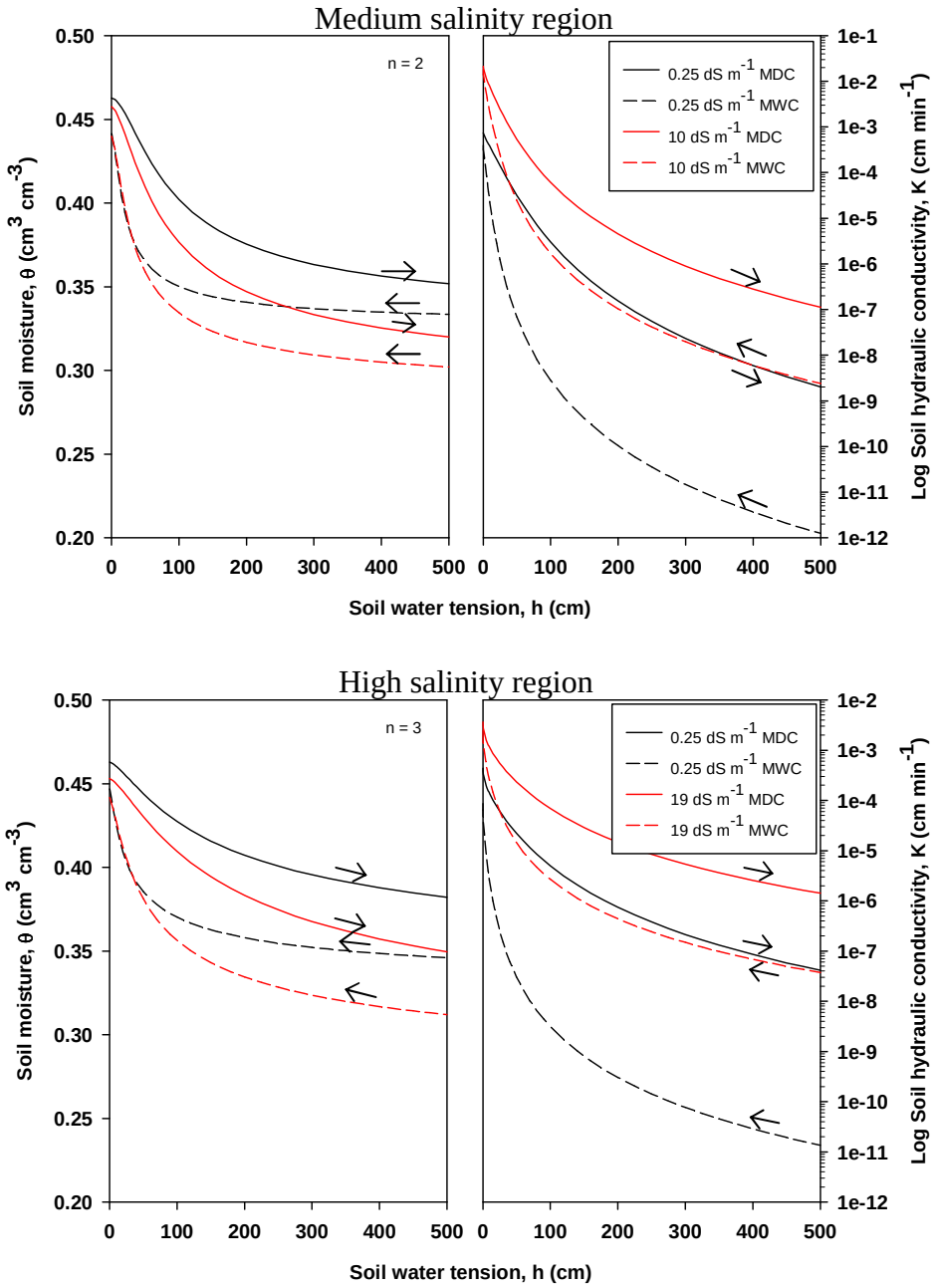

Figure 28 and 29: The change in hysteresis (main drainage curve, MDC, and main wetting curve, MWC) due to reduced soil solution EC in the average measured van Genuchten soil hydraulic conductivity, K(h), and moisture retention, θ(h), functions for the medium and high salinity regions in field 1. The EC reduction for the medium salinity region was reduced from the native value (10 dS m^{-1}) to 0.25 dS m^{-1}. The EC reduction for the high salinity region was reduced from the native value (~19 dS m^{-1}) to 0.25 dS m^{-1}.

It appears that the dispersion of clay platelets due to reduced EC causes constrictions or bottlenecks in the soil pores that increase the required soil water pressure to refill the pore space during rewetting but do not drastically change the porosity, and therefore do not drastically change the moisture retention of the soil.

Unlike the medium and high salinity regions however, the low salinity region shows a clear shift in the slope of K(h). Under native conditions, the van Genuchten L parameter for the low salinity region shows the greatest inherent pore connectivity for both the wetting and draining functions (Figure 30), which can be an indicator of greater soil development and structure. Although in this case, the high L value for the low salinity region, in context of the change in slope of K(h), is likely indicative of a narrower PSD where K_{sat} is dominated by just a few large pores, maintaining K near saturation but at higher soil water tensions K is severely reduced due to clogged of smaller pores. This also makes sense in terms of the θ(h) function for the low salinity region.

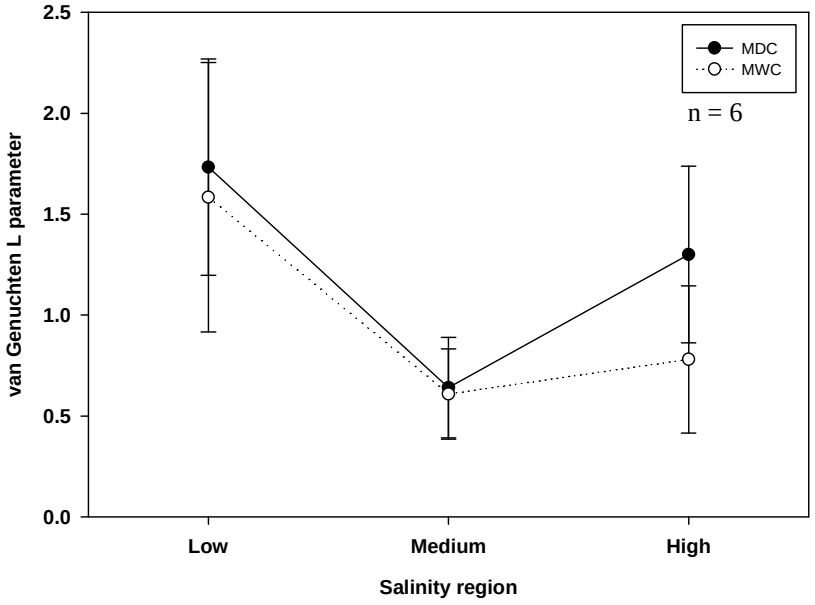

Figure 30: The difference in the van Genuchten L parameter between salinity regions and for the main draining and main wetting curves (MDC and MWC).

Specifically examining the change in the L parameter for the EC series shows a clear reduction in L with changing solution chemistry below 2-4 dS m^{-1}. The difference in L between the MDC and MWC for the EC series was less clear (Figure 31), and the only consistency between the low and high salinity regions is a reduction in hysteresis for L at the 0.25 dS m^{-1} solution treatment.

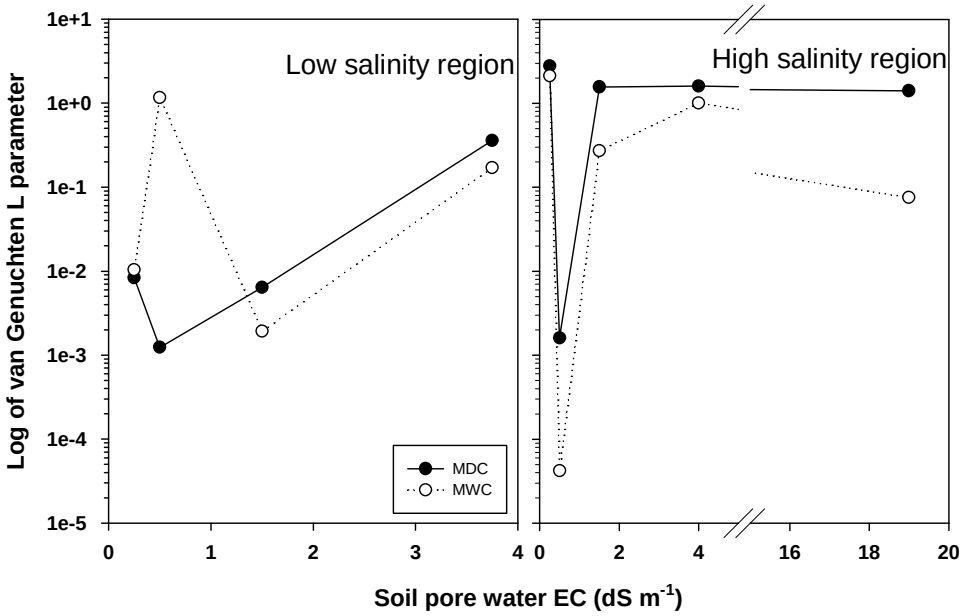

Figure 31: The difference in the van Genuchten L parameter for the low and high salinity regions, and for the main draining and main wetting curves (MDC and MWC) with reduced soil pore water electrical conductivity.

For the SAR series, hysteresis in both K(h) and θ(h) first appears to decrease with increasing SAR (Figure 32 and 33). However, that is only in comparison to native K(h) and θ(h), if compared to the lowest SAR treatment, there is little or no decrease in hysteresis with increasing SAR. In theory, an increase in SAR will cause expansion of interlayer spacing between clay particles when $Na{\cdot}6H_2O$ replaces $Ca{\cdot}2H_2O$ or $Mg{\cdot}2H_2O$. In contrast to reduced EC which causes substantial clay dispersion, the dominant physical

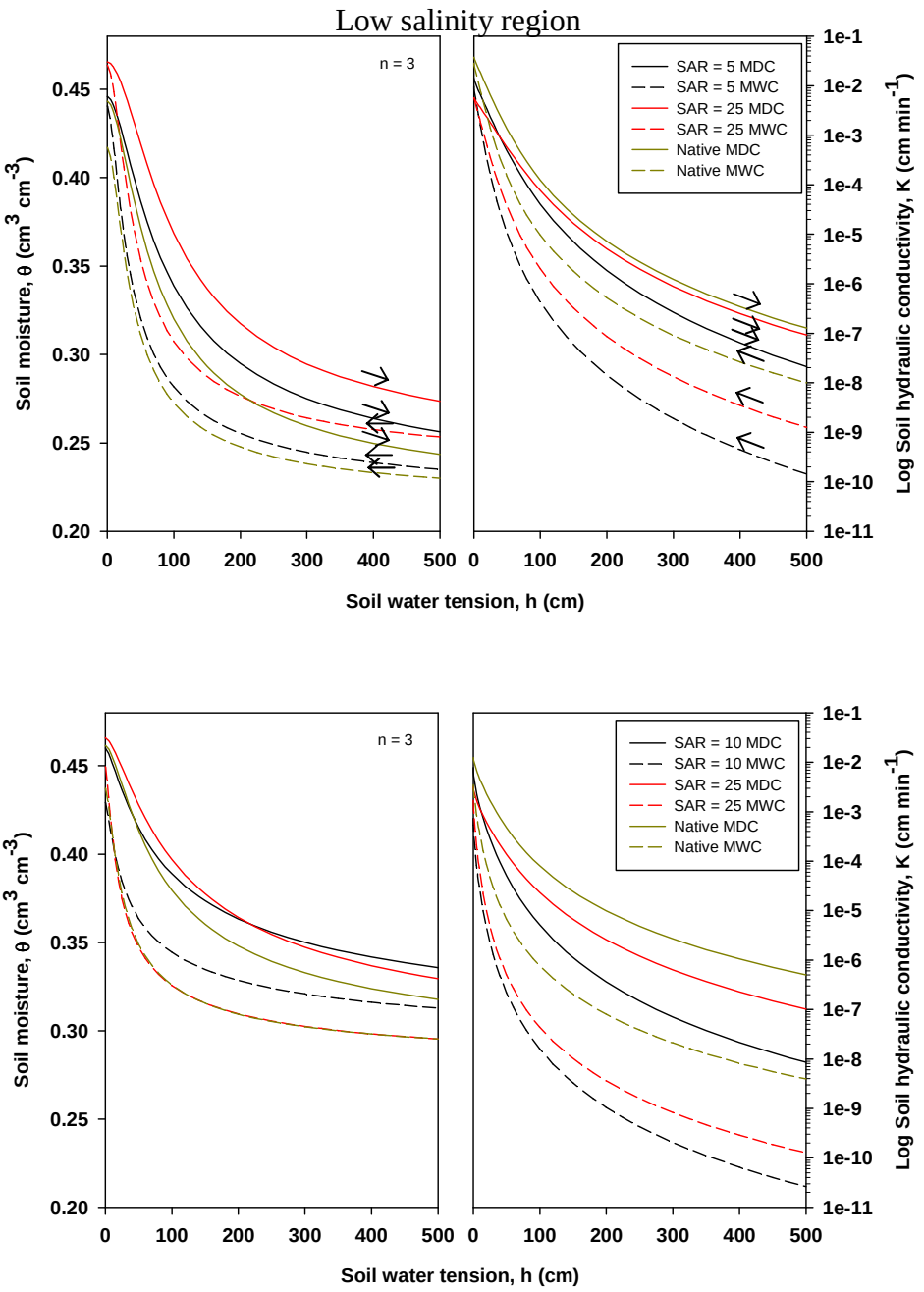

Figure 32 and 33: The change in hysteresis (main drainage curve, MDC, and main wetting curve, MWC) due to an increase in soil solution SAR in the average measured van Genuchten soil hydraulic conductivity, K(h), and moisture retention, θ(h), functions for the low and high salinity regions in field 1. SAR increase for the low and high salinity regions was changed from a starting value of 5 to 25.

change in the SAR treatment soils is swelling. This process changes the entire volume of soil, as well as effectively reducing the PSD and shifting it towards a smaller average pore radius and greater moisture retentions. The likely mechanism for reduced hysteresis is the overall shift in PSD towards smaller radii and a reduction in the required soil water pressure required to wet the soil. Another mechanism that may reduce hysteresis is reduced air entrapment with swelling soil.

The change in pore connectivity (L parameter) for the SAR series was minimal for the low salinity region (Figure 34).

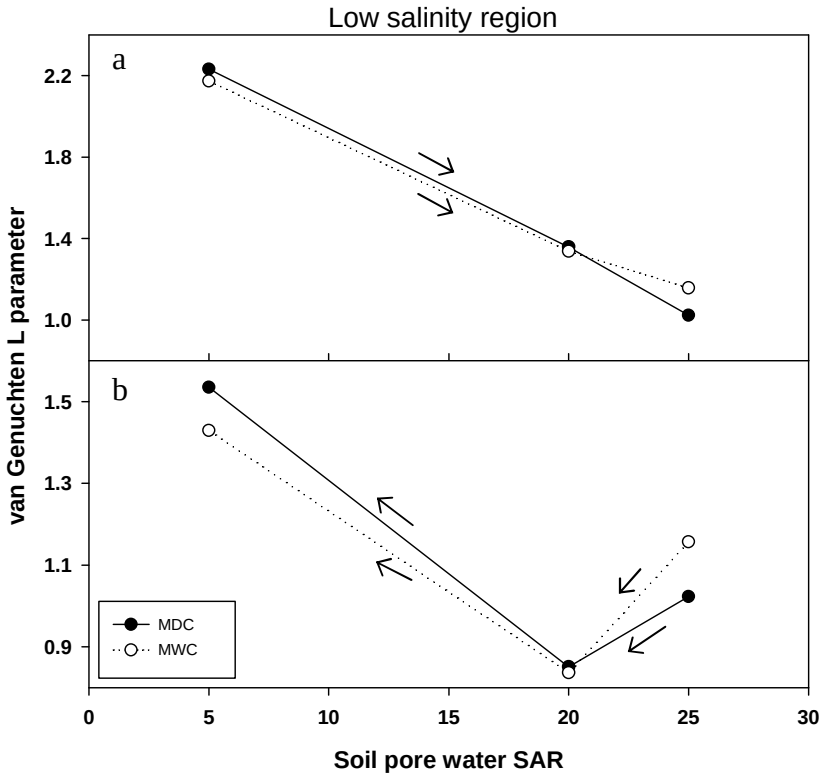

Figure 34: The difference in the van Genuchten L parameter for the low salinity region for the main draining and main wetting curves (MDC and MWC) with increased, a, and decreased, b, soil pore water sodium adsorption ratio (SAR).

For the entire SAR series, the average L value for the low salinity region changes much less than with the EC reduction series, which supports the swelling mechanism responsible for the reduction in K for the SAR series and the little to no change in hysteresis of the K(h) function. Note also the recovery in L with decreasing SAR which is expected with soil swelling.

For the high salinity region, the change in the L parameter is greater, although the L values increased which would suggest greater pore connectivity (Figure 35). Only at an SAR of 25 does the L value begin to decline and even then not below the lowest SAR treatment value.

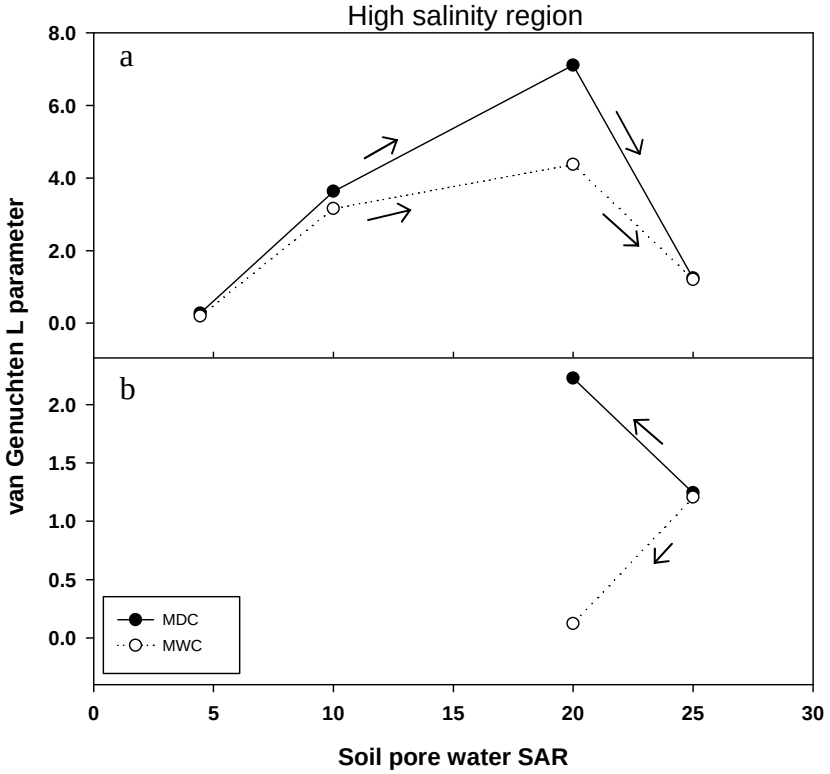

Figure 35: The difference in the van Genuchten L parameter for the high salinity region for the main draining and main wetting curves (MDC and MWC) with increased, a, and decreased, b, soil pore water sodium adsorption ratio (SAR).

Although the proportion of recovery in the L value with decreasing SAR was similar to that at the low salinity zone, the decline in L for the MWC with L increasing for the MDC is different and difficult to interpret. Exacerbating the interpretation of Figure 35 is the lack of data for the reduction in SAR.

The relationship between changing solution chemistry and pore connectivity is intriguing and potentially important. However, the L parameter for the K(h) function was not constrained during inverse analysis of the flow cell measurements which may add too much variability with only a single replicate to make any clear interpretation of the results. In fact, if the L parameter is plotted against the sum of squares (SSQ) for each individual inverse fit of the flow cell data (Figure 36), there is a significant correlation between the L value SSQ, with L values below approximately 0.15 having poor inverse fits (high SSQ), ($r^2 = 0.7741$, $p < 0.0001$, n = 36).

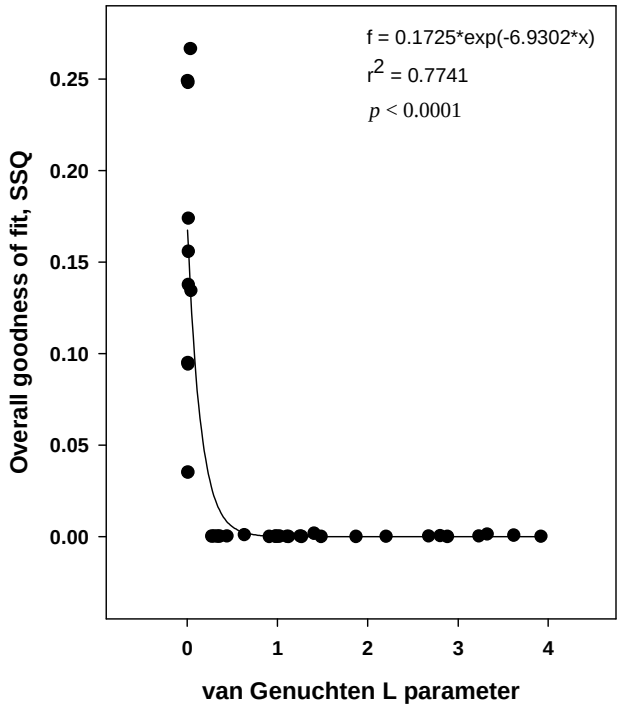

Figure 36: Regression of the van Genuchten L parameter with the sum of squares (SSQ) for the inverse fit of the flow cell measurements.

It may be that L should be constrained to retain a mechanistic relationship with pore connectivity and K(h), however a deliberate analysis of this issue is required to say definitively which is beyond the scope of this research project.

Spatial and Treatment Effects on Soil Air Entry Pressure

Changes in the air entry, h_i, soil water pressure with changing EC show ambiguous trends but are nevertheless significantly different with changing EC treatment, $F_{(3,8)} = 9.1133$, $p = 0.005847$. After removing the 0.25 dS m^{-1} treatment and repeating the ANOVA, the p-value was reduced only slightly, $F_{(2,6)} = 14.735$, $p = 0.004841$, but correlation between h_i and changes in EC was greatly improved, (r = -0.9033, $p = 0.0008$, n = 3; f=-20.0481+-1.3466*x), showing an increase (i.e. less negative) in air entry soil water pressure with reduced EC. Figure 37a shows the change in h_i for each salinity region with decreasing soil pore water EC.

The changes in h_i with increasing SAR show contrasting trends between salinity regions. Increases in SAR at the low salinity region induced a slight increase in h_i (Figure 37b). Increases in SAR at the high salinity region induced a decrease in h_i. Although h_i changes in opposite directions between the low and high salinity regions, the magnitude of change is small, and no significant difference between salinity regions in response to SAR treatments is observed, $W_{(n1 = 3,n2 = 3)} = 0.5$, $p = 0.1212$. Correlation between normalized h_i values and changes in SAR are modest and not significant for the low (r = +0.9749, $p = 0.1428$, n = 3; f=-25.5226+0.1112*x) or high (r = -0.8866, $p = 0.3061$, n = 3; f=-19.6181- 0.4712*x) salinity regions.

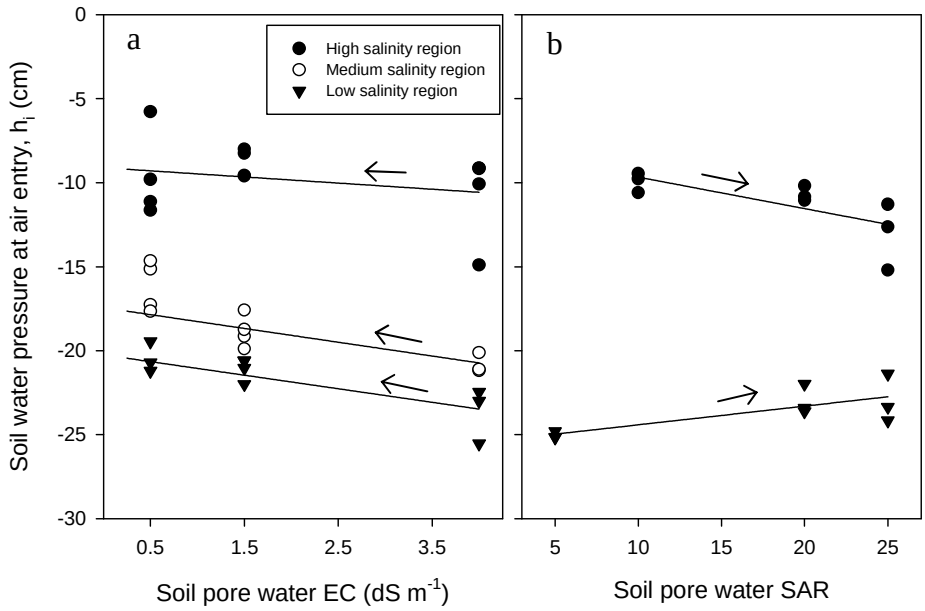

Figure 37: Change in soil water pressure (h_i) with changing soil pore water electrical conductivity, a, or sodium adsorption ration, b.

Attempts to recover native soil solution hydraulic properties by reducing the SAR back to native conditions (approximately SAR = 5) did result in modest improvements in h_i but also large variability between salinity regions which, along with an n = 2, resulted in no significant change in h_i from an SAR = 25, $W_{(n1=2,\ n2=2)} = 3.0$, $p = 0.6667$.

Effects of Solution Chemistry with Changing Soil Water Content

As noted several time in this discussion, the effects of changing soil solution EC or SAR on K(θ) do not appear constant between saturation and higher soil water tensions. This observation has been noted by several other studies (Chaudhari et al., 2010; Russo and Bresler, 1976, 1977; Wesseling and Oster, 1973) but has failed to draw much attention. In addition, most research have focused on the effects of solution SAR on K(θ)

in Na^+ dominated systems, ignoring changes not associated with shrink-swell behavior. This bias towards Na^+ dominated systems is understandable considering the systems in which the models were likely developed but appear to be ill suited to accurately predict $K(\theta)$ in Ca^{2+} dominated systems with limited shrink-swell potential.

Equation 12 shows the general model presented by Russo and Bresler (1976) to correct $K(\theta)$ for solution chemistry,

$$K^* = K(R, C, S_e) \,/\, K_{Ca}(S_e) \qquad \text{[Eq. 12]}$$

where K^* is the relative hydraulic conductivity and is a function of the Na^+ to Ca^{2+} ratio, R, the total soil solution concentration, C, and θ, which is expressed here as $S_e = (\theta_{obs} - \theta_r)/(\theta_s - \theta_r)$, and the reference hydraulic conductivity, $K_{ca}(S_e)$. The reference $K_{ca}(S_e)$ is for a soil in equilibrium with a 0.01 M $CaCl_2$ solution. Equation 12 was developed on clay soils dominated by montmorillonite which is not the case for the soils in this study. A modified form of the Russo and Bresler equation (Russo and Bresler, 1977) has been shown by Chaudhari *et al*. (2010) to deviate from observed $K(\theta)$ at lower water contents by underestimating K (i.e. over estimating the effects of solution chemistry).

Unlike the Russo and Bresler model, the Hydrus-1D model assumes solution chemistry affects K to the same extent at all θ. That is, the magnitude of reduction in K at saturation is applied across the entire $K(\theta)$ function. The virtue of this approach is that the Hydrus model is relatively simple and requires minimal work to determine parameter estimates. The general model used by Hydrus is,

$$K(h, pH, SAR, C_0) = r(pH, SAR, C_0)\, K(h) \qquad \text{[Eq. 13]}$$

where K at a particular h, pH, SAR, and total solution salt concentration, C_0, is equal to K at a non-salt affected condition multiplied by a reduction factor, r. Note that r is only a function of pH, SAR, and C_0, it does not consider water content or soil water tension. Similar to the Russo and Bresler models, the model used by Hydrus-1D is especially sensitive to changes in soil solution SAR, and is predominantly suited to address shrink/swell effects of solution chemistry on soils (see Šimůnek *et al*., 2009 for more details).

Relative Conductivity for the EC Reduction Series

Considering the results of this study, a similar approach to Russo and Bresler (1976) is used to examine $K(EC,S_e)$ or $K(SAR,S_e)$, where there relative hydraulic conductivity, K^*, is equal to the observed K, K_{obs}, at a particular EC or SAR, and S_e combination, divided by the reference K, K_{ref}, which is equal to the K under native soil solution concentrations (see table 2 for EC and SAR values). The $K(EC,S_e)$ functions are shown for the low, medium, and high salinity regions in Figure 32, 33, and 34.

The low salinity $K(EC,S_e)$ series shows a decline in K^* at saturation of more than 2 orders of magnitude with EC reduced from 3.73 to 0.25 dS m^{-1}. As S_e is reduced, K^* at all EC levels is reduced somewhat from K^* at saturation over the majority of the measured Se range. As S_e approaches θ_r, K^* declines sharply to over 5 orders of magnitude below saturated values. Figure 32 clearly illustrates a change in the effect of soil solution chemistry on hydraulic conductivity with changing water content.

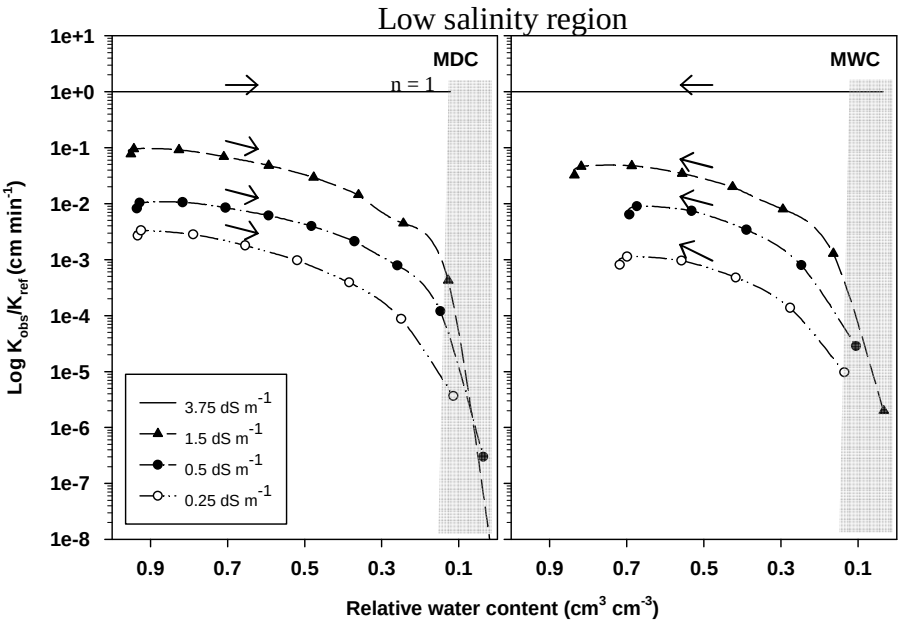

Figure 38: Ratio of K_{obs} (soil hydraulic conductivity at a particular electrical conductivity, EC, treatment) and K_{ref} (soil hydraulic conductivity at native salinity conditions) for the low salinity region at field 1. Functions are presented for both the main drainage curve, MDC, and main wetting curve, MWC. The shaded θ region represents portions of K(θ) extrapolated to water contents below the range measured by the flow cell using the inverse analysis and the 1.5 MPa water content.

As a point of emphasis, note that the plot of each K(EC,S_e) function should be horizontal if an equal reduction in K occurred at all θ values, which is clearly not the case for these soils. Recall that the Hydrus-1D model assumes the K(EC,S_e) functions are horizontal. All salinity regions (Figure 32-34) show a similar change in K(EC,S_e) in both the MDC and MWC.

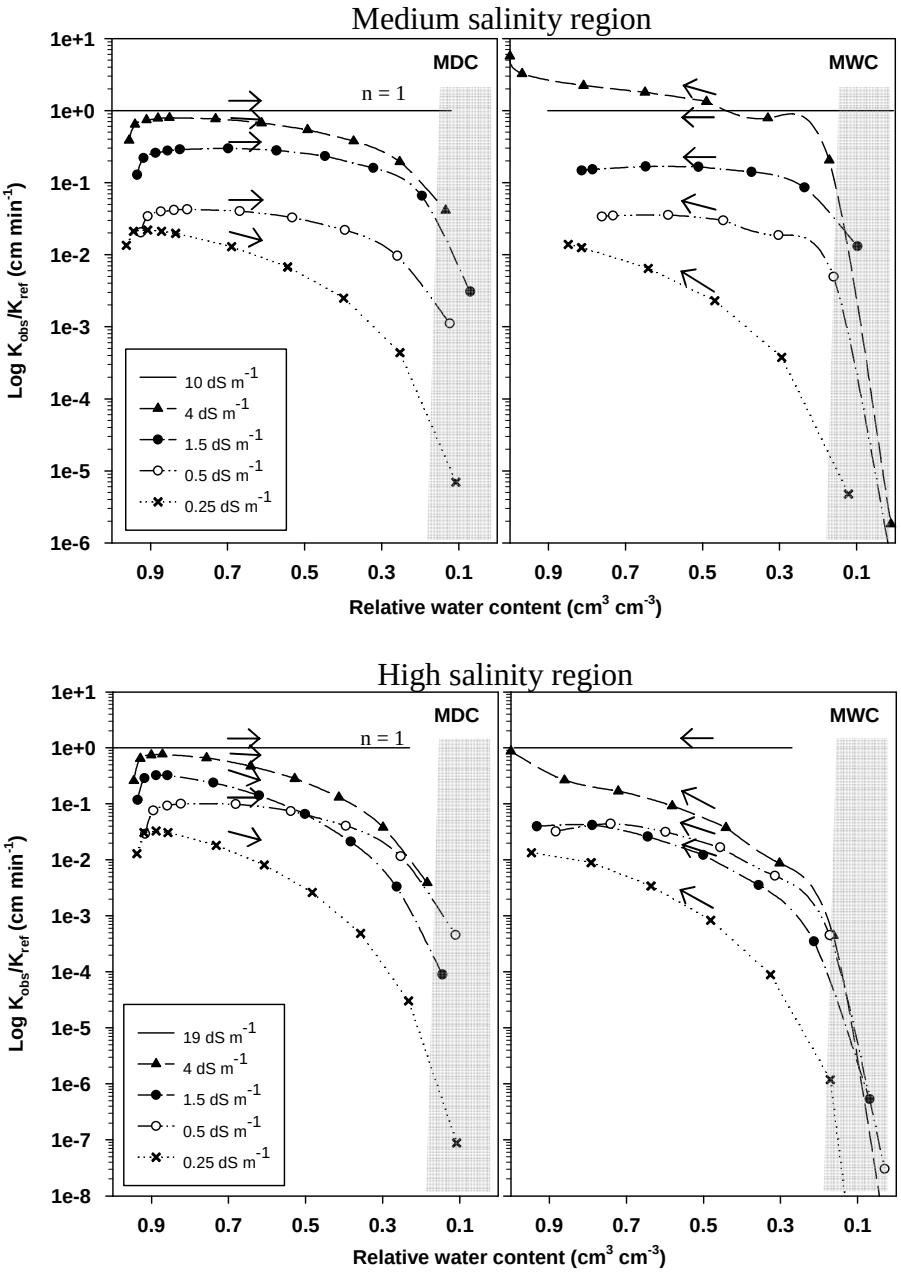

Figure 39 and 40: Ratio of K_{obs} (soil hydraulic conductivity at a particular electrical conductivity, EC, treatment) and K_{ref} (soil hydraulic conductivity at native salinity conditions) for the medium and high salinity regions at field 1. Functions are presented for both the main drainage curve, MDC, and main wetting curve, MWC. The shaded θ region represents portions of K(θ) extrapolated to water contents below the range measured by the flow cell using the inverse analysis and the 1.5 MPa water content.

Examining the relative hydraulic conductivity for the soils in this study, it is clear that consideration of solution chemistry on soil hydraulic properties is extremely important. Even without accounting for the change in K(θ) at lower soil water contents with changing solution chemistry, a significant portion of the reduction can be accounted for at Ks. However, because the Hydrus-1D model was likely developed for Na^+ dominated systems, its accuracy in predicting the soil K at different soil EC values in these soils is fairly poor. Experimentally determined values for Ks compared to predicted K_s values determined using the major ion chemistry model in Hydrus-1D are presented in Table 7 for the EC reduction series. The difference between measured vs. predicted K_s values increases significantly below a solution EC of 1.5 dS m^{-1} for the medium and high salinity regions. At or above 1.5 dS m^{-1}, the average measured decline for the medium salinity region from the native soil solution is 52.5%. For the predicted Ks, the decline at 1.5 dS m^{-1} is 18.1%. For the high salinity region, the average measured Ks actually increases by 19.5%. Recall that the native soil solution was at 19 dS m^{-1}, substantially higher than the medium or low regions. For the predicted Ks, the decline at 1.5 dS m^{-1} is 25.8%. Although the agreement between measured vs. predicted K_s values was not good above 1.5 dS m^{-1}, below 1.5 dS m^{-1} the Hydrus-1D model's ability to predict K_s becomes substantially worse. At 0.25 dS m^{-1}, the average measured decline for the medium salinity region from the native soil solution is 97.1% vs. only 55.0% for the Hydrus model. At 0.25 dS m^{-1}, the average measured decline for the high salinity region from the native soil solution is 88.3% vs. only 50.1% for the Hydrus-1D model.

Table 7: Comparison between measured and predicted K_{sd} values for the EC reduction series at each salinity region. The K_{sd} estimate by Hydrus-1D for each corresponding reduction in soil solution EC is higher for all EC solutions except for the 4 and 1.5 dS m^{-1} EC treatments for the high salinity region.

Salinity Region	EC Trmt (dS m^{-1})	SAR	K_{sd} Measured ------- (cm min^{-1}) -------	K_{sd} Hydrus	diff %
Low	3.73 N	7.78	$4.27e^{-2}$	$4.27e^{-2}$	0.0
	1.50	5.00	$1.16e^{-2}$	$3.87e^{-2}$	70.1
	0.50	5.00	$2.23e^{-3}$	$3.87e^{-2}$	94.2
	0.25	5.00	$3.69e^{-4}$	$1.88e^{-2}$	98.0
	5.00*	5.00	$2.96e^{-4}$	$4.58e^{-2}$	99.4
Medium	10.00 N	8.88	$2.21e^{-2}$	$2.21e^{-2}$	0.0
	4.00	5.00	$1.95e^{-2}$	$2.08e^{-2}$	6.3
	1.50	5.00	$1.05e^{-2}$	$1.81e^{-2}$	42.1
	0.50	5.00	$2.35e^{-3}$	$1.81e^{-2}$	87.0
	0.25	5.00	$6.38e^{-4}$	$9.95e^{-3}$	93.6
	5.00*	5.00	$1.29e^{-3}$	$2.14e^{-2}$	94.0
High	19.87 N	5.45	$3.41e^{-3}$	$3.41e^{-3}$	0.0
	4.00	5.00	$6.91e^{-3}$	$2.92e^{-3}$	136.2
	1.50	5.00	$4.07e^{-3}$	$2.53e^{-3}$	60.7
	0.50	5.00	$6.09e^{-4}$	$2.53e^{-3}$	76.0
	0.25	5.00	$3.98e^{-4}$	$1.70e^{-3}$	76.6
	5.00*	5.00	$7.59e^{-4}$	$3.00e^{-3}$	74.7

N = native soil conditions
* = soil solution EC increased back to 5 from 0.25 dS m^{-1}

For the low salinity region, the agreement between measured and predicted K_s values is poor even at 1.5 dS m^{-1}(62.5% vs. 9.5% predicted). The average measured decline at 0.25 dS m^{-1} for the low salinity region from the native soil solution is 99.1%. For the predicted K_s, the decline at 0.25 dS m^{-1} is 56%. Note, for all salinity regions, measured K_s does not recover after reduced EC vs. Hydrus-1D K_s values which recover 100%.

These large differences between observed and predicted K, especially at low EC values, reduce confidence in the model simulations in these salt affected soil. One

contributing factor to the poor model prediction may be the assumption that soil pH remained nearly constant during the EC sequence measurements. In hindsight, it would have been helpful to measure the pH of the effluent at each EC level to verify this and/or provide better information to the model.

Relative Conductivity for the SAR Reduction Series

For the SAR series, a similar trend in $K(SAR,S_e)$ was observed for both the MDC and MWC, with a decrease in K with higher SAR and lower S_e. The change in $K(SAR,S_e)$ for the low and high salinity regions is show in Figure 35 and 36. Once again, the relative K cures are not horizontal with diminishing water content illustrating a differential salinity effect. That is, the further from saturation, the greater the reduction in K with increasing SAR.

Although comparison between measured and predicted Ks values for the EC reduction series were poor, comparisons for the SAR soils showed much better agreement for the low salinity region. Experimentally determined values for Ks compared to predicted Ks values determined using the major ion chemistry model in

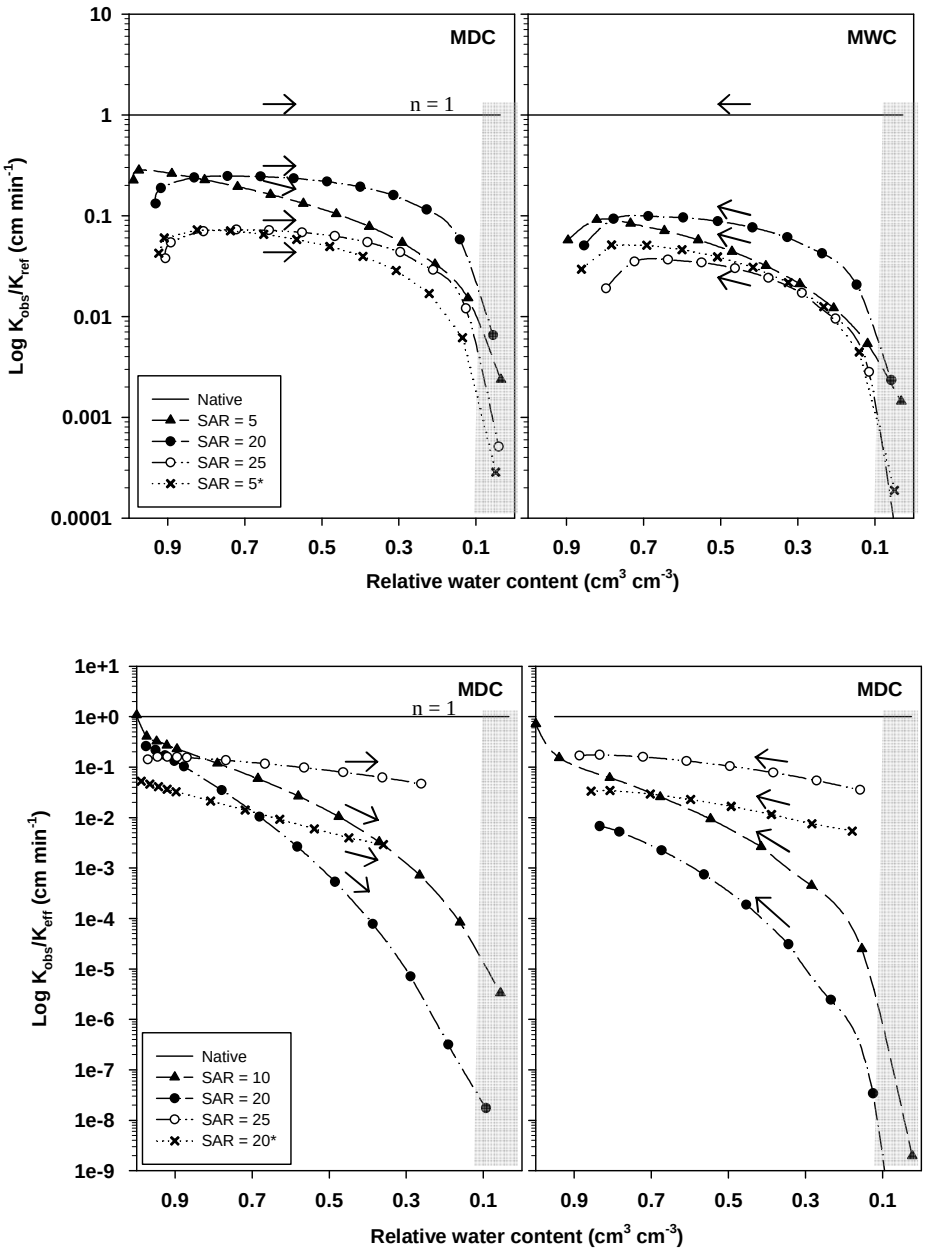

Figure 41 and 42: Ratio of K_{obs} (soil hydraulic conductivity at a particular sodium adsorption ration, SAR, treatment) and K_{ref} (soil hydraulic conductivity at native salinity conditions) measured along the moisture retention, θ(h), function for the low and high salinity region at field 1. Functions are presented for both the main drainage curve, MDC, and main wetting curve, MWC. The shaded θ region represents portions of K(θ) extrapolated to water contents below the range measured by the flow cell using the inverse analysis and the 1.5 MPa water content .

Hydrus-1D are presented in Table 8 for the SAR series. The difference between measured and predicted Ks values was moderate at all SAR treatments and showed no discernable trend with increasing SAR for the low salinity region. The percent difference between measured vs. predicted Ks values ranged from 5.1% to 87.8% and averaged 29.9% and 64.1% between SAR = 5 and 25 for the low and high salinity regions respectively. This is significantly better than agreement for the EC series (77.4%). Measurements of Ks recovery with reduced SAR agreed well with Hydrus-1D but only while still at relatively high SAR values (24.7%) and only for the low salinity region. At SAR values near native levels (and importantly at low total solution salt concentrations,

Table 8: Comparison between measured and predicted K_{sd} values for the SAR series for each salinity region. The K_{sd} estimate by Hydrus-1D for each corresponding increase in soil solution SAR is higher for all SAR treatment solutions.

Salinity Region	EC	SAR Trmt	K_{sd} Measured	K_{sd} Hydrus	diff
	($dS\ m^{-1}$)		($cm\ min^{-1}$)		%
Low	3.73	7.78 N	$3.87e^{-2}$	$3.87e^{-2}$	0.0
	0.65	5.00	$2.53e^{-2}$	$4.60e^{-2}$	45.0
	0.65	20.00	$1.50e^{-2}$	$1.58e^{-2}$	5.1
	0.65	25.00	$7.61e^{-3}$	$1.26e^{-2}$	39.6
	0.65	20.00*	$1.19e^{-2}$	$1.58e^{-2}$	24.7
	0.65	5.00*	$5.59e^{-3}$	$4.60e^{-2}$	87.8
High	19.87	5.45 N	$2.09e^{-2}$	$2.09e^{-2}$	0.0
	0.65	10.00	$6.90e^{-3}$	$2.04e^{-2}$	66.1
	0.65	20.00	$3.80e^{-3}$	$9.72e^{-3}$	60.9
	0.65	25.00	$2.60e^{-3}$	$7.51e^{-3}$	65.4
	0.65	20.00*	$1.30e^{-3}$	$9.72e^{-3}$	86.6

N = native soil conditions
* = soil solution SAR reduced from SAR =25

EC = 0.65) the agreement between measurements and predictions is poor (average of 87.2% for both regions). The agreement between measured and predicted values for the high salinity region was not as good (61.4%) but still averaged lower than EC series at

the low and high salinity regions. Agreement between K_s estimates for the SAR reduction for the high salinity regions was not good even at high SAR values (86.6%). Russo and Bresler (1977) note a similar discrepancy as stated earlier. They compared their findings, measured in a montmorillonite dominated clay soil, to those of Quirk and Scholfield (1955), who reported measurements for an illite dominated clay soil. Russo and Bresler (1977) equate the difference primarily to differences in mineralogy and mechanical composition of the two soils. The mineralogy of the soils in this system is closer to the illite dominated soil studied by Quirk and Scholfield (1955).

CONCLUSIONS AND IMPLICATIONS

Widespread issues with saline and sodic soils throughout the U.S. and else ware cause extensive losses in crop yields and income annually. And although the result of higher saline or sodic soils is the same everywhere, the conditions that lead to the buildup of salts and the management and remediation strategies can differ dramatically. Having a detailed and region specific understanding of the soil, water, and plant interactions with salinity is vital in developing an effective region specific salinity management strategy.

Solution Chemistry and Relative Hydraulic Conductivity

A key finding of this research is confirmation that the effect of solution chemistry on soil hydraulic conductivity is not constant with decreasing water content. The mechanisms responsible for the effect of soil water content on the solution chemistry reduction of soil hydraulic conductivity were not part of this study. However, it is possible to gain insight from the literature. As stated earlier, Russo and Bresler (1976) speculate that in swelling soils, the change in K^* with increasing soil water tension at high SAR values is due to a reduction in swelling as water is removed from the soil and thus pore space is partially recovered. This seems reasonable for swelling soils and high SAR levels but does not explain changes due to increasing SAR in this study since K^* clearly declines with increasing soil water tension.

Figure 37 show the characteristic curve of $K^*(EC,S_e)$ for the MDC at the low salinity region and is representative of $K^*(EC,S_e)$ functions for EC reduction series at all salinity regions. The overall reduction in K* at higher soil water tensions can be explained by hydraulic conductivity dominated by larger pores at or near saturation in which dispersed clay particles would have little effect. As K* is reduced, hydraulic conductivity is dominated by capillaries which become increasingly blocked or constricted by dispersed clays.

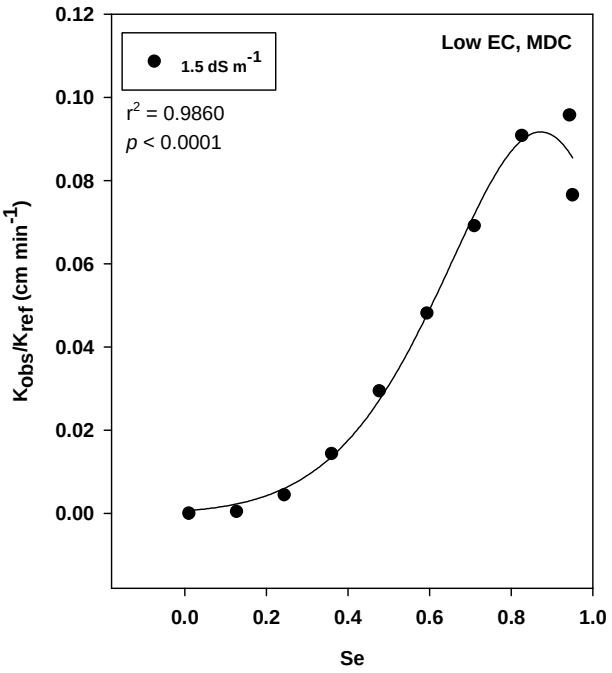

Figure 43: Regression of the characteristic reduction in K_{obs}/K_{ref} (K^*) with reducing S_e. Example curve is for the MDC of the low salinity region at EC = 1.5 dS m^{-1}. All K^* functions fit this general form.

The salinity impact on hydraulic conductivity clearly has important implications to salinity remediation practices. For example, models may over estimate drainage if soil

solution chemistry is not considered or only considered to be constant over the entire soil water tension range. Similarly, if drainage is actually less than expected, these same models are likely to underestimate groundwater salinity due to a lack of dilution from recharge.

Model Parameterization and Soil Heterogeneity

Predicting how a system will respond to changes in quantity and/or quality of water requires researchers to balance the capture of as much detail as possible through direct measurement or observations and the time and financial constraints of the project. Optimally, one would measure everything and know with certainty how the soils would respond. Of course this is not possible, even with projects as well funding and with extensive long term datasets such as the one associated with this research project, there is significant uncertainty in many of the estimates associated with salinity management.

The balance between accurate, detailed analysis and less accurate (although maybe no less precise) but fast and less expensive methods of parameter estimation is what prompted the comparison between the Rosetta PTF model and observed data. The results of this comparison show potential in estimating essential hydraulic model input parameters using basic soil measurements such as soil texture and bulk density as long as the heterogeneity of the system is well characterized. For these soils, $\theta(h)$ and Ks were highly correlated to percent sand. This relationship may be even better expressed if the error inherent in measuring the sand fraction of the soil is minimized. The hydrometer method is very sensitive to user error when determining the sand fraction. A more accurate method incorporates the hydrometer method for silt and clay fraction, but

gravimetrically determines the sand fraction following the 7 hour hydrometer reading by sieving with a 53 micron screen.

Continued management of the salinity issues in the Arkansas River Valley may benefit from future investigation of PTFs like Rosetta which were able to predict relative differences between soils with reasonably good precision in this study. It is clear from analysis of soil hydraulic properties from the 3 salinity regions, that the hydraulic properties of these soils are spatially variable. Burkhalter and Gates (2005) modeled groundwater recharge and salinity over a large section of the valley west of John Martin Reservoir. This study assumed homogeneity of soil properties on a scale of 250 m. Based off the current study, a cell size of 250 m is much too large to capture the heterogeneity of even the field scale. That said, the Burkhalter and Gates study examined basin scale recharge and considered more than 16,000 cells. Reducing the cell size to something that catches the heterogeneity of a soil like field 1 could easily place the number of cells well over 100,000 and out of the range of feasibility.

Surface Crusting and Leaching Efficiency

Considering data from both *in situ* and lab analyses, solution chemistry with an electrical conductivity below 1.5 dS m^{-1} and with a low to moderate sodium adsorption ratio (approx. 5), appears to be a threshold value for clay dispersion and disruption of these specific soils. The 1.5 dS m^{-1} value was nearly constant between all soils collected from all salinity and for *in situ* infiltration measurements. These findings agree well with those of Ayers and Westcot (1985), who predict a moderate reduction in infiltration capacity below an EC of 1.5 dS m^{-1} at an SAR ≈ to 7.5. Based off these results, use of

irrigation water at an EC much less than 1.5 dS m^{-1} should be discouraged to prevent crusting of the soil surface and to maintain the leaching efficiency of the system.

However, it is important to acknowledge the difference between *in situ* and lab observations in K reduction – *in situ* K_{sat} was significantly reduced only at EC values of 0.5 dS m^{-1} or less (trend in K_{sat} observed starting at 1 dS m^{-1} but not statistically significant from EC = 2), where as lab experiments saw a significant change at 1.5 and below. This slight difference between lab and field observations likely reflects the buffering capacity of the field soils due to high gypsum concentrations which was effectively removed from lab soil cores due to leaching prior to flow cell measurements. The reduction in hydraulic conductivity in field treatments was not as severe as lab measurements (approximately 1 vs. 2 to 4 orders of magnitude). Whether the reduction in infiltration under field conditions is significant to irrigation management was not part of this study but should be considered along with any irrigation water quality recommendation.

If the observed reductions in hydraulic conductivity are important practically speaking, there could be consequences if applying improved irrigation water. In the Burkhalter and Gates (2005) model mentioned above, the leaching efficiency is presumed constant. However, in any system where irrigation water below the suggested threshold value is applied or rainfall during the summer monsoon where large convective storms are typical, significant reductions in groundwater recharge could be observed. This lack of recharge, as mentioned above, will impact water quality for downstream users and may have water rights implications.

A simulation examining the effect of solution chemistry on cumulative infiltration for both the low and high salinity regions was performed using the major ion chemistry component of Hydrus-1D. The major ion chemistry component does consider solution chemistry effects on soil hydraulic properties but as mentioned above, the reduction factor applied to K is equal at all water content values. Although the model did not accurately match the salinity induced K_{sat} and K_{unsat} reductions observed in this soil, it is a useful tool to examine the relative impacts caused by changes in irrigation water quality in the field.

The simulated involved a 3 hour irrigation event on a free draining, 150 cm deep soil with a constant 5 cm head at the soil surface. The irrigation water quality was one of 4 treatments – rain water, ditch water, groundwater, and as a positive control coal bed methane (CBM) effluent (Table 9). Inputs for the water flow component of the simulation included the average native soil hydraulic properties for the low and high salinity regions. Soil chemistry input parameters were estimated from the soil chemical analyses performed for each salinity region; soil BD and CEC for each salinity region were also used. Because of high endemic gypsum concentrations and because soil extractions constitute total concentrations (i.e. both solution and solid concentrations), the fractionation of major ions in solution had to be estimated by iterating concentrations until they matched observed soil water EC values. The Gapon selectivity constants for Ca^{2+}, Mg^{2+}, and Na^{+} (i.e. the molar concentrations in solution) were determined from the final ion fractionations determined above along with empirical relationships with clay percentage and type.

Table 9: Simulated irrigation water quality chemistry for the simulation of water quality effects on cumulative infiltration for both the low and high salinity regions in field 1. Rain, ditch, and groundwater are all data collected from the Rocky Ford Experimental Station. The coal bed methane (CBM) effluent (McBeth *et al*., 2003) is used only as a positive control to induce a dramatic response in the cumulative infiltration of the soils.

Water source	Ca	Mg	Na	K	SO4	Cl	Alk	EC	SAR
	---------- (mg L^{-1}) ----------							($dS\ m^{-1}$)	
Rain	0.170	0.008	0.013	0.008	0.192	0.000	0.120	0.030	0.044
Ditch	5.540	2.780	2.790	0.110	4.680	0.100	3.010	1.370	1.300
Ground	14.120	6.320	5.780	0.070	21.940	2.400	1.470	3.700	1.810
CBM	1.910	2.550	16.410	0.340	2.480	0.390	18.140	1.900	11.000

For this simulation, soil pH was approximately equal to the average native value at each salinity region and estimated by iterating the alkalinity of the system until it approximated observed values. The actual measurement of changing soil solution pH with changing water quality treatments was not conducted for this project. For demonstration purposes this is reasonable; however, to accurately model the change in K for these soils, the soil pore water pH would need to be measured with changing irrigation water treatments.

Results of the simulation for cumulative infiltration are shown in Figure 38. There are several things to note; first, the cumulative infiltration for the high salinity region is approximately half that at the low salinity region for all irrigation water treatments except CBM effluent. This is because of the lower native K for the high salinity region. More importantly however, for the low salinity region, changing irrigation water quality induces a change in cumulative infiltration whereas at the high salinity region, cumulative infiltration is nearly identical for all irrigation water treatments. At the low salinity region cumulative infiltration is reduced with reducing irrigation water EC (i.e. infiltration for groundwater > ditch water > rain water). The

exception to this is the CBM effluent which has a low EC but high SAR; this induces a large reduction in infiltration due to swelling.

Here again we see more evidence for the buffering capacity of the high gypsum concentrations, especially at the high salinity region. Although this simulation does not say much about the overall importance of increased irrigation water quality, it follow that a higher EC threshold for irrigation water quality is more likely in regions with lower initial salt concentrations. The soils in Figure 38 were found in close association in a single field. Clearly, a threshold EC for irrigation water would be spatially variable and should probably be based on the most susceptible sub-region of a field, not by the average conditions.

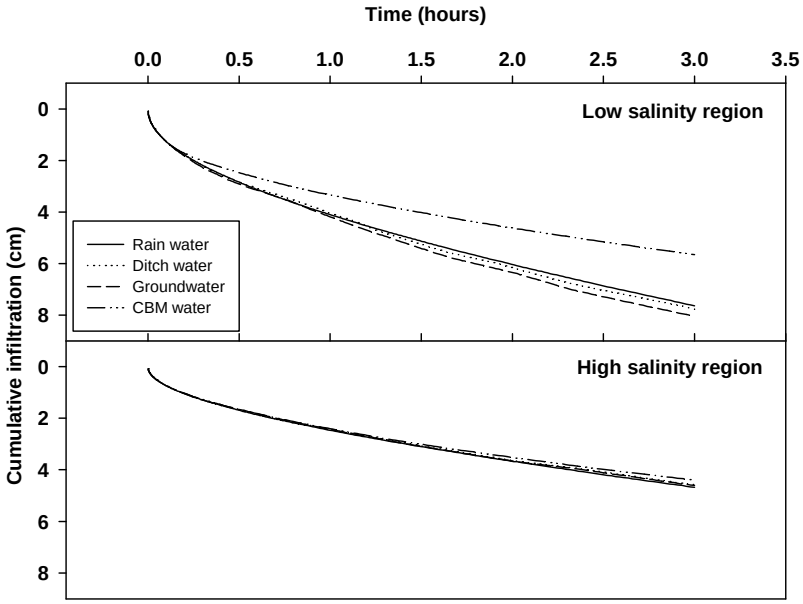

Figure 44: Simulated changes in soil hydraulic conductivity with changing solution chemistry.

Implications of Soil Water Hysteresis

The hysteresis, or difference, between the draining and wetting K(h) function in these soils was shown to become more pronounced with reduced EC. The reduction in

EC caused a slight reduction in hysteresis for the θ(h) function at the low salinity region and appeared to have no effect on θ(h) at the medium and high salinity regions. It is unclear from these results alone, whether an increase in soil water hysteresis will have implications in these fields.

To examine the potential effects of increasing soil water hysteresis on the drainage and water balance of a soil, a simulation involving multiple wetting and draining cycles was run using Hydrus-1D. The simulated ran for 80 days and involved a 3 hour irrigation event every 7 days at a rate of 1 cm hr^{-1}. The soil was a generic loam, free draining, and 90 cm deep. The simulation also included root growth and root water uptake for a crop of corn initiated at germination and increasing to a maximum rooting depth of 90 cm and maximum LAI after 50 days. Root water extraction for the crop was reduced at 0.1 MPa and ceased at 0.78 MPa. The potential evapotranspiration for the system was constant at 0.7 cm day^{-1}. No major ion chemistry or solution chemistry changes were considered for this simulation. Three hysteresis scenarios were considered, 1) no hysteresis in which the α_w/α_d ratio was equal to 1, 2) weak hysteresis in which the α_w/α_d ratio was equal to 1.5, and 3) strong hysteresis in which the α_w/α_d ratio was equal to 2.36 (absolute ratio values are arbitrary).

Results of the soil water hysteresis simulation are shown in Figure 39. As the α_w/α_d ratio increases and the soil becomes more hysteretic, the cumulative drainage for the strongly hysteretic soil in this simulation is reduced nearly one and a half times the no hysteresis amount after 80 days. For the cumulative evaporation, the trend is reversed, with increased evaporation with increasing soil water hysteresis and 25 to 30 percent

increase in evaporative loss after 80 days between the no hysteresis and strong hysteresis soils.

It appears that the changes in soil water hysteresis, which could be induced by changes in solution chemistry, have potential to cause important changes in the drainage and soil water storage of a region. The reduction in drainage from a soil due to hysteresis alone could have implications for groundwater recharge and water quality. Additional work is needed to determine the relevance of increased hysteresis *in situ* and whether the α_w/α_d ratio of the bulk soil must change in order to observe important changes in water storage

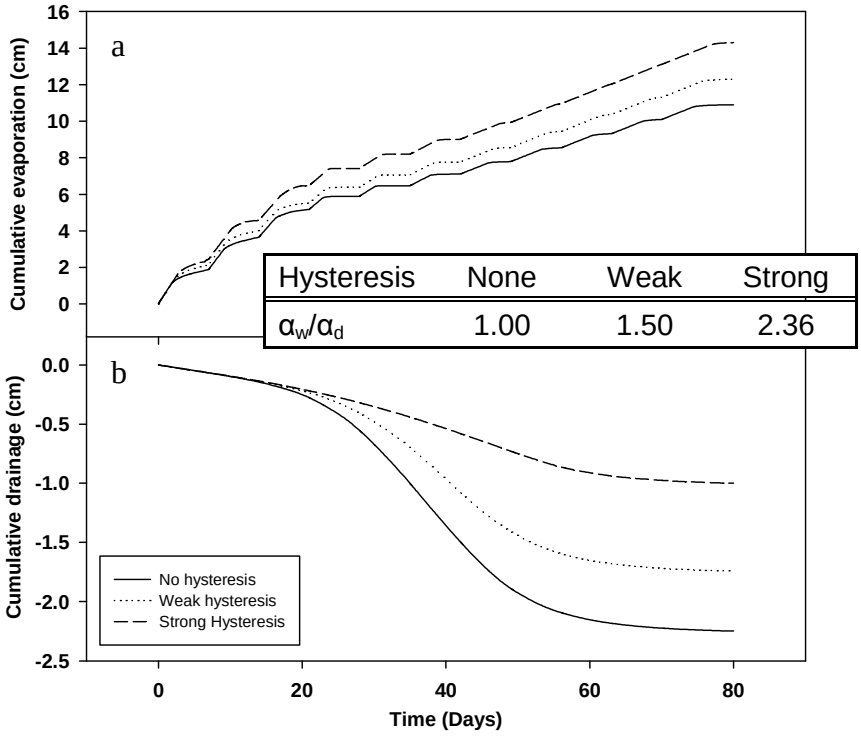

Figure 45: Simulated changes for a generic loam soil in cumulative soil evaporation (a), and cumulative drainage (b) under three different conditions of soil water hysteresis (none, weak, and strong). The larger the α_w/α_d ratio, the greater the hysteretic properties of the soil.

or if changes in the α_w/α_d ratio at the surface are enough to diminish drainage and/or increase evaporative loss.

This creates a system were irrigation water quality could be especially important because more of the salts therein will remain at or near the soil surface. Speculating about the potential effects of reduced drainage and increased evaporation, it is possible that the accumulation of salts would actually create a negative feedback to the effects of improved irrigation water quality and increased hysteresis. However, since the initial increase in hysteresis is caused by the dispersal of clay particles, the theoretical positive impacts of salt accumulation and reduction in hysteresis may effectively have no impact other than increased osmotic stress for crops.

Recommendations

Based on the findings of this and other research projects, management of salinity problems in the lower Colorado Arkansas River Valley should focus on four primary issues. 1) Although not directly examined as part of this study, lowering the groundwater level, in light of the mitigation practices focus on in this project, appears to be the most viable salinity mitigation option (Burkhalter and Gates, 2005). Without lowered water tables, it is unlikely that soil salt concentrations can be substantially reduced. 2) Application of the highest quality irrigation water possible but not below the suggested threshold value of 1.5 dS m^{-1}. This improved water quality will come as a result of reduced dissolution of endemic gypsum and increased overall water volume if water tables are lowered (Gates *et al*., 2006). 3) Integration of solution chemistry into soil hydraulic models to account for soil surface crusting, increased soil water hysteresis,

and overall reductions in groundwater recharge. 4) Incorporation and increased understanding of soil property heterogeneity in estimating soil hydraulic properties.

The lower Colorado Arkansas River Valley presents several unique challenges in managing and mitigating the highly saline soils of the region. In particular, large outtake upstream, low flow rates and channel silting, year round water storage in basins and ditches, and high concentrations of endemic gypsum have created conditions in which salts severely reduce crop yields and high water tables preventing effective salt mitigation through leaching. The larger group associated with this research project has worked extensively to understand the details and magnitude of salinity problems in the lower Arkansas River Valley and have developed many good management strategies for the region. However, by applying the major findings of this research project to current salinity/soil-water models, better success in mitigating problems associated with salinity is likely.

REFERENCES

Ayers, R. S., and D. W. Westcot. 1985. Water quality for agriculture. p. 13-74. *In* FAO irrigation and drainage paper 29, rev. 1. Food and Agriculture Organization of the United Nations, Rome, Greece.

Burkhalter, J. P. and T. K. Gates. 2005. Agroecological Impacts from Salinization and Waterlogging in an Irrigated River Valley. *Journal of Irrigation and Drainage Engineering*, 131:197–209.

Burkhalter, J. P., T. K. Gates, and J. W. Labadie. 2000. Pg. 205-223. Model and Field Studies to Manage Saline Shallow Water Tables in the Lower Arkansas Valley, Colorado. Proceedings of the USCID International Conference: Challenges Facing Irrigation and Drainage in the New Millennium, Vol. I, Technical Sessions, U.S. Committee on Irrigation and Drainage, Fort Collins, CO.

Butters, G. L., and P. Duchateau. 2002. A continuous flow method for rapid measurement of soil hydraulic properties. I. Experimental considerations. *Vadose Zone Journal*, 1:239-251.

Chaudhari, S. K., R. Singh, and A. Kumar. 2010. Suitability of a hydraulic-conductivity model for predicting salt effects on swelling soils. *Journal of Plant Nutrition and Soil Science*, 173:360–367.

Dane, J. H., and J. W. Hopkans. 2002. The Soil Solution Phase: Laboratory. pp.688-689. *In* J.H. Dane and G.C. Topp editors. Methods of Soil Analysis, Part 3 - Physical Methods. Soil Science Society of America. Madison, WI.

Dane, J. H. and A. Klute. 1977. Salt Effects on the Hydraulic Properties of a Swelling Soil. *Soil Science Society of America Journal*, 41:1043-1049.

DiNatale, K., W. Davis, R. Brown, S. Morea, J. Rehring, and N. Rowan. 2005. Colorado State Wide Supply Initiative. American Water Works Association Annual Conference, Denver, CO.

Duncan, R. R., R. N. Carro, and M. Huck . 2000. Understanding Water Quality and Guidelines to Management: An overview of challenges for water usage on golf courses for the 21st century. *Green Section Record*, United States Geological Association, 14-24.

Eldeiry, A. A. and L. A. Garcia. 2008. Detecting Soil Salinity in Alfalfa Fields using Spatial Modeling and Remote Sensing. *Soil Science Society of America Journal*, 72:201-211.

Gates, T. K., L. A. Garcia, and J. W. Labadie. 2006. Toward optimal water management in Colorado's Lower Arkansas River Valley: monitoring and modeling to enhance agriculture and environment. *Colorado Water Resources Res. Inst. Completion Report No. 205, Colorado Agric. Exp. Station Tech. Report TR06-10*, Colorado State University, Fort Collins, CO.

Gates, T. K., J. P. Burkhalter, J. W. Labadie, J. C. Valliant and I. Broner. 2002. Monitoring and Modeling Flow and Salt Transport in a Salinity-Threatened Irrigated Valley. *Journal of Irrigation and Drainage Engineering*, 128:87-99.

Gates, T. K. and M. E. Grismer. 1989. Irrigaton and Drainage Strategies in Salinity-affected Regions. *Journal of Irrigation and Drainage Engineering*, 115:255-284.

Gee, G.W., and D. Or. 2002. Particle-Size Analysis. p. 255-283. *In* J.H. Dane and Clark Topp, F. editors, Methods of Soil Analysis. Part 4, Physical Methods. Soil Science Society of America, Inc., Madison, Wisconsin, USA.

Ghassemi, F., A. Close, and J. R. Kellett. 1997. Numerical models for the management of land and water resources salinization. *Mathematics and Computers in Simulation*, 43:323-329.

Ghassemi, F., A. J. Jackeman, and H. A. Nix. 1995. Salinization of land and water resources: Human causes, extent, management and case studies. *CAB Int*., Wallingford, UK.

Gillham, D. 2004. Data and Modeling of Irrigated Fields with Saline High Water Tables. *M.S. thesis*, Department of Civil and Environmental Engineering, Colorado State University, Fort Collins, CO.

Goff, K., M. E. Lewis, M. A. Person, and L. F. KoniKow. 1998. Simulated Effects of Irrigation on Salinity in the Arkansas River Valley in Colorado. *Ground Water*, 36:76-86.

Green, C. H. 2001. The Solubility of Manganese and Coincident Release of Copper, Iron, Nickel, and Zinc Based on the Reduction-Oxidation of Alamosa River Basin Soils. M.S. thesis. Colorado State University, Fort Collins.

Hillel, D. 2000. Salinity Management for Successful Irrigation: integrating science, environment, and economics. *The World Bank*, Washington D.C., USA.

Houk, E., M. Frasier, and E. Schuck. 2006. The agricultural impacts of irrigation induced waterlogging and soil salinity in the Arkansas Basin. *Agricultrual Water Management*, 85:175-183.

Integrated Decision Support Group. Unpublished figures. Dep. of Civil and Environmental Engineering, Colorado State University, Fort Collins, CO.

Keren, R., and G. A. O'Connor. 1982. Gypsum Dissolution and Sodic Soil Remediation as Affected by Water Flow Velocity. *Soil Science Society of America Journal*, 46:726-732.

Keren, R., and I Shainberg. 1981. Effect of Dissolution Rate on the Efficiency of Industrial and Mined Gypsum in Improving Infiltration of a Sodic Soil. *Soil Science Society of America Journal*, 45:103-107.

Khavari-Nejad, R. A. and N. Chaparzadeh. 1998. The effects of NaCl and CaCl2 on photosynthesis and growth of alfalfa plants. *Photosynthetica*, 35:461- 466.

Klute, A. 1986. Water retention: Laboratory methods. p. 635–662. *In* A. Klute (ed.) Methods of soil analysis. Part 1. 2nd. ed. Agron. Monogr. 9. ASA and SSSA, Madison, WI.

Lajtha, K., and W. H. Schlesinger. 1988. The effects of CaCO3 on the uptake of phosphorous by two desert shrub species, Larrea tridentate (DC.) cov and Parthenium incanum H. B. K. *Botanical Gazette* 149:328-334.

Lefkoff, L. J. and S. M. Gorelick. 1990. Simulating physical processes and economic behavior in saline, irrigated agriculture: model development . *Water Resources Research*, 26:1359-1369.

Levy, G. J., D. Goldstein, and A. I. Mamedov. 2005. Saturated Hydraulic Conductivity of Semiarid Soils: Combined Effects of Salinity, Sodicity, and Rate of Wetting. *Soil Science Society of America Journal*, 69:653–662.

Mamedov, A. I., G. J. Levy, I. Shainberg, and J. Letey. 2001. Wetting rate, sodicity, and soil texture effects on infiltration rate and runoff. *Australian Journal of Soil Resources*, 39:1293–1305.

McBeth, I. H., K. J. Reddy, and Q. D. Skinner. 2003. Coalbed Methane Product Water Chemistry in Three Wyoming Watersheds. *Journal of the American Water Resources Association – JAWRA*, 39:575-585.

McNeal, B. L. 1968. Prediction of the Effect of Mixed-Salt Solutions on Soil Hydraulic Conductivity. *Soil Science Society of America Proceedings*, 32:190-193.

McNeal, B. L., N. T. Coleman. 1966. Effect of Solution Composition on Soil Hydraulic Conductivity. *Soil Science Society of America Proceedings*, 30:308-312.

Mer, R. K., P. K. Prajith, D. H. Pandya and A. N. Pandey. 2000. Effect of Salts on Germination of Seeds and Growth of Young Plants of Hordeum vulgare, Triticum aestivum, Cicer arietinum and Brassica juncea. *Journal of Agronomy and Crop Science*, 74:198-106.

Miller, L. D., K. R. Watts, R. F. Ortiz, and T. Ivahnenko. 2010. Occurrence and Distribution of Dissolved Solids, Selenium, and Uranium in Groundwater and Surface Water in the Arkansas River Basin from the Headwaters to Coolidge, Kansas, 1970–2009. Scientific Investigations Report 2010–5069. U.S. Geological Survey, Reston, Virginia.

Miles, D. L. 1977. Salinity in the Arkansas Valley of Colorado. Colorado State University, Cooperative Extension Service. Region VIII, Environmental Protection Agency, Denver, Colorado.

Moore, D. M. and R. C. Reynolds, Jr. 1997. X-Ray Diffraction and the Identification and Analysis of Clay Minerals: 2nd ed. Oxford University Press, New York.

Nelson, D. W. and L. E. Sommers. 1996. Total Carbon, Organic Carbon, and Organic Matter. pp.975-977. *In* D.L. Sparks editor. Methods of Soil Analysis, Part 3 – Chemical Methods. Soil Science Society of America. Madison, WI.

Oster, J. D. 1994. Irrigation with poor quality water. *Agricultural Water Management*, 25:271-297.

Oster, J. D. and F. W. Schroer. 1979. Infiltration as Influence by Irrigation Water Quality. *Soil Science Society of America Journal*, 43:444-447.

Purkey, D. R. and W. W. Wallender. 2001a. Habitat Restoration and Agricultural Production Under Land Retirement. *Journal of Irrigation and Drainage Engineering*, 127:140-145.

Quirk, J. P. 1994. Interparticle Forces: A Basis for the Interpretation of Soil Physical Behavior. *Advances in Agronomy*, 53:121-183.

Quirk, J. P. and R. K. Schofield. 1955. The effect of electrolyte concentration on soil permeability. *Journal of Soil Science*, 6:163-178.

R Development Core Team. 2008. R: A language and environment for statistical computing. R Foundation for Statistical Computing, Vienna, Austria. ISBN 3-900051-07-0, URL http://www.R-project.org.

Reynolds, W. D. and D. E. Elrick. 1995. Pounded Infiltration From a Single Ring: I. Analysis of Steady Flow. *Soil Science Society of America Journal*, 54:1233-1241.

Rhoades, J.D. 1996. Salinity: Electrical Conductivity and Total Dissolved Solids. pp.417-435. *In* D.L. Sparks editor. Methods of Soil Analysis, Part 3 – Chemical Methods. Soil Science Society of America. Madison, WI.

Rietz, D. N. and R. J. Haynes. 2003. Effects of irrigation-induced salinity and sodicity on soil microbial activity. *Soil Biology and Biochemistry*, 35:845-854.

Russo, D. and E. Bresler. 1977. Analysis of the Saturated-unsaturated Hydraulic Conductivity in a Mixed Sodium-Calcium soil System. *Soil Science Society of America Journal*, 41:706-710.

Russo, D. and E. Bresler. 1976. Soil-Water-Suction Relationships as Affected by Soil Solution Composition and Concentration. Pp.287-296. *In* A. Banin and U. Kafkafi editors. Agrochmicals in soils. Pergamon Press Inc. New York, NY.

Sarig, S., E. B. Roberson, and M. K. Firestone. 1993. Microbial activity-soil structure: Response to saline water irrigation. *Soil Biology and Biochemistry*, 25:693-697.

Schaap, M. G., Leij F. J. and van Genuchten M. Th. 1998. Neural network analysis for hierarchical prediction of soil water retention and saturated hydraulic conductivity. *Soil Science Society of America Journal*, 62:847-855.

Schaap, M. G. and F. J. Leij. 1998a. Using Neural Networks to predict soil water retention and soil hydraulic conductivity. *Soil & Tillage Research* 47:37-42.

Shainberg, I. and J. Lety. 1984. Response of Soils to Sodic and Saline Conditions. *Hilgardia*, 52:1-57.

Sherrod, L. A., G. Dunn, G. A. Peterson and R. L. Kolberg. 2002. Inorganic Carbon Analysis by Modified Pressure-Calcimeter Method. *Soil Science Society of America Journal* 66:299-305.

Šimůnek, J., M. Šejna, H. Saito, M. Sakai, and M. Th. van Genuchten. 2009. The HYDRUS-1D Software Package for Simulating the One-Dimensional Movement of Water, Heat, and Multiple Solutes in Variably-Saturated Media. Version 4.08, IGWMC-TPS70. Int. GroundWater Modeling Center, Colorado School of Mines, Golden, CO.

Singh, P. N., W. W. Wallender, M. P. Maneta, S. L. Lee, and B. A. Olsen. 2010. Sustainable Root Zone Salinity and Shallow Water Table in the Context of Land Retirement. *Irrigation and Drainage Engineering*, 136:289-299, DOI: 10.1061/_ASCE_IR.1943-4774.0000065

Soltanpour, P. N. and A. P. Schwab. 1977. New Soil Test for Simultaneous Extraction of Macro-Nutrients and Micro-Nutrients in Alkaline Soils. *Communications in Soil Science and Plant Analysis*, 8:195-207.

Sumner, M. E. and W. P. Miller. 1996. Cation Exchange Capacity and Exchange Coefficients. pp.1209-1222. *In* J.H. Dane and G.C. Topp editors. Methods of Soil Analysis, Part 3 - Chemical Methods. Soil Science Society of America. Madison, WI.

SYSTAT. 2002. SYSTAT for Windows, Version 10.2. SYSTAT Software Inc., Richmond, California.

Thomas, G. W. 1996. Soil pH and Soil Acidity. pp.475-490. *In* J.H. Dane and G.C. Topp editors. Methods of Soil Analysis, Part 3 - Chemical Methods. Soil Science Society of America. Madison, WI.

Thorvaldson, J. and J. Pritchett. 2006. Economic Impact Analysis of Reduced Irrigated Acreage in Four River Basins in Colorado. *Colorado Water Resources Res. Inst. Completion Report No. 205,*Colorado State University, Fort Collins, CO.

van Genuchten, M. T. 1980. A Closed-Form Equation for Predicting the Hydraulic Conductivity of Unsaturated Soils. *Soil Science Society of America Journal*, 44:892-898.

Wang, H. L., M. J. Hedly, N. S. Bolan, D. J. Horne. 1999. The influence of surface incorporated lime and gypsiferous by-products on surface and sub-surface soil acidity: II. root growth and agronomic implications. *Australian Journal of Soil Resources*, 37:181-190.

Wesseling, J. and J. D. Oster. 1973. Response of Salinity Sensors to Rapidly Changing Salinity. *Soil Science Society of America Journal*, 37:553-557.

Whittemore, D. O., M. S. Tsou, and C. McElwee. 2000. Arkansas River Salinity and Contamination of the High Plains Aquifer. Pg. 225-247. Proceedings of the USCID International Conference: Challenges Facing Irrigation and Drainage in the New Millennium, Vol. I, Technical Sessions, U.S. Committee on Irrigation and Drainage, Fort Collins, CO.

Wittler, J. M., G. E. Cardon, T. K. Gates, C. A. Cooper, and P. L. Sutherland. 2006. Calibration of electromagnetic induction for regional assessment of soil water salinity in an irrigated valley. *Journal of Irrigation and Drainage Engineering-ASCE*, 132:436-444.

Yellow Springs Incorporated. 1989. YSI-35 conductivity meter manual. Yellow Springs, Ohio, USA.

Youngs, E. G. 1995. Development in the Physics of Infiltration. Soil *Science Society of America Journal*, 59:307-313.

SUPPLEMENTAL APPENDIX

Table 1: Average drainage curve van Genuchten parameters measured from flow cell runs for each salinity region in field 1 under native soil EC and SAR conditions. Parameters estimated using inverse analysis of drainage flow cell data only in Hydrus-1D.

Salinity Region	Core No.	EC	SAR	θ_r	θ_{sd}	K_{sd}	α_d	n	L	SSQ	Sample Size
		(dS m^{-1})		--- (cm^3 cm^{-3}) ---		(cm min^{-1})	(1 cm^{-1})				
Low	1	3.73	7.78	0.213	0.441	$4.27e^{-2}$	0.017	2.026	$1.27e^{+0}$	$2.37e^{-5}$	3
	2	3.73	7.78	0.204	0.442	$4.78e^{-2}$	0.019	1.673	$1.22e^{-2}$	$1.38e^{-1}$	3
	3	3.73	7.78	0.215	0.430	$5.04e^{-2}$	0.015	1.868	$3.92e^{+0}$	$7.93e^{-5}$	3
	4	3.73	7.78	0.211	0.442	$3.87e^{-2}$	0.020	1.657	$1.00e^{-2}$	$2.48e^{-1}$	3
	5	3.73	7.78	0.206	0.440	$4.35e^{-2}$	0.019	1.679	$1.31e^{-2}$	$1.56e^{-1}$	4
	6	3.73	7.78	0.203	0.447	$3.20e^{-2}$	0.016	1.975	$1.87e^{+0}$	$4.30e^{-5}$	4
Medium	1	10.00	8.88	0.277	0.458	$2.21e^{-2}$	0.017	1.858	$1.12e^{+0}$	$3.69e^{-5}$	3
	2	10.00	8.88	0.269	0.488	$3.96e^{-2}$	0.020	1.853	$1.00e^{+0}$	$9.82e^{-5}$	3
	3	10.00	8.88	0.270	0.467	$9.30e^{-3}$	0.019	1.624	$3.58e^{-2}$	$2.67e^{-1}$	3
	4	10.00	8.88	0.255	0.465	$1.25e^{-2}$	0.020	1.607	$6.43e^{-3}$	$9.51e^{-2}$	3
	5	10.00	8.88	0.261	0.444	$2.40e^{-2}$	0.019	1.65	$4.28e^{-2}$	$1.34e^{-1}$	3
	6	10.00	8.88	0.275	0.481	$1.48e^{-2}$	0.018	1.634	$4.18e^{-3}$	$2.49e^{-1}$	3
High	1	19.87	5.45	0.262	0.471	$1.25e^{-2}$	0.012	1.563	$2.80e^{+0}$	$4.90e^{-4}$	4
	2	19.87	5.45	0.259	0.451	$1.90e^{-2}$	0.020	1.703	$9.77e^{-1}$	$1.89e^{-4}$	3
	3	19.87	5.45	0.251	0.461	$2.93e^{-2}$	0.025	1.579	$3.00e^{-1}$	$3.74e^{-4}$	5
	4	19.87	5.45	0.263	0.453	$3.41e^{-3}$	0.017	1.579	$1.19e^{-2}$	$1.74e^{-1}$	5
	5	19.87	5.45	0.276	0.464	$1.42e^{-2}$	0.014	2.068	$2.88e^{+0}$	$9.39e^{-6}$	3
	6	19.87	5.45	0.281	0.462	$2.09e^{-2}$	0.015	1.942	$3.23e^{+0}$	$3.43e^{-4}$	3

Table 2: Average drainage curve van Genuchten parameters measured from flow cell runs for each salinity region in field 1 under native soil EC and SAR conditions. Parameters estimated using inverse analysis of both drainage and wetting flow cell data in Hydrus-1D.

Salinity Region	Core No.	EC	SAR	θ_r	θ_{sd}	K_{sd}	α_d	n	L	SSQ	Sample Size
		(dS m^{-1})		--- (cm^3 cm^{-3}) ---		(cm min^{-1})	(1 cm^{-1})				
Low	1	3.73	7.78	0.212	0.441	$4.10e^{-2}$	0.022	1.80	$3.58e^{-1}$	$2.12e^{-4}$	2
	2	3.73	7.78	0.208	0.442	$5.28e^{-2}$	0.025	1.90	$4.40e^{-1}$	$2.29e^{-4}$	2
	3	3.73	7.78	0.207	0.430	$5.00e^{-2}$	0.029	1.44	$3.62e^{+0}$	$7.57e^{-4}$	2
	4	3.73	7.78	0.211	0.443	$3.75e^{-2}$	0.023	1.81	$1.10e^{+0}$	$9.01e^{-5}$	2
	5	3.73	7.78	0.207	0.440	$4.44e^{-2}$	0.020	1.69	$2.20e^{+0}$	$7.09e^{-5}$	3
	6	3.73	7.78	0.195	0.447	$3.31e^{-2}$	0.022	1.54	$2.67e^{+0}$	$2.17e^{-4}$	2
Medium	1	9.99	8.88	0.279	0.458	$2.14e^{-2}$	0.023	1.60	$1.02e^{+0}$	$1.82e^{-4}$	2
	2	9.99	8.88	0.269	0.488	$4.07e^{-2}$	0.025	1.76	$3.36e^{-1}$	$2.13e^{-4}$	2
	3	9.99	8.88	0.270	0.467	$7.81e^{-3}$	0.019	1.62	$1.01e^{-2}$	$9.42e^{-2}$	2
	4	9.99	8.88	0.254	0.465	$1.15e^{-2}$	0.020	1.60	$7.18e^{-3}$	$3.52e^{-2}$	2
	5	9.99	8.88	0.263	0.444	$2.36e^{-2}$	0.018	1.83	$9.81e^{-1}$	$7.53e^{-5}$	2
	6	9.99	8.88	0.276	0.481	$1.43e^{-2}$	0.017	1.75	$1.48e^{+0}$	$3.22e^{-5}$	2
High	1	19.87	5.45	0.248	0.471	$1.14e^{-2}$	0.015	1.40	$3.33e^{+0}$	$1.32e^{-3}$	3
	2	19.87	5.45	0.252	0.451	$1.47e^{-2}$	0.025	1.50	$1.25e^{+0}$	$3.60e^{-4}$	2
	3	19.87	5.45	0.238	0.461	$3.06e^{-2}$	0.030	1.42	$6.34e^{-1}$	$9.44e^{-4}$	3
	4	19.87	5.45	0.228	0.453	$3.68e^{-3}$	0.011	1.37	$1.41e^{+0}$	$1.72e^{-3}$	3
	5	19.87	5.45	0.276	0.464	$1.43e^{-2}$	0.023	1.73	$9.10e^{-1}$	$2.97e^{-5}$	1
	6	19.87	5.45	0.274	0.462	$1.25e^{-2}$	0.022	1.60	$2.73e^{-1}$	$1.40e^{-4}$	1

Table 3: Average wetting curve van Genuchten parameters measured from flow cell runs for each salinity region in field 1 under native soil EC and SAR conditions. Parameters estimated using inverse analysis of both drainage and wetting flow cell data in Hydrus-1D.

Salinity Region	Core No.	EC	SAR	θ_r	θ_{sw}	K_{sw}	α_w	n	L	SSQ	Sampl Size
		(dS m^{-1})		--- (cm^3 cm^{-3}) ---		(cm min^{-1})	(1 cm^{-1})				
Low	1	3.73	7.78	0.213	0.403	$1.21e^{-2}$	0.046	1.79	$1.70e^{-1}$	$2.51e^{-4}$	2
	2	3.73	7.78	0.209	0.404	$3.05e^{-2}$	0.049	1.90	$9.45e^{-2}$	$3.40e^{-4}$	2
	3	3.73	7.78	0.214	0.403	$2.18e^{-2}$	0.056	1.45	$4.32e^{+0}$	$9.27e^{-4}$	2
	4	3.73	7.78	0.214	0.417	$2.85e^{-2}$	0.043	1.84	$7.94e^{-1}$	$1.38e^{-4}$	2
	5	3.73	7.78	0.209	0.419	$2.14e^{-2}$	0.056	1.69	$1.52e^{+0}$	$2.46e^{-5}$	3
	6	3.73	7.78	0.198	0.434	$1.40e^{-2}$	0.045	1.54	$2.60e^{+0}$	$1.02e^{-4}$	2
Medium	1	9.99	8.88	0.279	0.440	$1.86e^{-2}$	0.059	1.59	$8.36e^{-1}$	$1.15e^{-4}$	2
	2	9.99	8.88	0.266	0.450	$3.21e^{-2}$	0.053	1.74	$9.20e^{-4}$	$1.20e^{-3}$	2
	3	9.99	8.88	0.271	0.448	$4.29e^{-3}$	0.030	1.80	$5.59e^{-1}$	$1.18e^{-5}$	2
	4	9.99	8.88	0.253	0.443	$5.04e^{-3}$	0.039	1.66	$3.93e^{-5}$	$5.32e^{-5}$	2
	5	9.99	8.88	0.263	0.408	$8.98e^{-3}$	0.043	1.81	$8.39e^{-1}$	$2.60e^{-5}$	2
	6	9.99	8.88	0.277	0.455	$7.49e^{-3}$	0.031	1.75	$1.42e^{+0}$	$2.75e^{-5}$	2
High	1	19.87	5.45	0.263	0.455	$1.48e^{-3}$	0.063	1.42	$2.33e^{+0}$	$7.26e^{-4}$	3
	2	19.87	5.45	0.255	0.429	$3.64e^{-3}$	0.063	1.50	$1.20e^{+0}$	$1.51e^{-4}$	2
	3	19.87	5.45	0.231	0.443	$1.15e^{-2}$	0.090	1.39	$1.26e^{-2}$	$3.40e^{-2}$	3
	4	19.87	5.45	0.247	0.442	$2.50e^{-3}$	0.043	1.37	$7.53e^{-2}$	$1.05e^{-3}$	3
	5	19.87	5.45	0.276	0.430	$3.20e^{-3}$	0.054	1.73	$8.74e^{-1}$	$1.01e^{-5}$	1
	6	19.87	5.45	0.276	0.437	$3.48e^{-3}$	0.069	1.60	$1.97e^{-1}$	$4.59e^{-5}$	1

Table 4: Average drainage curve van Genuchten parameters measured from flow cell runs for each salinity region in field 1 with EC reduction series. Parameters estimated using inverse analysis of drainage flow cell data only in Hydrus-1D.

Salinity Region	Core No.	EC	SAR	θ_r	θ_{sd}	K_{sd}	α_d	n	L	SSQ	Sample Size
		(dS m^{-1})		--- (cm^3 cm^{-3}) ---		(cm min^{-1})	(1 cm^{-1})				
Low	1	3.73 N	7.78	0.213	0.441	$4.27e^{-2}$	0.017	2.03	$1.27e^{+0}$	$2.37e^{-5}$	3
	1	1.50	5.00	0.279	0.450	$1.16e^{-2}$	0.020	1.62	$2.28e^{-1}$	$3.83e^{-1}$	5
	1	0.50	5.00	0.305	0.453	$2.23e^{-3}$	0.019	1.64	$3.95e^{-2}$	$2.76e^{-1}$	3
	1	0.25	5.00	0.302	0.451	$3.69e^{-4}$	0.019	1.63	$4.82e^{-2}$	$3.63e^{-1}$	2
	1	5.00*	5.00	0.296	0.442	$2.96e^{-4}$	0.019	1.63	$1.45e^{-4}$	$3.19e^{-1}$	3
Medium	1	10.00 N	8.88	0.277	0.458	$2.21e^{-2}$	0.017	1.86	$1.12e^{+0}$	$3.69e^{-5}$	3
	1	4.00	5.00	0.298	0.465	$1.95e^{-2}$	0.016	1.81	$2.01e^{+0}$	$4.88e^{-5}$	3
	1	1.50	5.00	0.310	0.468	$1.05e^{-2}$	0.019	1.63	$1.88e^{-3}$	$3.80e^{-2}$	5
	1	0.50	5.00	0.315	0.469	$2.35e^{-3}$	0.020	1.60	$1.35e^{-2}$	$6.79e^{-2}$	4
	1	0.25	5.00	0.325	0.468	$6.38e^{-4}$	0.017	2.07	$1.71e^{+0}$	$2.70e^{-3}$	3
	1	5.00*	5.00	0.306	0.458	$1.29e^{-3}$	0.014	1.73	$4.18e^{+0}$	$2.17e^{-5}$	3
High	4	19.87 N	5.45	0.263	0.453	$3.41e^{-3}$	0.017	1.58	$1.19e^{-2}$	$1.74e^{-1}$	3
	4	4.00	5.00	0.287	0.463	$6.91e^{-3}$	0.013	1.44	$1.95e^{+0}$	$8.54e^{-4}$	4
	4	1.50	5.00	0.302	0.464	$4.07e^{-3}$	0.013	1.44	$1.21e^{+0}$	$1.06e^{-3}$	5
	4	0.50	5.00	0.324	0.465	$6.09e^{-4}$	0.018	1.56	$2.95e^{-3}$	$1.94e^{-1}$	4
	4	0.25	5.00	0.302	0.463	$3.98e^{-4}$	0.012	1.46	$1.59e^{+0}$	$5.26e^{-4}$	3
	4	5.00*	5.00	0.280	0.453	$7.59e^{-4}$	0.011	1.36	$2.65e^{+0}$	$1.98e^{-3}$	3

N = native soil conditions

* = soil solution EC increased from 0.25 dS m^{-1}

Table 5: Average drainage curve van Genuchten parameters measured from flow cell runs for each salinity region in field 1 with EC reduction series. Parameters estimated using inverse analysis using both the drainage and wetting flow cell data only in Hydrus-1D.

Salinity Region	Core No.	EC	SAR	θ_r	θ_{sd}	K_{sd}	α_d	n	L	SSQ	Sample Size
		(dS m^{-1})		--- (cm^3 cm^{-3}) ---		(cm min^{-1})	(1 cm^{-1})				
Low	1	3.73 N	7.78	0.212	0.441	$4.10e^{-2}$	0.022	1.80	$3.58e^{-1}$	$2.12e^{-4}$	2
	1	1.50	5.00	0.278	0.450	$1.02e^{-2}$	0.020	1.63	$6.42e^{-3}$	$2.09e^{-1}$	3
	1	0.50	5.00	0.274	0.453	$1.29e^{-3}$	0.016	1.63	$1.24e^{-3}$	$1.60e^{-1}$	3
	1	0.25	5.00	0.303	0.451	$4.31e^{-4}$	0.020	1.63	$8.31e^{-3}$	$5.56e^{-1}$	1
	1	5.00*	5.00	0.297	0.442	$2.60e^{-4}$	0.020	1.60	$7.30e^{-3}$	$4.50e^{-1}$	3
Medium	1	10.00 N	8.88	0.279	0.458	$2.14e^{-2}$	0.023	1.60	$1.02e^{+0}$	$1.82e^{-4}$	2
	1	4.00	5.00	0.298	0.465	$2.29e^{-2}$	0.019	1.74	$1.64e^{+0}$	$7.00e^{-5}$	3
	1	1.50	5.00	0.309	0.468	$1.02e^{-2}$	0.017	1.67	$4.51e^{-1}$	$4.35e^{-4}$	3
	1	0.50	5.00	0.322	0.469	$2.00e^{-3}$	0.020	1.60	$2.70e^{-3}$	$8.74e^{-2}$	2
	1	0.25	5.00	0.325	0.463	$7.44e^{-4}$	0.018	1.74	$2.25e^{+0}$	$3.62e^{-5}$	2
	1	5.00*	5.00	0.300	0.458	$1.54e^{-3}$	0.016	1.48	$4.29e^{+0}$	$7.11e^{-4}$	2
High	4	19.87 N	5.45	0.228	0.453	$3.68e^{-3}$	0.011	1.37	$1.41e^{+0}$	$1.72e^{-3}$	3
	4	4.00	5.00	0.288	0.462	$6.28e^{-3}$	0.014	1.42	$1.60e^{+0}$	$1.21e^{-3}$	2
	4	1.50	5.00	0.296	0.464	$4.20e^{-3}$	0.014	1.37	$1.57e^{+0}$	$1.65e^{-3}$	4
	4	0.50	5.00	0.325	0.465	$6.32e^{-4}$	0.018	1.54	$1.60e^{-3}$	$2.00e^{-1}$	4
	4	0.25	5.00	0.303	0.463	$4.38e^{-4}$	0.012	1.39	$2.79e^{+0}$	$1.75e^{-3}$	2
	4	5.00*	5.00	0.293	0.453	$9.22e^{-4}$	0.012	1.28	$2.90e^{+0}$	$4.47e^{-3}$	3

N = native soil conditions

* = soil solution EC increased from 0.25 dS m^{-1}

Table 6: Average wetting curve van Genuchten parameters measured from flow cell runs for each salinity region in field 1 with EC reduction series. Parameters estimated using inverse analysis using both the drainage and wetting flow cell data only in Hydrus-1D.

Salinity Region	Core No.	EC	SAR	θ_r	θ_{sw}	K_{sw}	α_w	n	L	SSQ	Sample Size
		(dS m^{-1})		--- (cm^3 cm^{-3}) ---		(cm min^{-1})	(1 cm^{-1})				
Low	1	3.73 N	7.78	0.213	0.403	$1.21e^{-2}$	0.046	1.79	$1.70e^{-1}$	$2.51e^{-4}$	2
	1	1.50	5.00	0.275	0.428	$3.22e^{-3}$	0.035	1.70	$1.92e^{-3}$	$1.09e^{-1}$	3
	1	0.50	5.00	0.305	0.446	$1.24e^{-3}$	0.046	2.13	$1.16e^{+0}$	$1.27e^{-6}$	3
	1	0.25	5.00	0.301	0.443	$2.21e^{-4}$	0.032	1.68	$1.04e^{-2}$	$4.45e^{-1}$	1
	1	5.00*	5.00	0.274	0.442	$2.56e^{-4}$	0.048	1.80	$3.81e^{-5}$	$8.49e^{-2}$	3
Medium	1	10.00 N	8.88	0.279	0.440	$1.86e^{-2}$	0.059	1.59	$8.36e^{-1}$	$1.15e^{-4}$	2
	1	4.00	5.00	0.299	0.424	$1.61e^{-2}$	0.040	1.75	$1.14e^{+0}$	$7.60e^{-5}$	3
	1	1.50	5.00	0.306	0.451	$4.46e^{-3}$	0.052	1.67	$9.21e^{-5}$	$3.08e^{-3}$	3
	1	0.50	5.00	0.318	0.457	$1.48e^{-3}$	0.049	1.69	$8.24e^{-5}$	$1.10e^{-3}$	2
	1	0.25	5.00	0.326	0.442	$3.94e^{-4}$	0.084	1.73	$2.21e^{+0}$	$4.38e^{-5}$	2
	1	5.00*	5.00	0.307	0.458	$5.24e^{-4}$	0.132	1.49	$2.86e^{+0}$	$2.25e^{-4}$	2
High	4	19.87 N	5.45	0.247	0.442	$2.50e^{-3}$	0.043	1.37	$7.53e^{-2}$	$1.05e^{-3}$	3
	4	4.00	5.00	0.297	0.440	$8.00e^{-4}$	0.036	1.42	$1.00e^{+0}$	$7.96e^{-4}$	2
	4	1.50	5.00	0.310	0.449	$3.10e^{-4}$	0.069	1.39	$2.72e^{-1}$	$1.11e^{-3}$	4
	4	0.50	5.00	0.316	0.456	$3.63e^{-4}$	0.056	1.44	$4.21e^{-5}$	$5.79e^{-4}$	4
	4	0.25	5.00	0.318	0.447	$8.65e^{-5}$	0.087	1.41	$2.13e^{+0}$	$9.67e^{-4}$	2
	4	5.00*	5.00	0.320	0.453	$1.45e^{-4}$	0.071	1.30	$1.15e^{+0}$	$5.77e^{-3}$	3

N = native soil conditions

* = soil solution EC increased from 0.25 dS m^{-1}

Table 7: Average drainage curve van Genuchten parameters measured from flow cell runs for each salinity region in field 1 with EC reduction series. Parameters estimated using inverse analysis of drainage flow cell data only in Hydrus-1D.

Salinity Region	Core No.	EC	SAR	θ_r	θ_{sd}	K_{sd}	α_d	n	L	SSQ	Sample Size
		(dS m^{-1})		--- (cm^3 cm^{-3}) ---		(cm min^{-1})	(1 cm^{-1})				
Low	4	3.73	7.78 N	0.211	0.442	$3.87e^{-2}$	0.020	1.66	$1.00e^{-2}$	$2.48e^{-1}$	3
	4	0.65	5.00	0.212	0.446	$2.53e^{-2}$	0.019	1.65	$4.19e^{-2}$	$3.20e^{-1}$	3
	4	0.65	20.00	0.224	0.459	$1.50e^{-2}$	0.019	1.66	$6.98e^{-3}$	$1.77e^{-1}$	3
	4	0.65	25.00	0.228	0.466	$7.61e^{-3}$	0.018	1.66	$5.33e^{-4}$	$1.63e^{-1}$	3
	4	0.65	20.00*	0.229	0.463	$1.19e^{-2}$	0.015	1.99	$2.67e^{+0}$	$7.79e^{-6}$	3
	4	0.65	5.00*	0.227	0.461	$5.59e^{-3}$	0.019	1.65	$3.01e^{-3}$	$1.95e^{-1}$	3
High	6	19.87	4.45 N	0.281	0.462	$2.09e^{-2}$	0.015	1.94	$3.23e^{+0}$	$3.43e^{-4}$	3
	6	0.65	10.00	0.266	0.463	$6.90e^{-3}$	0.018	1.60	$1.78e^{+0}$	$2.57e^{-4}$	3
	6	0.65	20.00	0.276	0.465	$3.80e^{-3}$	0.017	1.62	$5.77e^{+0}$	$1.32e^{-4}$	4
	6	0.65	25.00	0.268	0.466	$2.60e^{-3}$	0.016	1.58	$7.74e^{-1}$	$1.02e^{-3}$	4
	6	0.65	20.00*	0.253	0.463	$1.30e^{-3}$	0.016	1.41	8.74e-^{1}	$1.31e^{-2}$	4

N = native soil conditions

* = soil solution SAR reduced from SAR = 25

Table 8: Average drainage curve van Genuchten parameters measured from flow cell runs for each salinity region in field 1 with SAR series. Parameters estimated using inverse analysis using both the drainage and wetting flow cell data only in Hydrus-1D.

Salinity Region	Core No.	EC	SAR	θ_r	θ_{sd}	K_{sd}	α_d	n	L	SSQ	Sample Size
		(dS m^{-1})		--- (cm^3 cm^{-3}) ---		(cm min^{-1})	(1 cm^{-1})				
Low	4	3.73	7.78 N	0.211	0.443	$3.75e^{-2}$	0.023	1.81	$1.10e^{+0}$	$9.01e^{-5}$	2
	4	0.65	5.00	0.212	0.446	$1.41e^{-2}$	0.020	1.73	$2.23e^{+0}$	$3.71e^{-5}$	1
	4	0.65	20.00	0.227	0.459	$1.42e^{-2}$	0.018	1.94	$1.36e^{+0}$	$5.05e^{-6}$	2
	4	0.65	25.00	0.230	0.465	$5.75e^{-3}$	0.015	1.83	$1.02e^{+0}$	$3.22e^{-5}$	2
	4	0.65	20.00*	0.227	0.463	$5.72e^{-3}$	0.016	1.78	$8.51e^{-1}$	$4.92e^{-5}$	2
	4	0.65	5.00*	0.229	0.461	$5.71e^{-3}$	0.017	1.83	$1.54e^{+0}$	$1.37e^{-5}$	2
High	6	19.00	4.45 N	0.274	0.462	$1.25e^{-2}$	0.022	1.60	$2.73e^{-1}$	$1.40e^{-4}$	1
	6	0.65	10.00	0.269	0.460	$7.78e^{-3}$	0.028	1.40	$3.63e^{+0}$	$1.27e^{-3}$	1
	6	0.65	20.00	0.261	0.465	$1.16e^{-2}$	0.028	1.33	$7.11e^{+0}$	$2.67e^{-3}$	2
	6	0.65	25.00	0.269	0.466	$3.18e^{-3}$	0.018	1.53	$1.24e^{+0}$	$3.87e^{-4}$	3
	6	0.65	20.00*	0.240	0.463	$1.49e^{-3}$	0.016	1.32	$2.23e^{+0}$	$3.18e^{-3}$	3

N = native soil conditions

* = soil solution SAR reduced from SAR = 25

Table 9: Average wetting curve van Genuchten parameters measured from flow cell runs for each salinity region in field 1 with SAR series. Parameters estimated using inverse analysis using both the drainage and wetting flow cell data only in Hydrus-1D.

Salinity Region	Core No.	EC	SAR	θ_r	θ_{sw}	K_{sw}	α_w	n	L	SSQ	Sample Size
		(dS m^{-1})		--- (cm^3 cm^{-3}) ---		(cm min^{-1})	(1 cm^{-1})				
Low	4	3.73	7.78 N	0.214	0.417	$2.85e^{-2}$	0.043	1.84	$7.94e^{-1}$	$1.38e^{-4}$	2
	4	0.65	5.00	0.213	0.441	$9.59e^{-3}$	0.050	1.73	$2.17e^{+0}$	$1.10e^{-5}$	1
	4	0.65	20.00	0.227	0.449	$8.28e^{-3}$	0.047	1.94	$1.34e^{+0}$	$8.29e^{-7}$	2
	4	0.65	25.00	0.234	0.464	$5.75e^{-3}$	0.037	1.84	$1.16e^{+0}$	$6.98e^{-5}$	2
	4	0.65	20.00*	0.230	0.456	$5.45e^{-3}$	0.039	1.79	$8.37e^{-1}$	$5.69e^{-5}$	2
	4	0.65	5.00*	0.229	0.447	$5.39e^{-3}$	0.042	1.83	$1.43e^{+0}$	$4.25e^{-6}$	2
High	6	19.00	4.45 N	0.276	0.437	$3.48e^{-3}$	0.069	1.60	$1.97e^{-1}$	$4.59e^{-5}$	1
	6	0.65	10.00	0.277	0.439	$7.25e^{-4}$	0.073	1.40	$3.16e^{+0}$	$7.40e^{-4}$	1
	6	0.65	20.00	0.277	0.460	$5.61e^{-4}$	0.174	1.35	$4.37e^{+0}$	$1.49e^{-3}$	2
	6	0.65	25.00	0.272	0.450	$1.70e^{-3}$	0.098	1.52	$1.21e^{+0}$	$5.02e^{-5}$	3
	6	0.65	20.00*	0.266	0.457	$1.06e^{-3}$	0.194	1.34	$1.22e^{-1}$	$1.20e^{-3}$	3

N = native soil conditions

* = soil solution SAR reduced from SAR = 25